



2015-06-01

A Study of Allylic Aminations as Catalyzed by Heterobimetallic Pd-Ti Complexes

Diana Lauren Ellis

Brigham Young University - Provo

Follow this and additional works at: <https://scholarsarchive.byu.edu/etd>

 Part of the [Biochemistry Commons](#), and the [Chemistry Commons](#)

BYU ScholarsArchive Citation

Ellis, Diana Lauren, "A Study of Allylic Aminations as Catalyzed by Heterobimetallic Pd-Ti Complexes" (2015). *All Theses and Dissertations*. 5471.

<https://scholarsarchive.byu.edu/etd/5471>

This Thesis is brought to you for free and open access by BYU ScholarsArchive. It has been accepted for inclusion in All Theses and Dissertations by an authorized administrator of BYU ScholarsArchive. For more information, please contact scholarsarchive@byu.edu, ellen_amatangelo@byu.edu.

A Study of Allylic Aminations as Catalyzed by Heterobimetallic Pd-Ti Complexes

Diana Lauren Ellis

A thesis submitted to the faculty of
Brigham Young University
in partial fulfillment of the requirements for the degree of

Master of Science

David J. Michaelis, Chair
Daniel H. Ess
Roger G. Harrison

Department of Chemistry and Biochemistry

Brigham Young University

June 2015

Copyright © 2015 Diana Lauren Ellis

All Rights Reserved

ABSTRACT

A Study of Allylic Aminations as Catalyzed by Heterobimetallic Pd-Ti Complexes

Diana Lauren Ellis
Department of Chemistry and Biochemistry, BYU
Master of Science

Heterobimetallic complexes present a unique approach to catalyzing challenging reactions. By having two metals in close proximity to each other, the metals are able to interact and alter their electronics in a way that simple organic ligands (carbon, nitrogen, sulfur etc.) cannot. Our studies of heterobimetallic complexes focus on a Pd–Ti complex. The complex features a dative interaction between the palladium and the titanium held together by a phosphoramidate scaffold. This interaction increases the electrophilicity of the palladium and makes it a very suitable catalyst for allylic amination reactions. We have conducted extensive studies of this catalyst in allylic aminations, the results of which will be discussed.

Our first studies with heterobimetallic Pd–Ti complexes focused on their potential to catalyze challenging allylic amination reactions. These studies showed that the Pd-Ti complex was effective at catalyzing allylic aminations with sterically hindered secondary amines, a reaction which had heretofore proved challenging. We then developed a method for synthesizing the catalyst *in situ*, greatly simplifying the procedure by which the catalyst is used and making it that much more accessible. We also tested the substrate scope and varied the structure of both the amine and chloride substrates. Our results demonstrated the high catalytic activity of heterobimetallic catalysts with most substrates, in spite of steric hindrance of notoriously challenging substrates.

Next, we investigated the origin of the fast catalysis we had observed with heterobimetallic Pd–Ti complexes. We confirmed the catalytic cycle and determined the activation barrier for the rate-determining step. We computationally investigated the reactivity of various control catalysts in which the Pd-Ti interaction was severed. These results were compared with the reactivity of the heterobimetallic catalyst. We found that the activation barrier for turnover-limiting reductive amine addition was lowered with the bimetallic complex because of an increased electrophilicity at palladium. We further supported our claim by synthesizing a phosphinoamide palladium complex lacking a titanium atom and testing it in the allylic amination reaction. Our findings in the lab corroborated our calculations. We also ensured that the Pd-Ti catalyst was not transformed prior to catalysis by examining various decomposition pathways and determining that they all resulted in higher energy pathways. We discovered that the Pd-Ti interaction is made possible only by the steric interaction provided by *N-tert*-butyl groups on the amines which sterically reinforce the Pd–Ti interaction. Lastly, we tested the catalytic activity of the complex with allylic acetates and found them to be ineffective due to catalyst decomposition. It is our hope that these findings can serve as guiding principles when designing heterobimetallic complexes for future catalytic applications.

Keywords: [Heterobimetallic, Catalysis, Allylic Aminations]

ACKNOWLEDGEMENTS

I am very grateful for the support I have received from Dr. Michaelis, my advisor, throughout my time here at Brigham Young University. His patience and instruction have taught and inspired me to achieve my very best. I am grateful to Dr. Harrison for his instruction and encouragement. And I am grateful to Dr. Ess as well, for allowing me work with his group and training me in computational chemistry so that I might continue my studies and research in spite of my recently becoming a mother. I am also grateful to my coworkers in the Michaelis lab and the Ess lab, especially Whitney Walker and Benjamin Kay, for their collaboration and guidance.

I am grateful to my family for the countless sacrifices they have made to help me get to this point. I am grateful to my father for his example and for instilling in me a love for learning, and for years of encouragement and counsel. I am grateful to my mother for her innumerable hours of travel to help watch my daughter as I worked on my research and thesis. I am also grateful to my sister for her unending support in helping take care of my daughter, often on a moment's notice, so that I could continue to progress in my scholastic endeavors.

Most of all, I am grateful to my husband, Tyler, for his immeasurable love and support throughout my career here at BYU. I am grateful for all the sacrifices he has made in order to allow me to return to school and the added weight he has so willingly carried because of it. He is a wonderful husband and father and I could not have accomplished this without him. It is to him and my sweet baby daughter, Mckenzie, whom I dedicate this thesis.

TABLE OF CONTENTS

TABLE OF CONTENTS	iv
LIST OF FIGURES	viii
LIST OF SCHEMES	x
LIST OF TABLES	xi
Chapter 1 Catalytic Applications of Heterobimetallic Complexes.....	1
1.1 INTRODUCTION	1
1.1.1 Inspiration For Heterobimetallic Catalysts	3
1.1.2 Types of Metal-Metal Interactions.....	4
1.2 METAL-METAL BONDS	4
1.2.1 H ₂ Addition.....	5
1.2.2 Hydrogenation of Alkynes	5
1.2.3 Hydrosilylation	6
1.2.4 CO ₂ Activation and Functionalization	7
1.2.5 Binuclear Oxidative Addition	8
1.3 COOPERATIVITY BETWEEN TWO METALS	8
1.3.1 Dehydrogenation of Dimethylamine-Borane.....	9
1.3.2 Hydroformylation.....	10
1.3.3 Carbon-Carbon Bond Forming Reactions.....	10
1.3.4 Hydroacylation	12

1.3.5 Ethylene Polymerization	13
1.4 A SECOND METAL AS A SPECIAL LIGAND	13
1.4.1 Carbon-Carbon Coupling	14
1.4.2 Hydrogenation of CO	15
1.4.3 Hydrogenation of CO ₂	16
1.4.4 Cross Coupling of Stannanes	16
1.4.5 Hydrosilylation of Alkynes	16
1.4.6 Copolymerization of Olefin Monomers	17
1.4.7 Hydrogenation of Olefins	18
1.5 ELECTRONIC TUNING USING A SECOND METAL	20
1.5.1 Allylic Amination	20
1.5.2 Polymerization of Olefins	21
1.5.3 Metal Carbenoid Transformations	22
1.6 CONCLUSION AND OUTLOOK	22
1.7 REFERENCES	24
 Chapter 2 Heterobimetallic Pd–Ti Complexes for Fast Catalysis In Allylic Amination	
Reactions	29
2.1 INTRODUCTION	29
2.2 RESULTS AND DISCUSSION	32
2.2.1 Optimization of Allylic Amination using Hindered Amine	32

2.2.2 In Situ formation of Catalyst.....	34
2.2.3 Synthesis and Reactions of Metal Containing Ligands	35
2.2.4 Reaction with Hindered Amin Nucleophiles	37
2.2.5 Intramolecular Cyclizations	38
2.3 CONCLUSION.....	40
2.4 REFERENCES.....	42
Chapter 3 Origin of Fast Catalysis in Allylic Amination Reactions Catalyzed by Pd–Ti	
Heterobimetallic complexes.....	46
3.1 INTRODUCTION	46
3.2 RESULTS AND DISCUSSION.....	48
3.2.1 A Brief Review of Density Functional Theory.....	48
3.2.2 Computational Assessment of Heterobimetallic Pd-Ti Complex 1 and Mechanism for Allylic Amination	51
3.2.3 Experimental and Computational Evaluation of the Impact of Replacing TiCl ₂ to Remove the Pd-Ti Interaction	59
3.2.4 Impact of Coordination Angle and Electronic Effects on Catalysis.....	61
3.2.5 Testing the Limits of The Pd-Ti Interaction	64
3.3 CONCLUSION.....	67
3.4 REFERENCES.....	68
Chapter 4 Supporting Information.....	76

4.1 Supporting Information for Chapter 2.....	76
4.1.1 General Information	76
4.2 Supporting Information for Chapter 3.....	124

LIST OF FIGURES

Chapter 1

Figure 1: Dative interaction between two electronically disparate metals in close proximity	2
Figure 2: Example of Heterobimetallic Mo/Ir and W/Ir catalysts active in alkyne hydrogenation.....	6
Figure 3: Nb/Rh catalysts used in the hydrosilylation	7
Figure 4: Hydroformylation of alkenes using heterobimetallic Zr/Rh catalyst	10
Figure 5: Formation of enol esters using heterobimetallic Ru/Re complex.....	12
Figure 6: Ti/Rh catalyst active in hydroacylation reactions.....	12
Figure 7: Zr/M polymerization catalysts.	13
Figure 8: Carbon-carbon coupling catalyzed by a Zr/Co heterobimetallic catalyst.....	15
Figure 9: Ti/Rh and Ti/Ru CO Hydrogenation catalysts.....	15
Figure 10: Active hydrosilylation Pt/Ir heterobimetallic complex	17
Figure 11: Olefin Polymerization catalysts	18
Figure 12: Olefin Polymerization Catalyst.....	21

Chapter 2

Figure 1. Stoichiometric allylic amination with heterobimetallic complex 1.....	31
Figure 2. Allylic amination of hindered amines using heterobimetallic complex 1	32
Figure 3. <i>In situ</i> formation of catalyst using titanium-containing ligand	35
Figure 4: Novel titanium-containing ligands.....	36
Figure 5: Aminations with titanium-containing ligands.....	37
Figure 6: Intramolecular aminations for heterocycle synthesis.....	40

Chapter 3

Figure 1: Mechanism for allylic amination catalyzed by 1	52
Figure 2: M06 free energy landscape for Et ₂ NH reductive addition and methallyl chloride oxidative addition & transition-state structures.....	53
Figure 3. Possible alternative species involved in catalysis.....	54
Figure 4. Boat and flat conformations of catalyst 1.	56
Figure 5: Comparison of allylic amination M06 free energy landscapes catalyzed by 1 (boat) and 1 (flat). (kcal/mol)	57
Figure 6: Significance of phosphinoamide ligand to enforcing Pd-Ti interaction and fast catalysis	59
Figure 7: Bidentate phosphinoamine Pd-Ti mimic.....	60
Figure 8: Allylic amination using allyl acetates and 13 catalyzed by 1	66

LIST OF SCHEMES

Chapter 1

Scheme 1:H ₂ activation across polar M-M' bond.....	5
Scheme 2:CO ₂ insertion across a polarized M-M' bond	7
Scheme 3:Addition of Me-I across a polarized Cu-Fe bond.....	8
Scheme 4:Mechanism proposed for amine-borane dehydrogenation by cooperativity of Zr/Ru catalyst.	9
Scheme 5:Proposed mechanism for epoxide/CO ₂ coupling.....	11
Scheme 6:Cross coupling of stannanes by Fe/Pd heterobimetallic complex	16
Scheme 7:Proposed catalytic cycle for hydrogenation of olefins using Ta/Ir catalysts...	19
Scheme 8:Catalytic activity as facilitated by Pd-Ti interaction vs monometallic analogue	20

Chapter 3

Scheme 1 A study by Nagashima of allylic aminations using heterobimetallic Pd-Ti complex	47
---	----

LIST OF TABLES

Chapter 2

Table 1 : Optimization Studies on Allylic Aminations with **3** 33

Table 2: Substrate Scope with Hindered Amines 39

Chapter 3

Table 1: Reactivity comparison for monometallic Pd catalyzed allylic aminations 62

Table 2. Reactivity of sterically-hindered amine **13** 65

Chapter 1

Catalytic Applications of Heterobimetallic Complexes

1.1 INTRODUCTION

Chemists have long employed organometallic complexes as homogeneous catalysts for organic synthesis. These catalysts are carefully designed by incorporating specific organic ligands onto a transition metal center to control catalytic activity and reaction selectivity. Catalysis takes place as substrates interact with the metal center and the ligands of the catalyst and generate the desired product. By altering the steric and electronic properties of these ligands, chemists can control both the reactivity and selectivity of a catalyst in a given transformation. However, the potential of organic ligands (phosphorous, nitrogen, oxygen, carbon, sulfur-based ligands) to tune the reactivity of transition metals is limited, and many difficult and unselective transformations still exist.

Introducing a second metal as a ligand for transition metal catalysts represents a novel approach to tuning of the redox properties and reactivity of organometallic complexes through formation of a metal-metal interaction. Heterobimetallic complexes offer an alternative solution to ligand design that addresses the limitations of classic ligand design by providing an alternative strategy, for modifying reactivity independent of the supporting ligands. This strategy has the potential to increase reaction rates in traditionally slow and unselective reactions.

Heterobimetallic complexes feature two different metals held in close proximity, either through a ligand scaffold or a direct metal–metal bond, which allows them to interact or work together to facilitate catalysis. The disparity between the electronic properties of the two metals, such as in early/late heterobimetallic complexes, can impart unique metal reactivity due to electron-sharing. This pairing of two electronically different metals creates a dative interaction between an electron deficient, Lewis-acidic early transition metal and an electron rich, Lewis-basic late transition metal and drastically alters the reactivity of the original metals⁽¹⁾ (Figure 1). The new properties introduced by the presence of a second metal allow for each metal center to behave differently than its monometallic analogue and thereby achieve unprecedented reactivity. In addition, modifications to the structure of the supporting ligands at either of the metal centers serve as a strategy for improving selectivity while maintaining reactivity with the metal- metal interaction.

Electron Withdrawing Dative Interaction

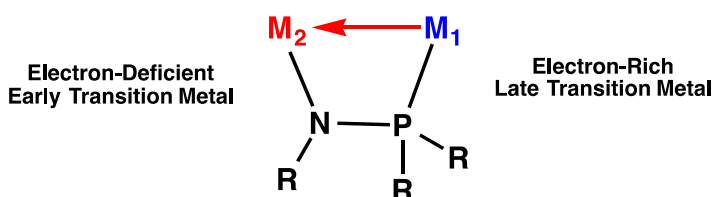


Figure 1: Dative interaction between two electronically disparate metals in close proximity

In this review, we will briefly discuss the origins of heterobimetallic catalysis, and then focus our attention on catalytic applications of heterobimetallic complexes where the presence of two metals is essential for reactivity. Several recent reviews cover the synthesis and structure of heterobimetallic complexes.^{2,3} This review is organized based on how the two metals in heterobimetallic complexes interact with each other and facilitate

catalysis. Specifically, we will discuss 1) heterobimetallic complexes containing metal-metal bonds, 2) cooperativity effects between two metals, 3) a second metal acting as a unique ligand, and 4) electronic tuning through dative M–M bond formation.

1.1.1 Inspiration For Heterobimetallic Catalysts

The design of catalytically active heterobimetallic complexes has its roots in heterogeneous catalysis, where deposition of a catalytically active transition metal onto a heterogeneous support can alter the activity of the metal catalyst. In 1978, Tauster and coworkers found that reactivity of a rhodium catalyst was dramatically increased when deposited on a titania support, as opposed to a silica or an alumina support. They attributed the increased reactivity to the participation of the d-orbitals from the titania and hypothesized that the noble metals were donating electrons from their filled d-shells to the empty d-orbitals of the Lewis-acidic titania. This donation of electron density drastically improved the reactivity of the noble metals studied.⁴

Since this discovery, many have sought to employ a second transition metal to tune the reactivity of a catalytically active metal in homogenous systems. While in many systems the presence of a second metal led to improved catalysis, the presence of a second metal has also been shown to inhibit catalysts in certain systems. One suggested reason for this lies in the design of a suitable scaffold capable of maintaining the heterobimetallic interaction throughout the reaction. An inadequate scaffold might cause the bimetallic system to degenerate and behave as a 1:1 mixture of the monometallic analogues.

Therefore, great care must be taken in catalyst design to ensure the metals are able to maintain interaction.

1.1.2 Types of Metal-Metal Interactions

Many cases have been reported in which the presence of a second metal is necessary for or greatly enhances the reactivity of certain catalytic processes. The remainder of this review is broken down to discuss catalytic applications of heterobimetallic complexes based on how the two metals interact or work cooperatively to enable catalysis. Specifically, we will first discuss systems where the two metals form an actual M–M bond and facilitate oxidative processes across that bond.⁵ Second, we will cover systems where the two metals work in a cooperative manner, and both metals are active participants in the catalytic process.⁶⁻⁸ Third, we will describe systems where the second metal acts as a special ligand that facilitates a novel mechanism, but is not actively participating in the mechanism. Finally, we will discuss systems where a second metal is used to tune the electronic properties of the catalytically active metal center through formation of a dative metal-metal interaction. Particular attention will be given to heterobimetallic complexes that enable catalytic transformations in which the second metal is involved or necessary for reactivity.

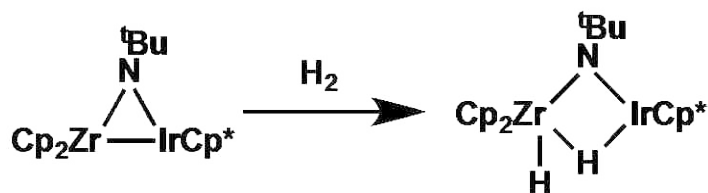
1.2 METAL-METAL BONDS

The systems described in this section involve formation of a polarized M–M' bond and its subsequent participation in the reaction mechanism. This polar bond is capable of activating various substrates as they align with the polarized M–M bond and interact with the each of the two metals and the ligand framework. In some cases, the presence of this

metal-metal bond improves catalytic rates, while in others this type of interaction is shown to inhibited catalysis.

1.2.1 H₂ Addition

The Bergman group reported⁹ that reversible oxidative addition of H₂ can occur across a Zr-Ir bond in the complex Cp₂Zr(μ-N^tBu)IrCp*. In this example, oxidative addition happens by reaction with the metal-metal bond, and the two substituents end up coordinated to different metal centers. This is another example of utilizing the polarized metal-metal bond to activate small molecule substrates (Scheme 1).



Scheme 1: H₂ activation across polar M-M' bond

1.2.2 Hydrogenation of Alkynes

The Hidai group reported the hydrogenation of alkynes at room temperature using several sulfide bridged Group 6/Group 9 bimetallic complexes (Figure 2). However, in this case, they found that the catalysis occurred faster with a monometallic RhH₂(PPh₃)₂(Me₂CO)(EtOH)][PF₆] (Figure 4). They do not explain the origin of the fast catalysis but they do point out that the shortest bond distance between the metal centers was merely 2.87 Å. This indicates a veritable bond between the two metals and warrants further investigation to better understand the mechanism observed with the bimetallic system as compared with that of the monometallic system.¹⁰

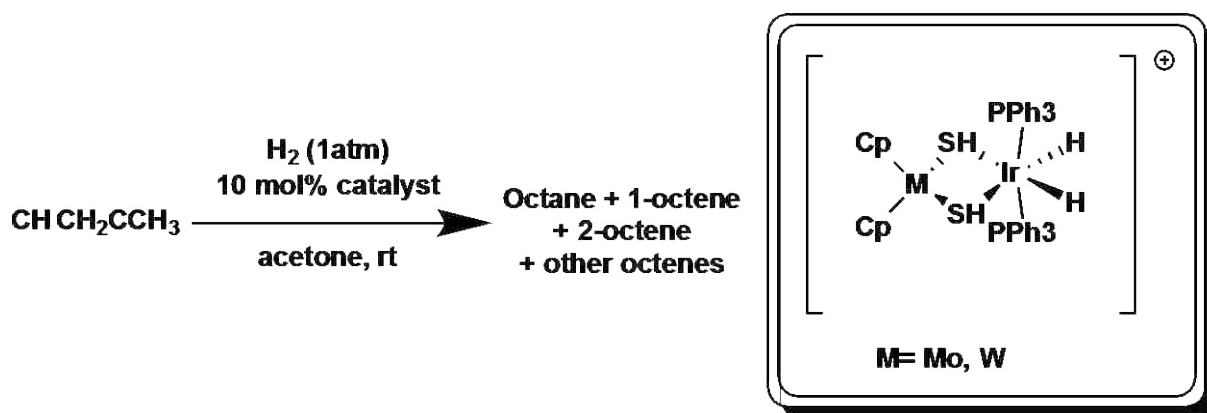


Figure 2: Example of Heterobimetallic Mo/Ir and W/Ir catalysts active in alkyne hydrogenation

1.2.3 Hydrosilylation

The Nikonov group recently reported¹¹ the use of a Nb/Rh complexes, $\text{Cp}_2\text{Nb}(\mu\text{-PPh}_2)(\mu\text{-N}^t\text{Bu})\text{RhCp}$ and $[\text{Cp}_2\text{Nb}(\mu\text{-PPh}_2)(\mu\text{-N}^t\text{Bu})\text{Rh}(\text{cod})][\text{BF}_4]$, in the hydrosilylation of benzaldehyde and acetophenone. (Figure 3). In this study, they found the first two Nb/Rh complexes to have strong intermetallic interactions, while the third complex had the metals over 4 angstroms apart, indicating a lack of interaction. Contrary to their predictions, the catalysts lacking the M-M' interaction more efficiently effected the hydrosilylation than those with very strong M-M' interactions. The authors attribute the lack of reactivity to the exceptionally strong bonds of the bridging imido groups to the Rh. This suggests that hemilabile scaffolds are essential for enabling the catalytic activity of these types of heterobimetallic complexes by allowing access to the metal- metal bond.

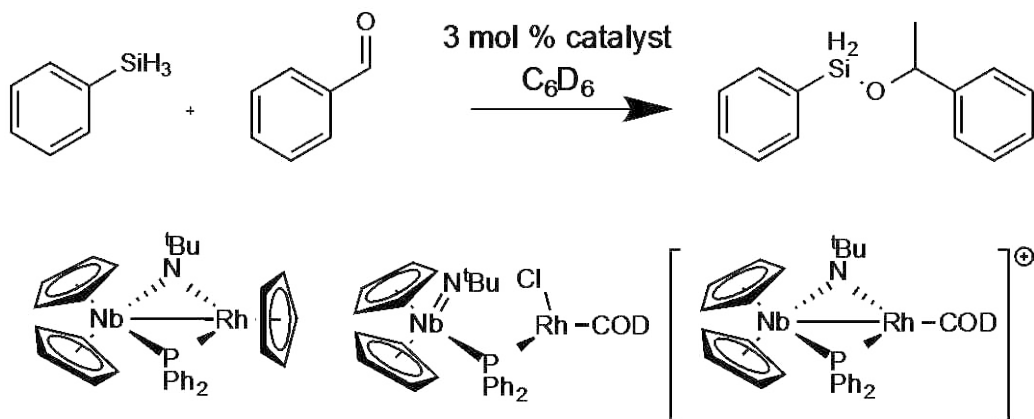
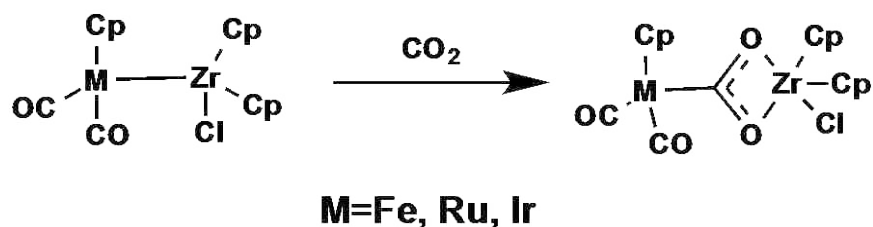


Figure 3: Nb/Rh catalysts used in the hydro-silylation of benzaldehyde and acetophenone

1.2.4 CO₂ Activation and Functionalization

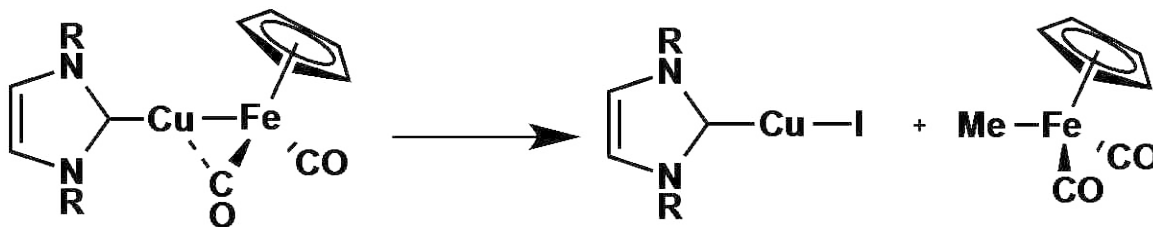
Several groups have reported the stoichiometric activation of functionalization of CO₂ across a polarized M-M' bond.¹²⁻¹⁴ Although stoichiometric, the heterobimetallic complex used serves to illustrate the utility of a polarized bond between metals in functionalizing substrates. In each case, the oxygen interacts with the early, Lewis-acidic transition metal. This Lewis acid activation of CO₂ makes the central carbon more electrophilic, facilitating nucleophilic addition by the late transition metal. These studies used Zr as the early transition metal and Fe, Ru or Ir as the late transition metal (Scheme 2).



Scheme 2: CO₂ insertion across a polarized M-M' bond

1.2.5 Binuclear Oxidative Addition

The Mankad group recently published their findings³⁴ on the synthesis and reactivity of Cu-Fe and Zn-Fe systems. Although they studied a late/late transition metal system and the reactions reported are also not catalytic, the principles governing their reactivity are worth mentioning in the context of this review. They reported the synthesis of a Cu-Fe heterobimetallic complex containing an unsupported Cu-Fe bond. The highly polarized bond between Fe and Cu was found to be active in the binuclear oxidative addition of methyl iodide where the methyl group and the iodide end up on iron and copper respectively. The iodide exclusively added to the Cu and the methyl always added to the Fe (Scheme 3). This result was consistent with the predicted $\text{Cu}^+\text{-Fe}^-$ polarity. This study provides a valuable example in which the polarized bond between two metals can be used to activate substrates.



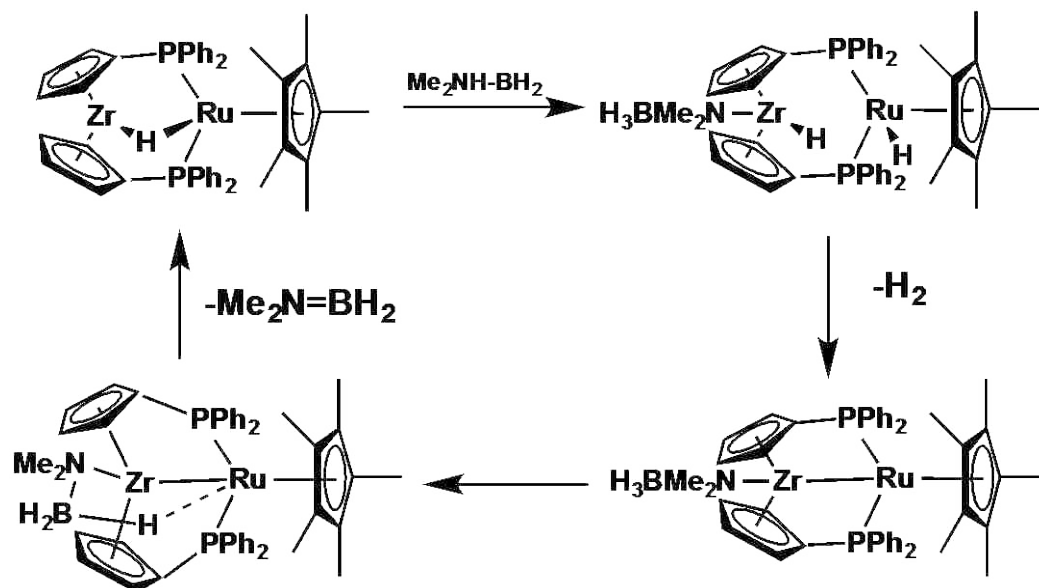
Scheme 3: Addition of Me-I across a polarized Cu-Fe bond

1.3 COOPERATIVITY BETWEEN TWO METALS

In this section, we will discuss systems where the two metals each play a distinctive role necessary to enable fast catalysis. This cooperation between the metals allows for catalysis to be enabled in previously inactive monometallic systems.

1.3.1 Dehydrogenation of Dimethylamine-Borane

Several Group 4/Group 8 metal complexes have been studied¹⁶ in the dehydrogenation of dimethylamine-borane. These include Zr/Ru, Hf/Ru, and Zr/Fe complexes bridged by cyclopentadienylphosphino linkers (Scheme 6). It was reported that each of these bimetallic complexes was quite active in the dehydrogenation reaction. In contrast, the monometallic Zr and Hf analogues were completely inactive and the ruthenium monometallic catalyst was only moderately active. The proposed mechanism suggests cooperativity between the Zr and Ru in reductive elimination and in the activation of B-H bond. The amine-borane oxidatively adds across the Zr/Ru bond and breaks the bond between Zr and the bridging hydrogen. Then the Zr and Ru cooperatively reductively eliminate H₂ and cooperatively activate the B-H bond before releasing the product and regenerating the catalyst (Scheme 4)



Scheme 4: Mechanism proposed for amine-borane dehydrogenation by cooperativity of Zr/Ru catalyst.

1.3.2 Hydroformylation

The Kotila group investigated hydroformylation reactions using the Zr/Rh bimetallic catalyst, $\text{MeZr}(\mu\text{-Co-PPH}_2)_2\text{Rh}(\text{CO})(\text{PPh}_3)$.¹⁷ Their findings indicate that $\text{MeZr}(\mu\text{-Cp-PPH}_2)_2\text{Rh}(\text{CO})(\text{PPh}_3)$ readily catalyzes 1-hexene much more efficiently than other standard Rh phosphine systems (Figure 4). They attribute the fast reactivity to additional bridging or formation of a metal-metal bond to alter the electronics and reactivity of the system. However, they also found that regioselectivity decreased dramatically with the bimetallic system.

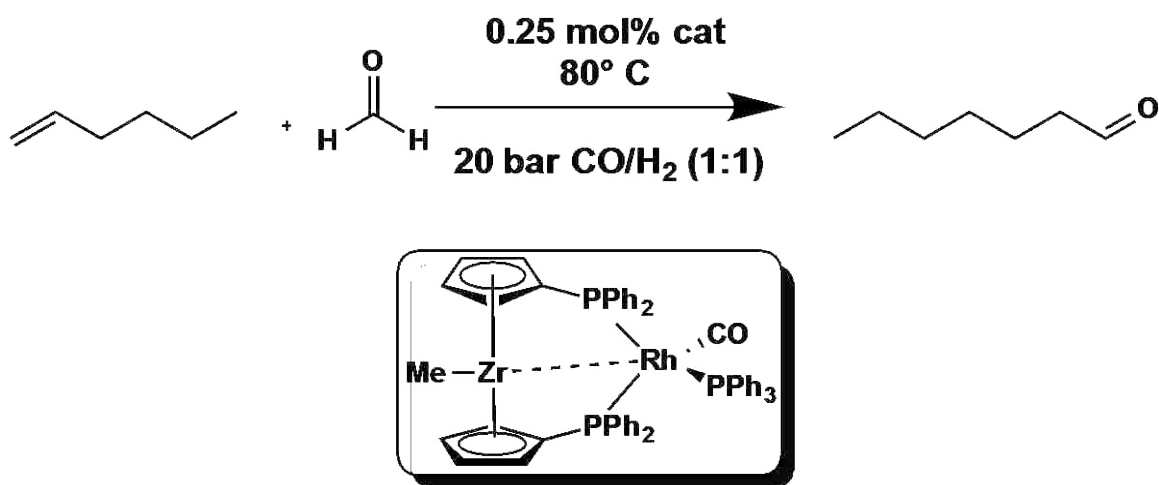
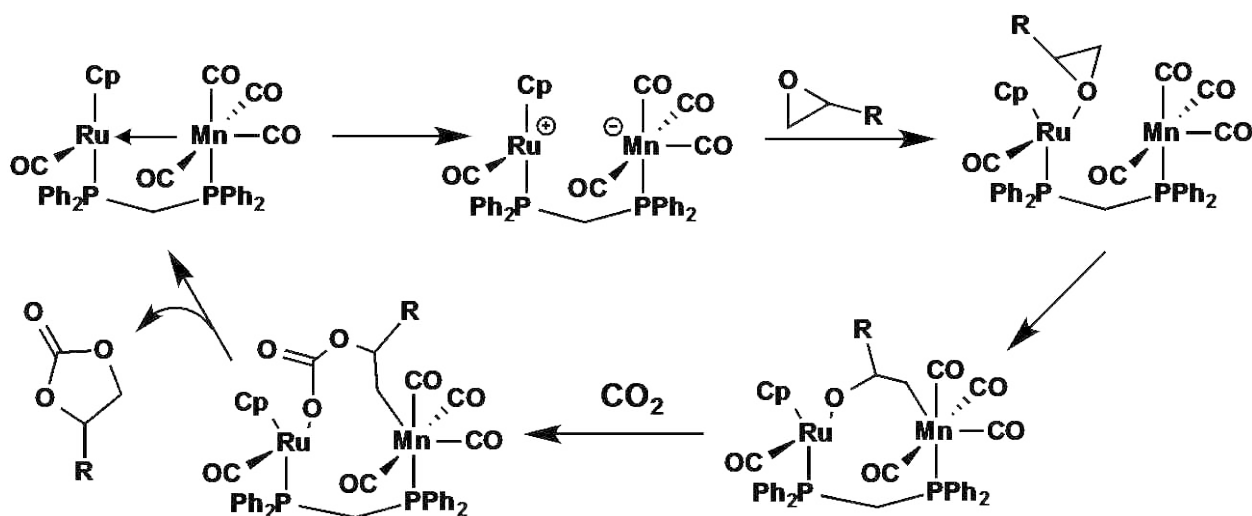


Figure 4: Hydroformylation of alkenes using heterobimetallic Zr/Rh catalyst

1.3.3 Carbon-Carbon Bond Forming Reactions

In 2006, the Lau group reported the reactivity of a Ru/Mn complex in the catalytic coupling of CO₂ and epoxides to form cyclic carbonates (Scheme 5). The metals in this complex are linked by a 1,1-bis(diphenylphosphino)methane (dppm) chain. This link allows the electron rich Mn(-I) to be between 2.85 and 2.87 angstroms apart from the electrophilic Ru (II). Because of the electronic disparity of the metals, they were able to

work cooperatively to facilitate catalysis. To initiate the reaction, the M-M' bond is cleaved, resulting in highly electronically disparate metal centers in very close proximity. Then the epoxide binds to the electrophilic Ru and undergoes ring opening to create a Mn-C bond. The CO₂ is then inserted and the product reductively eliminated from the two metals, regenerating the catalyst (Scheme 7). This mechanism relies heavily upon the interaction of the early and late transition metal to facilitate catalysis. Their findings also showed that monometallic Mn or Ru catalysts were less active or inactive respectively.¹⁸



Scheme 5: Proposed mechanism for epoxide/CO₂ coupling

Similarly, the Ru/Re system, Cp*₂Ru(μ-dppm)(μ-CO)₂Re(CO)₃, was explored in the formation of enol esters from carboxylic acids and 1-alkynes (Figure 5). However, the investigators found the dinuclear complexes were no more efficient than the mononuclear catalysts in facilitating the reaction.¹⁹ Perhaps in this case, the metal centers were not sufficiently electronically dissimilar to create a polarized bond to facilitate fast catalysis.

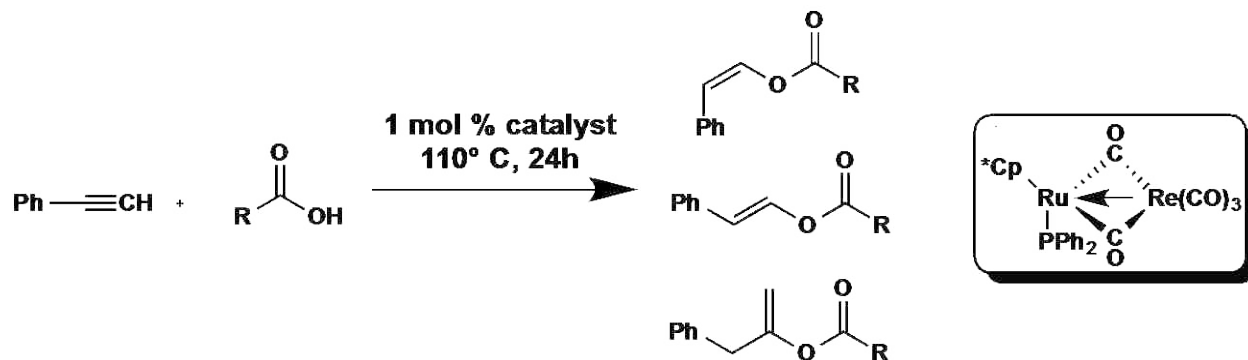


Figure 5: Formation of enol esters using heterobimetallic Ru/Re complex

1.3.4 Hydroacylation

Fast catalysis was also reported in the hydroacylation of 3-phenyl-4-pentenal and styrene using a Ti/Rh. The complex, as originally designed by Slaughter and Wolczanski²⁰ features an alkoxy-phosphine bridge linking the Ti (IV) and the Rh (I) as shown below in figure 6. This catalyst was found to be exceptionally active while monometallic and mixtures of monometallic analogues were found to be inactive in this reaction. Furthermore, the turnover frequency reported is approximately one order of magnitude higher when compared to monometallic analogues. The authors attribute the fast catalysis of polar substrates to the ability of Ti to act as an anchor to the oxygen of the aldehyde, helping facilitate rhodium C–H insertion.²¹

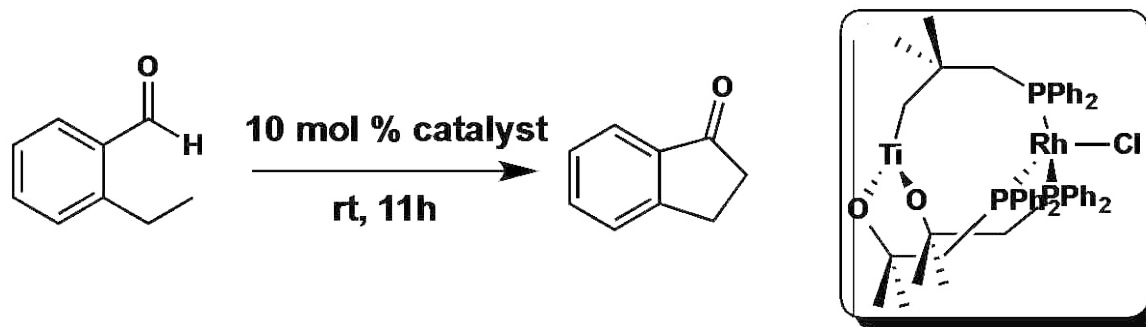


Figure 6: Ti/Rh catalyst active in hydroacylation reactions

1.3.5 Ethylene Polymerization

The Osakada group reported²² the polymerization of ethylene as catalyzed by Zr/Pd, Zr/Co and Zr/Ni complexes (Figure 7). By varying the late transition metal, they were able to synthesize polymers with different properties. For example, when they used Ni with Zr, they synthesized highly branched polymers. In this case, the Zr would generate a growing polymer chain and the Ni would simultaneously be forming oligomers and these oligomers would incorporate themselves to the polymer chain.

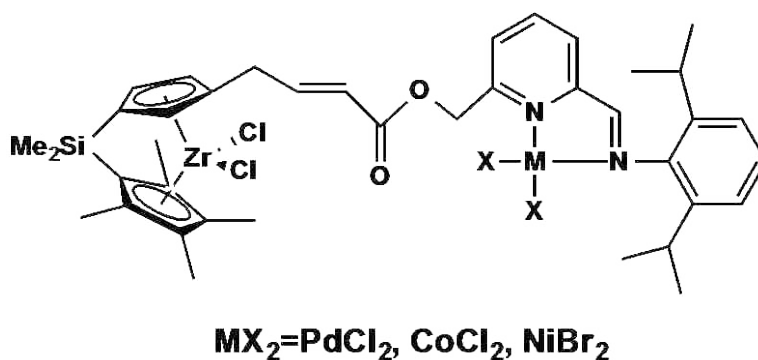


Figure 7: Zr/M polymerization catalysts.

1.4 A SECOND METAL AS A SPECIAL LIGAND

In several of the heterobimetallic systems studied, the nature of the metal-metal interaction is not well understood or defined. Several systems are reported in which catalysis is enhanced by the presence of a second metal but the second metal simply acts as a special ligand to create an environment better suited to catalysis. In some cases, it is clear that reactivity takes place at only one of the metal centers while in other cases, the mechanism is harder to decipher and catalysis is attributed to special ligand effects of the metalloligand. This section will describe examples of heterobimetallic complexes where the

second metal serves as a special ligand to enable catalysis without direct electronic communication.

1.4.1 Carbon-Carbon Coupling

The Thomas group recently reported the use of a Co/Zr complexes $\text{ClZr}(\text{R}'\text{NPR}_2)_3\text{CoI}$ ($\text{R}' = \text{}^i\text{Pr}$, $\text{R} = \text{Ph}$, or $\text{R}' = 2,4,6\text{-trimethylphenyl}$, $\text{R} = \text{}^i\text{Pr}$, or $\text{R}' = \text{R} = \text{}^i\text{Pr}$) as catalysts in Kumada coupling of alkyl chlorides and alkyl Grignard reagents (Figure 8). Their results showed the catalyst to be active in oxidative addition of primary and secondary alkyl chlorides and bromides at room temperature. The fast catalysis observed was especially pronounced for the coupling of alkyl chlorides. However, the alkyl bromides showed only moderate improvements when compared with the monometallic analogues. In light of their results, the authors tried similar reactions using a Co/Hf system. However, the results of that study pale in comparison to the catalysis achieved by the Co/Zr system. They attribute this decreased reactivity to a weaker Co/Zr interaction. They were unable to clearly identify the mechanism and therefore are unsure of the role that Zr plays in catalysis. It may be playing an active role in the catalytic cycle or it may be withdrawing electron density from the Co to facilitate reductive processes. Although it is not clear which role the Zr plays, the authors do propose that fast catalysis is enabled by the early/late heterobimetallic system. Their results suggest that the alteration of redox behavior at each of the metals enhances the catalytic activity of this particular early/late heterobimetallic complex.²³

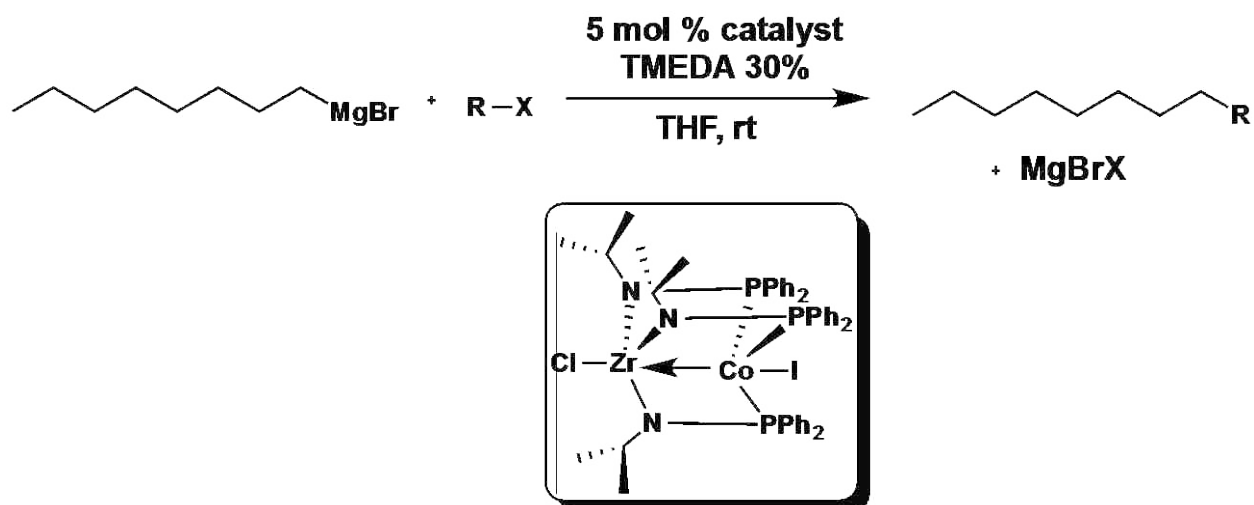


Figure 8: Carbon-carbon coupling catalyzed by a Zr/Co heterobimetallic catalyst

1.4.2 Hydrogenation of CO

The Terroros group reports the hydrogenation of CO using a Ti/Rh or Ti/Ir system, linked by alkoxide groups with varying steric environments²⁴. A few examples of these complexes are depicted in Figure 9. The catalysts were compared to the Rh-based catalyst used in Fisher Tropsh synthesis and were found to have higher catalytic activity: 56.0% vs. 4.2%.¹¹ However, neither the mechanism for this reaction nor the role of each of the metals was discussed by the authors.

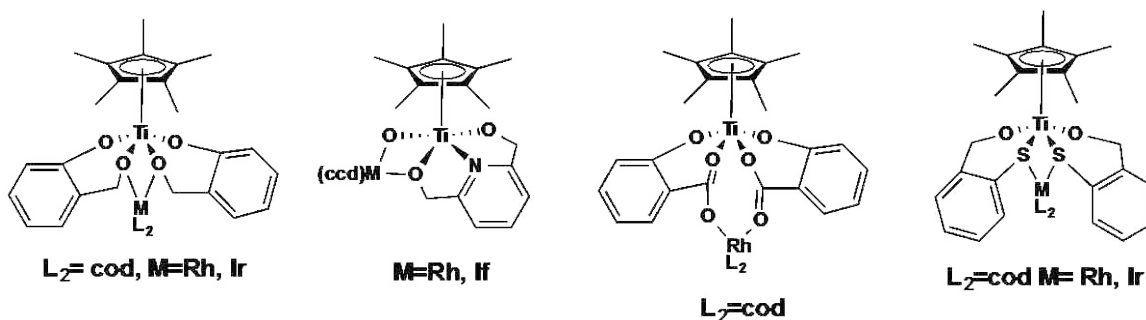


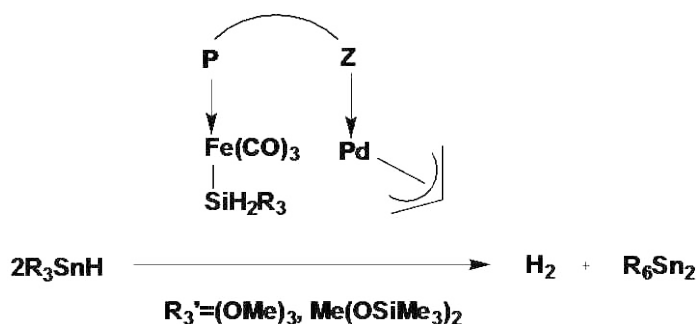
Figure 9: Ti/Rh and Ti/Ru CO Hydrogenation catalysts

1.4.3 Hydrogenation of CO₂

Results were also recently reported for the use of a Ru/Group 6 heterobimetallic system, (C₅X₅)(CO)Ru(μ-dppm)M(CO)₂ (X=H, Me, M=Mo, W), in the hydrogenation of CO₂. The authors show that, although these complexes were not exceptionally catalytically active, monometallic analogues with Ru, Mo, or W were incapable of facilitating the reaction to any extent. From this observation, they concluded that the catalysis occurred with the heterobimetallic interaction intact and inferred each metal played a role in the reaction.²⁵

1.4.4 Cross Coupling of Stannanes

A Pd/Fe heterobimetallic complex was studied in the dehydrogenative coupling of stannanes. Although catalysis was observed, the author attributes this not to a cooperative effect of the two metals, but to particularly reactive ligand environment created by the Fe metalloligands (Scheme 6).²⁶



Scheme 6 Cross coupling of stannanes by Fe/Pd heterobimetallic complex

1.4.5 Hydrosilylation of Alkynes

The Ishii group recently reported²⁷ the hydrosilylation of alkynes using a Pt-Ir system:

$[(PPh_3)_2Pt(\mu-SRS)Ir(\eta^5-Cp)][SbF_6]$ (SRS=cis-C₈H₁₄ or trans-C₈H₁₄) (Figure

10). These complexes provided moderate yields of b-(Z) vinylsilanes selectively but the solid state structure shows the distance between Pt and Ir to be 3.39 Å. At such great distance, there is unlikely any interaction between the two metal centers. In conjunction with this observation, the proposed mechanism shows reactivity occurring exclusively at the Ir, suggesting that the Pt serves only to dictate sterics and help with selectivity.

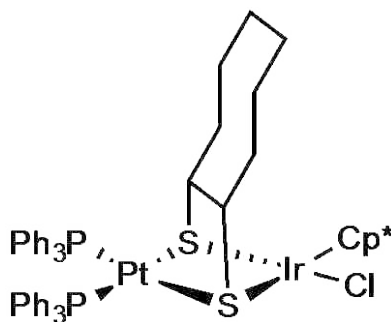


Figure 10: Active hydrosilylation Pt/Ir heterobimetallic complex

1.4.6 Copolymerization of Olefin Monomers

A W/Ti system was studied²⁸ in the copolymerization of ethylene and 1-hexene (Figure 11). These catalysts were found to be 3 times more active than their monometallic Ti analogues. However, it was concluded that polymerization occurs exclusively at the Ti center and the WN₂ fragment was simply a special metalloligands that influences the electronic properties or chloride lability at titanium.

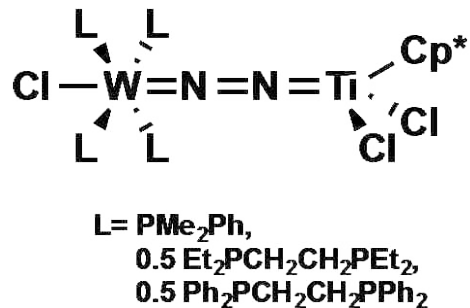
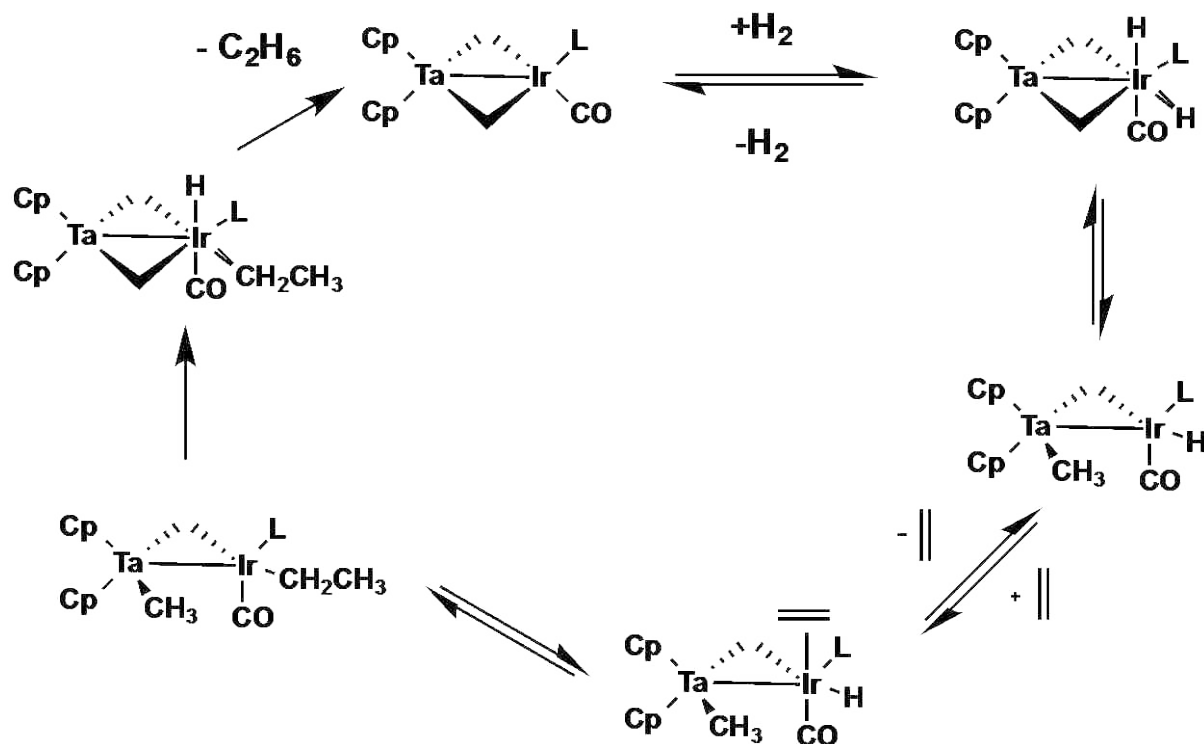


Figure 11: Olefin Polymerization catalysts

1.4.7 Hydrogenation of Olefins

Ligand effects are also observed in the catalytic hydrogenation of olefins as reported by the Bergman group.²⁹ The catalyst features a tantalum-iridium interaction in which the hydrogen adds oxidatively to the iridium and is followed by the insertion of hydrogen into the bridging methyl group, opening a coordination site in which the alkene may associate. The hydrogen on iridium then inserts into the M—C bond and the hydrogen in the ligand system re-associates to the iridium and reductively eliminates with the alkane (Scheme 7). The authors suggest that the Ta-Ir bond remains intact throughout the reaction and the Ta serves as a special ligand in stabilizing the reductive elimination in formation of the methyl group.



Scheme 7 Proposed catalytic cycle for hydrogenation of olefins using Ta/Ir catalysts

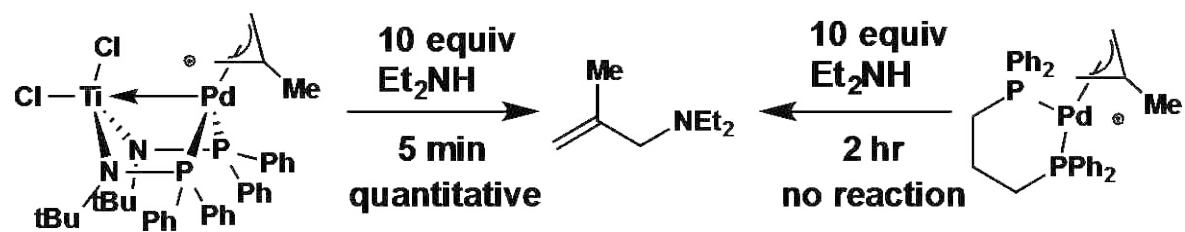
The Ess group recently reported³⁰ the mechanism and significance of the heterobimetallic interaction in the hydrogenation of alkenes using a Ir/Ta interaction linked by methyl groups, as reported by the Bergman group.²⁹ Through DFT calculations, they determined that the mechanism for hydrogenation. It begins with H₂ oxidatively adding to the Ir, followed by reductive elimination of a hydrogen and one of the bridging methyl groups. The electron withdrawing properties of the nearby TaCp₂ facilitates the synthesis of this precatalyst.

1.5 ELECTRONIC TUNING USING A SECOND METAL

Much of the research done with respect to early/late heterobimetallic complexes shows the alteration of redox properties of the individual metal centers. The systems described in the following section exploit the altered redox activity of the complexes to enable fast catalysis through a dative interaction between the two metals.

1.5.1 Allylic Amination

The Nagashima group reports the catalytic activity of a Pd-Ti interaction linked by phosphonamide bridges (Scheme 8). They proposed that the dative interaction between the electron-rich palladium and the electron-deficient titanium facilitates fast catalysis. The monometallic Pd catalyst used as a control exhibits no reaction while the Pd-Ti catalysts took the reaction to completion within 5 minutes at room temperature.³¹



Scheme 8 Catalytic activity as facilitated by Pd-Ti interaction vs monometallic analogue

The Michaelis group continued studies of this complex in order to better understand the nature of the fast catalysis observed. Their studies showed that monometallic analogues were similarly effective in these aminations with diethylamine, however, the electronic donation from Pd to Ti was found to be essential to catalyze aminations of more sterically

hindered amines.³² The results of these studies will be extensively discussed in chapters 2 and 3 of this work.

1.5.2 Polymerization of Olefins

The Suzuki group³³ reported an interesting usage of heterobimetallic complexes in the polymerization of olefins. The catalyst used was a Rh/Zr system, however the metals were over 6 Å apart (Figure 12). Despite the large distance, they observed a significant impact on catalytic rates compared to zirconocene or a mixture of monometallic Zr and monometallic Rh complexes. They also reported higher polymer weights with the heterobimetallic catalysts. Through cyclic voltammetry studies, they determined that the Rh in the system is donating a significant amount of electron density through the ligand system to zirconium. They concluded that this increased electron donation causes the enhanced catalysis.

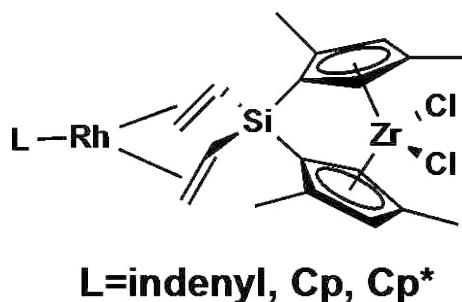


Figure 12: Olefin Polymerization Catalyst

1.5.3 Metal Carbenoid Transformations

The Davies group³⁴ reports the synthesis and catalytic application of a Bi/Rh paddlewheel complex and its catalytic applications. They found that these complexes were able to effectively carry out cyclopropanation reactions, similar to the Rh-Rh analogues, as well as C-H insertion processes. They also catalyzed reactions involving zwitterionic intermediates with diazo compounds. It was found that the heterobimetallic complexes displayed similar chemoselectivity and stereoselectivity as di-rhodium analogues. In the decomposition of methyl phenyldiazoacetate, the di-rhodium catalyst was actually significantly more efficient than the heterobimetallic Rh/Bi system. A charge distribution analysis reveals that the Rh-Bi core acts as an “electron pool” capable of facilitating processes similar to its di-rhodium analogue.

1.6 CONCLUSION AND OUTLOOK

In summary, early/late heterobimetallic complexes have been studied in various reactions and in the many cases, the intermetallic interaction was found to enable fast catalysis. The dative interaction between the electron-rich late transition metal and the electron-deficient early transition metal alters the redox activity at each metal and thereby alters the reactivity of the complex. In some cases, the polarized environment is capable of activating small molecule substrates, provided that the ligand structure does not interfere. In other cases, the metals work cooperatively to facilitate reductive or ring opening processes otherwise unachievable by monometallic substrates. Additionally, the second metal can also act as a ligand and facilitate reaction by simply altering the ligand environment or reaction mechanism. In a few reported cases, the heterobimetallic systems

were less active than monometallic systems. However, in many systems, catalysis was improved by the addition of a second metal to the catalyst. Because of the variable roles that each metal plays in these reactions, further investigation is warranted in order to better understand their potential and apply it to previously unattainable or difficult reactions.

1.7 REFERENCES

- 1) Zhang, Y.; Roberts, S. P.; Bergman, R. G.; Ess, D. H. *ACS Catal.* **2015**, *5*, 1840
- 2) Thomas, C. Metal-Metal Multiple Bonds in Early/Late Heterobimetallic Complexes: Applications Toward Small Molecule Activation and Catalysis. *Comments on Inorganic Chemistry.* **2011**, *32*, 14-38.
- 3) Cooper, B. G.; Napoline, J. W.; Thomas, C. M. *Catal. Rev. Sci. Eng.* **2012**, *54*, 1.
- 4) Tauster, S.J.; Fung, S.C.; Garten, R.L. Strong Metal-Support Interactions. Group 8 Noble Metals Supported on Titanium Dioxide. *J. Am. Chem. Soc.* **1978**, *100*, 170-175
- 5) Morgan, J.P.; Kundu, K.; Doyle, M.P. A Readily Prepared Neutral Heterobimetallic Titanium(IV)- Rhodium(I) Catalyst for Intramolecular Hydroacylation. *Chem Commun.* **2005**, 3307-3309.
- 6) Casey, C. P.; Palermo, R. E.; Jordan, R. F.; Rheingold, A. L.; *J. Am. Chem. Soc.* **1985**, *107* (15), 4597-4599.
- 7) Bosch, B.E.; Brummer, I; Kunz, K; Erker, G.; Frolich, R.; Kotila, S. Structural Characterization of Heterodimetallic Zr/Pd and Zr/Rh Catalyst Precursors Containing the C₅H₄PPH₂ Ligand. *Organometallics*, **2000**, *19*, 1255-1261.
- 8) Kuwabara, J.; Takeuchi, D.; Osakada, K. Early-Late Heterobimetallic Complexes as Initiator for Ethylene Polymerization. Cooperative Effect of Two Metal Centers to Arrod Highly Branched Polyethylene *Chem. Commun.* **2006**, 3815- 3817.
- 9) Kuwabara, J.; Takeuchi, D.; Osakada, K. Early-Late Heterobimetallic Complexes as Initiator for Ethylene Polymerization. Cooperative Effect of Two Metal Centers to Arrod Highly Branched Polyethylene *Chem. Commun.* **2006**, 3815- 3817.

- 10) Kato, H.; Seino, H.; Mizobe, Y.; Hidai, M. Synthesis and Reactivities of Hydrosulfido-or Sulfido-Bridged Heterobimetallic Complexes Containing Group 6 and Group 9 Metals. *Dalton Trans.* **2002**, 1494-1499
- 11) Leeasubcharoen, S.; Zhizhiko, P.A.; Kuzmina, L.G.; Churakov, A.V.; Howard, J.A.K.; Nikonov, G.I. Niobium/Rhodium Bimetallic Complexes: Synthesis, Structure and Catalytic Hydrosilylation of Acetophenone and Benzaldehyde. *Organometallics*, **2009**, 28, 4500-4506.
- 12) Hanna, T.A.; Baranger, A.M.; Bergman, R.G. Reaction of Carbon Dioxide and Heterocumulenes with an Unsymmetrical Metal-Metal Bond. Direct Addition of Carbon Dioxide across a Zirconium-Iridium Bond and Stoichiometric Reduction of Carbon Dioxide to Formate. *J. Am. Chem. Soc.* **1995**, 117 (45), 11363-11364.
- 13) Pinkes, J.R.; Steffey, B. D.; Vites, J.C.; Cutler, A.R. Carbon Dioxide Insertion into the Fe-Zr and RuZr Bonds of the Heterobimetallic Complexes Cp(CO)₂M-Zr(Cl)Cp₂; Direct Production of the $\mu - \eta^1(C): \eta^2(O,O')$ -Co₂ Compounds Cp(CO)₂M-CO₂-Zr(Cl)Cp₂ *Organometallics* **1994**, 13 (1), 21-23.
- 14) Memmler, H.; Kauper, U.; Gade, L. H.; Scowen, I.J.; McParlin, M. Insertion of X=C=Y Heteroallenes into Unsupported Zr-M Bonds (M=Fe, Ru). *Chem Commun.* **1996**, (15), 1751-1752
- 15) Jayarathne, U.; Mazzacano, T.; Bagherzadeh, S.; Mankad, N. Heterobimetallic OComplexes with Polar, Unsupported Cu-Fe and Zn-Fe Bonds Stabilized by N-Heterocyclic Carbenes *Organometallics* **2013**, 32, 3986-3992
- 16) Miyazaki, T.; Tanabe, Y.; Yuki, M.; Miyake, Y.; Nishibayashi, Y. Synthesis of Group IV(Zr, Hf)- Group VIII (Fe, Ru) Heterobimetallic Complexes Bearing Metallocenyl

Diphosphine Moieties and Their Application to Catalytic Dehydrogenation of Amine-Boranes. *Organometallics* **2011**, 30, 2394-2404.

17) Bosch, B.E.; Brummer, I; Kunz, K; Erker, G.; Frolich, R.; Kotila, S. Structural Characterization of Heterodimetallic Zr/Pd and Zr/Rh Catalyst Precursors Containing the C₅H₄PPH₂ Ligand. *Organometallics*, **2000**, 19, 1255-1261.

18) Man, M.L.; Zhou, Z.Y.; Ng, S.M.; Lau, C.P. Synthesis, Characterization and Reactivity of Heterbimetallic Complexes. *Dalton Trans.* **2003**, 3727-3735.

19) Ye, S.; Leong, W.K. Synthesis and Structure of Some Ruthenium-Rhenium Heterodinuclear Complexes and Their Catalytic Activity in the Addition of Carboxylic Acids to Phenylacetylene. *J. Organomet. Chem.* **2006**, 691, 1216- 1222.

20) Slaughter, L.M; Wlaczanski, *Chem Commun.* **1997**, 2109-2110.

21) Wheatley, N.; Kalck, P. Structure and Reactivity of Early-Late Heterobimetallic Complexes. *Chem Rev.* **1999**, 99 (12), 3379-3420.

22) Kuwabara, J.; Takeuchi, D.; Osakada, K. Early-Late Heterobimetallic Complexes as Initiator for Ethylene Polymerization. Cooperative Effect of Two Metal Centers to Arrod Highly Branched Polyethylene *Chem. Commun.* **2006**, 3815- 3817.

23) Zhou, W.; Napoline, J.W.; Thomas, C.M. A Catalytic Application of Co/Zr Heterobimetallic Complexes : Kumada Coupling of Unactivated Alkyl Halides with AlkylGrignard Reagents. *Eur. J. Inorg. Chem.* **2011**, 2011, 2029-2033.

24) Fandos, R.; Hernandez, C; Otero, A.; Rodriguez,A.; Ruiz, M.J.; Terroros, P. Early-Late Heterbimetallic Alkoxides as model Systems for Late-Transition Metal Catalysts Supported on Titania. *Chem. Eur. J.* **2003**, 9, 671-677.

- 25) Man, M.L.; Zhou, Z.Y.; Ng, S.M.; Lau, C.P. Synthesis, Characterization and Reactivity of Heterbimetallic Complexes. *Dalton Trans.* **2003**, 3727-3735.
- 26) Braunstein, P.; Durand, J.; Morise, X.; Tiripichio, A.; Ugozzoli, F.; Catalytic Dehydrogenative Coupling of Stannanes by Alkoxysilyl Heterobimetallic Complexes: Influed of the Assembling Ligand. *Organometallics* **2000**, 19, 444- 450.
- 27) Nakata, N.; Sakashite, M.; Komatsubara, C; Ishii, A. Snthesis, Strucutre and Catalytic Activity of Bimetallic Pt-II-Ir-III Complexes Bridged by Cyclooctane- 1,2-Dithiolato Ligands. *Eur. J. Inorg. Chem.* **2010**, 447-453.
- 28) Ishino, H.; Takemoto, S.; Hirate, K.; Kanaizuka, Y.; Hidai, M.; Nabika, M.; Seki, Y.; Miyatkae, T.; Suzuki, N. Preparation and Properties of Molybdenum and Tungsten Dinitrogen Complexes. Part 72. Olefin Polymerization Catalyzed by Titanium-Tungsten Dinitrogen Complexes. *Organometallics.* **2004** 23, 4544, 4544-2446.
- 29) Hostetler, M.J.; Butts, M.D.; Bergman, R.G. Scope and Mechanism of Alkene Hydrogenation/Isomerization Catalyzed by Complexes of the Type $R_2E(CH_2)_2M(CO)(L)$ (R=Cp, Me, Ph; E= Phosphorous, Tantalum; M= Rhodium, Iridium; L=CO, PPH₃). *J Am. Chem. Soc.* **1993**, 115, 2743-2752.
- 30) Braunstein, P.; Durand, J.; Morise, X.; Tiripichio, A.; Ugozzoli, F.; Catalytic Dehydrogenative Coupling of Stannanes by Alkoxysilyl Heterobimetallic Complexes: Influed of the Assembling Ligand. *Organometallics* **2000**, 19, 444- 450.
- 31) Tsutsumi, H.; Sunada, Y.; Shiota, Y.; Yoshizawa, K.; Nagashima, H. *Organometallics*, **2009**, 28, 1988.

- 32) Walker, W. K.; Anderson, D. L.; Stokes, R. W.; Smith, S. J.; Michaelis, D. J. *Org. Lett.* **2015**, 17, 752.
- 33) Takayama, C.; Yamaguchi, Y.; Mise, T.; Suzuki, N. Electronic Effects in Homogenous Ziegler-Natta Catalysts: Zr/Rh Early/Late Heterobimetallic Complexes. *Dalton Trans.* **2001**, 948-953
- 34) Hansen, J.; Li, B.; Dikarev, E.; Autschbach, J.; Davies, H.; Combined Experimental and Computation Studies of Heterobimetallic Bi-Rh Paddlewheel Carboxylates as Catalysis for Metal Carbenoid Transformations. *J. Org. Chem.* **2009**, 74, 6564-6571

Chapter 2

Heterobimetallic Pd–Ti Complexes for Fast Catalysis In Allylic Amination Reactions

2.1 INTRODUCTION

Heterobimetallic transition metal complexes present a unique approach to catalyst development where the rate of catalysis can be influenced through direct metal–metal communication. Having two electronically disparate metals in close proximity allows them to influence one another through formation of a dative bonding interaction, thereby alter the electronic properties of the catalytically active metal. It has been shown that early/late transition metal heterobimetallic complexes can form particularly strong metal–metal interactions in which the late, electron-rich metal donates electron density to the early, electron-deficient metal. However, it has not been shown whether this metal–metal electronic communication provides electronic tuning of the active catalyst that is unattainable using exclusively organic ligands.¹ In spite of a recent surge² in the design and synthesis of heterobimetallic complexes, there are few catalytic applications reported that take advantage of metal–metal communication in catalysts known to form dative M–M bonds.^{1a} We have sought to better understand these dative interactions in early/late heterobimetallic complexes and exploit them in catalytic applications where the metal–metal bond can facilitate fast or novel catalysis unachievable with monometallic catalysts. In this chapter, we will discuss our efforts to develop heterobimetallic catalysts capable of

fast catalysis in allylic amination reactions with traditionally unreactive hindered secondary amine substrates.

Basic, *N*-alkyl substituted amines are an important structure in bioactive molecules, and over 30% of the top 200 drugs (by US sales in 2012) contain a basic nitrogen group.¹³ However, amines in this class are notoriously challenging to synthesize and manipulate in organic synthesis due to their high basicity and low nucleophilicity, as well as their potential to bind to and deactivate transition metal catalysts. Yet, strategies to incorporate hindered, *N*-alkyl secondary amines via direct C–N bond formation could provide a more direct synthetic strategy to drug molecules and minimize the use of protecting groups in synthesis. We hypothesized that heterobimetallic Pd–Ti complexes could enable reactions with hindered amine nucleophiles in Pd-catalyzed allylic aminations by creating exceptionally electrophilic Pd catalysts that accelerate the addition of amine nucleophiles

In 2006, the Nagashima group reported the use of a Pd–Ti heterobimetallic complex in the allylic amination of methallyl chloride with diethylamine. This complex relies on a phosphoramidate scaffold to bring the palladium and titanium into close proximity (2.7 Å), which enables formation of a dative Pd–Ti bond. In their study, they found that addition of diethyl amine to complex **1** proceeded to completion within 5 minutes at room temperature (Figure 1). To further substantiate the significance of their findings, they synthesized a monometallic palladium analogue and found that it yielded no product even after two hours. The authors hypothesized that the palladium was forming a dative interaction with the titanium in which the titanium accepts electrons from the palladium, causing it to

become more electrophilic. And it is this dative interaction that enables the fast catalysis by accelerating the rate of the turnover-limiting reduction amine addition step.

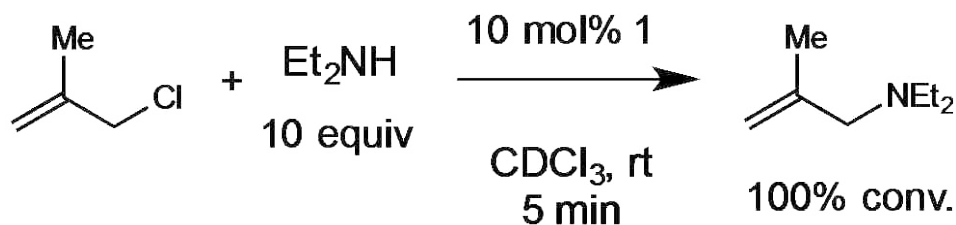


Figure 1. Stoichiometric allylic amination with heterobimetallic complex **1**.

Inspired by their findings, our group wondered whether these Pd–Ti catalysts could achieve reactivity that is inaccessible using traditional ligands in palladium catalysis and thus expand the classes of nucleophiles that undergo catalysis in allylic amination reactions. We first investigated the catalytic activity of the heterobimetallic complex **1** in the allylic amination of methallyl chloride using a sterically hindered secondary amine (Figure 2). Next, we conducted experiments involving several Pd monometallic analogues in order to verify the impact and importance of the M–M interaction to catalysis in allylic aminations. We then demonstrated that the heterobimetallic catalyst could be assembled in situ from a titanium-containing ligand, precluding the need to synthesize and isolate the discrete bimetallic complex. We also synthesized additional titanium-containing ligands and tested their catalytic applications in the allylic amination reaction. Lastly, we examined the substrate scope of the heterobimetallic catalyst by varying the structure of

both the amine and the allylic chloride substrates. The specific details of these pursuits are described below.

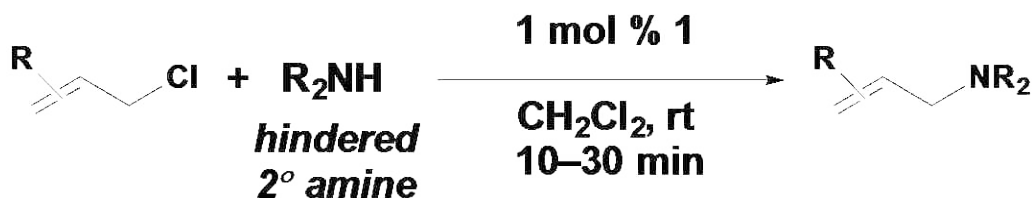


Figure 2. Allylic amination of hindered amines using heterobimetallic complex **1** (data collected with Whitney Walker)

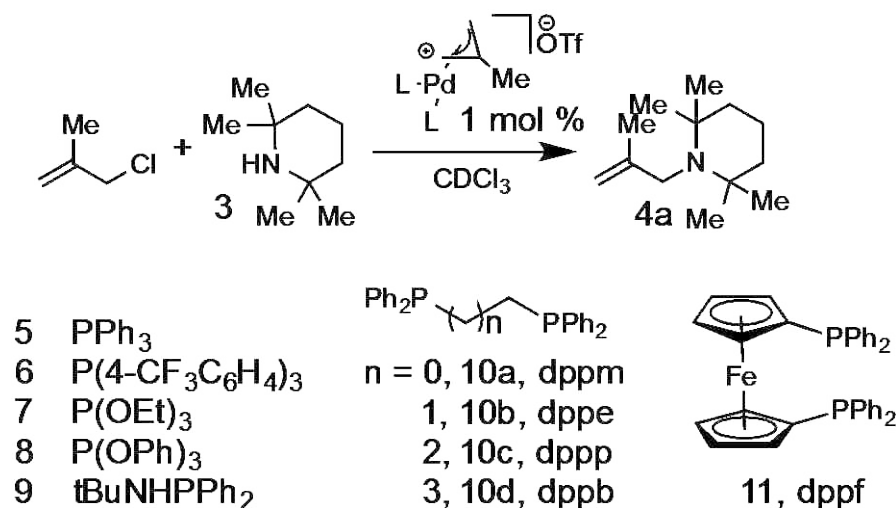
2.2 RESULTS AND DISCUSSION

2.2.1 Optimization of Allylic Amination using Hindered Amine

We first investigated the ability of heterobimetallic catalyst **1** to enable allylic aminations with traditionally unreactive hindered secondary amine nucleophiles. We found that the reaction of 2,2,6,6-tetramethylpiperidine **3** (TMP) with methallyl chloride proceeded at room temperature to provide quantitative yield of the amination product in just 35 minutes (Table 1, entry 1). Remarkably, this reaction proceeds with just 1 mol% catalyst loading. To show the significance of this result, we next performed the allylic amination with several reported monometallic palladium catalysts. When triphenylphosphine (**6**) was used as a ligand for palladium, no reaction was observed, even after 24 hours (entry 2). When this reaction was heated to 90 °C, a small amount of product was observed (entry 3). We next explored the reactivity of palladium complexes containing a variety of monodentate phosphine ligands (entries 4–7), as well as bidentate ligand structures (entries 8–12). Only the triphenylphosphite ligand (**8**) provided any reasonable levels of product formation, yet required elevated temperatures and a long reaction time. Importantly, the phosphinoamide

ligand lacking the titanium center (**9**) failed to provide significant levels of product formation, confirming the importance of the titanium to catalysis. The findings of this study substantiate our hypothesis: the heterobimetallic catalyst was much more efficient in catalyzing the allylic amination of sterically hindered secondary amines than traditional palladium catalysts.

Table 1 : Optimization Studies on Allylic Aminations with **3**



entry ^a	ligand	temp	time	% conv ^b
1 ^c	1	rt	35 min	100
2	5	rt	24 h	N.R.
3	5	90°C	24 h	7
4	6	90°C	24 h	6
5	7	90°C	10 h	14
6	8	90°C	24 h	67
7	9	90°C	24 h	<5
8	10a	90°C	24 h	11
9	10b	90°C	24 h	<5
10	10c	90°C	24 h	<5
11	10d	90°C	24 h	<5
12	11	90°C	24 h	<5

^aReactions performed using 1 mmol of methallyl chloride, 2.2equiv. of **3**, and 0.05 mmol of the indicated allyl complex formed *in situ* (0.025 mmol $[\text{Pd}(\text{methallyl})\text{Cl}]_2$, 0.05 mmol of AgOtf , and either 0.05 mmol of bisphosphine or 0.10 mmol of monophosphine) in CDCl_3 (1M) for the indicated time. ^bDetermined by

¹HNMR. ^cRun with 1 mol % of preformed complex **1**

2.2.2 *In Situ* formation of Catalyst

We next performed several control experiments to verify that the phosphonamide ligand scaffold was necessary to assemble the Pd–Ti interaction. As discussed above, no reaction proceeds when phosphinoamide ligand **9** is employed in the absence of titanium. If titanium tetrachloride is added to the reaction with ligand **9**, no conversion is observed after 24 h. When titanium tetrachloride was added to the reaction with phosphite ligand **9**, ~20 % conversion to product was observed after 24 hrs. These results suggest that the titanium-phosphinoamide ligand structure is uniquely capable of scaffolding the Pd–Ti interaction, which is essential for catalysis to occur in this system.

We next explored the possibility of forming the heterobimetallic complex *in situ* from titanium-containing ligand **2** (Figure 3). Such a finding would greatly simplify the process of using this catalyst by eliminating the need for prior synthesis and purification of the catalyst. Preformation of the catalyst was accomplished by mixing 0.5 mol % [Pd(methallyl)Cl]₂ and 1 mol % of silver triflate and 1 mol % of the titanium-containing ligand in CDCl₃. ¹H and ³¹P NMR confirmed that formation of the heterobimetallic complex had occurred in the solution. We then added the substrates and found that within 20 minutes, the reaction had gone to 99% completion at room temperature. This result confirms that the catalyst can self-assemble under reaction conditions and retain reactivity. The titanium-containing ligand used in this study was readily synthesized using air-free Schlenk line techniques as reported in the literature.²¹ Because it is stable in the solid state, it can easily be used on the bench-top, eliminating the need for a glovebox, provided it is stored under argon and solvents and reagents are dried prior to reaction.

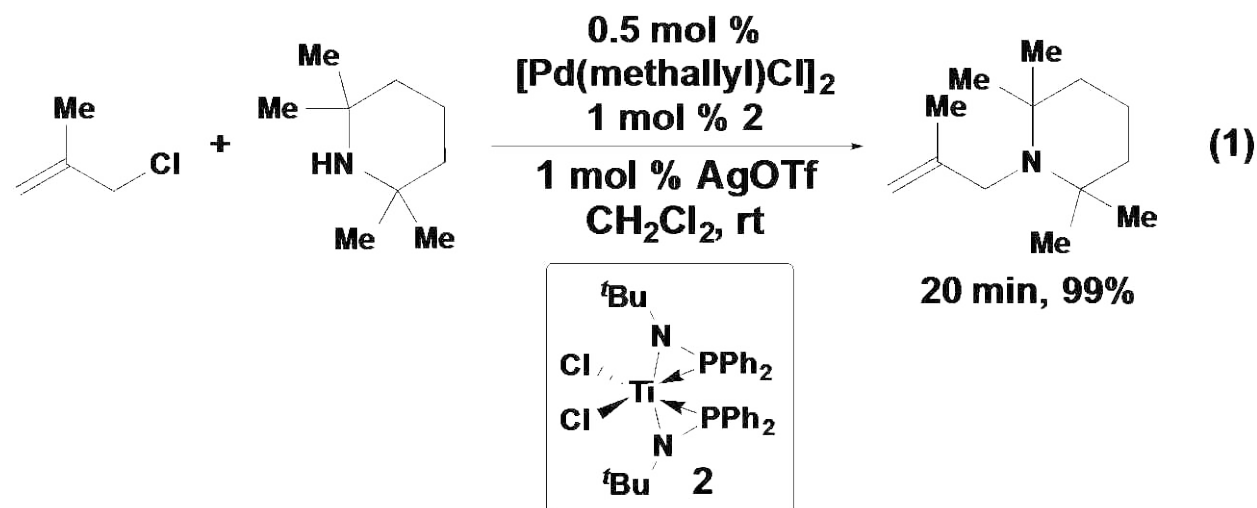


Figure 3. *In situ* formation of catalyst using titanium-containing ligand

(experiments conducted with Ryjul Stokes)

2.2.3 Synthesis and Reactions of Metal Containing Ligands

Our next experiment was designed to test the impact of the structure of the Ti- ligand on catalysis. We synthesized complexes **12** and **13** by careful manipulation of the reaction conditions and stoichiometries used in the reaction for the formation of **2**. These ligands are the first of their kind reported and their structure was confirmed by single crystal X-ray analysis (Figure 4).

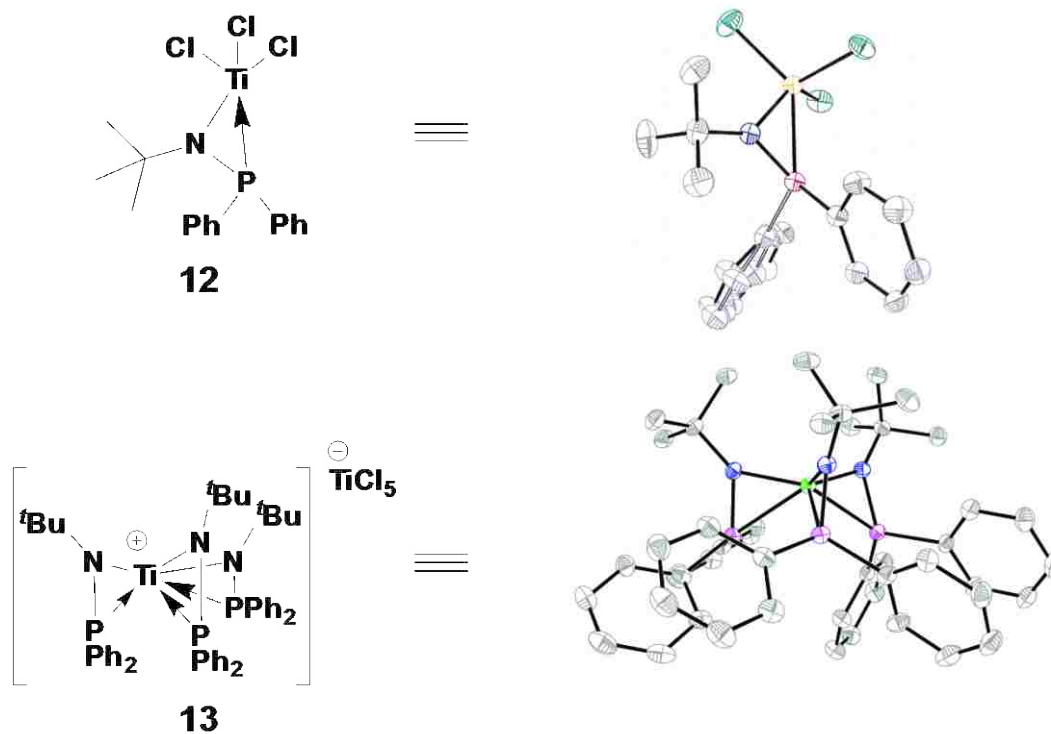


Figure 4: Novel titanium-containing ligands

(Ligands synthesized with Ryjul Stokes and Michael Talley, Crystallography by Stacey Smith)

Phosphinoamide ligands in this class are known to contain a dynamic titanium-phosphorous bond, which can sever, enabling coordination of a late transition metal to the phosphine ligand, and assembly of the metal–metal dative bond.¹¹ With this result in mind, we added $[\text{Pd}(\text{methallyl})\text{Cl}]_2$ and AgOTf to the ligand **12** and monitored the reaction using ^{31}P NMR. The spectra showed the peak corresponding to the starting material (-11.0 ppm) disappear as a new peak appeared at -2.6ppm, corresponding to a Pd-P bond. Although we have not yet been successful in isolating the heterobimetallic complexes with **12** and **13**, we believed that these preliminary results provided strong evidence that such ligands can

be used to form catalytically active heterobimetallic complexes *in situ*. Therefore, we used ligand **12** and **13** in the allylic amination with TMP, methallyl chloride, and $[\text{Pd}(\text{methallyl})\text{Cl}]_2$ and found that both ligands provided quantitative yields of the amination product after ~2.5 h (Figure 5). To date, no monometallic catalysts have been able to catalyze this reaction at room temperature. This result further substantiates our claim that these metalloligands are exceptionally useful in enabling fast catalysis in these systems. The dative interaction formed between the two electronically disparate metals allows for electron density to transfer from the Pd to the Ti and thereby create a more electrophilic and catalytically active palladium center.

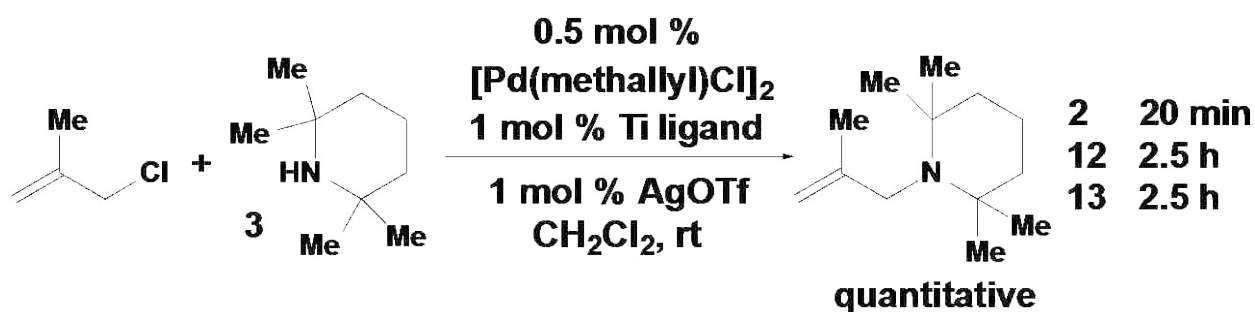


Figure 5: Aminations with titanium-containing ligands

(Reactions performed with Ryjul Stokes and Michael Talley)

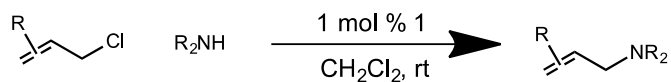
2.2.4 Reaction with Hindered Amin Nucleophiles

To conclude our studies of this system, we examined the substrate scope of the allylic amination with a variety of hindered amine nucleophiles (Table 2). We first tested a variety of amines in the reaction methallyl chloride (entries 1–7). We chose to use a variety of sterically hindered secondary amines as these have historically been very challenging substrates in this type of reaction. In all cases, the reaction proceeded to completion in

around 10 minutes at room temperature. Even the exceptionally hindered bis(trimethylsilyl)amine underwent allylic substitution in 4.5 hours at room temperature. However, the *tert*-amyl-*tert*-butylamine produced less than 5% yield, making it the only substrate tested that failed to provide decent results. We also varied the allylic electrophiles to test the scope of electrophiles subject to reaction in this system. Crotyl, cinnamyl and allyl chlorides (Entries 8-10) reacted in high yields. However allyl acetates and carbonates did not provide high conversions. We attributed this lowering in reactivity to the formation of Lewis basic acetate or alkoxide ions, which resulted in decomposition of the Pd-Ti catalyst.

2.2.5 Intramolecular Cyclizations

Lastly, we varied the amine substrate in order to investigate the catalyst's potential to enable intramolecular cyclizations to form cyclic products. If successful, this would enable the synthesis of piperidine and pyrrolidine derivatives, which are important structures in many natural products and pharmaceuticals. The challenge is that these kinds of cyclizations with hindered amines often require harsh reaction conditions to force the reaction to take place, and in some cases they still fail to react altogether. However, using 3 mol % of catalyst **1**, we observed that these substrates would undergo cyclization at room temperature in under 10 minutes (Figure 6).

Table 2: Substrate Scope with Hindered Amines

entry ^a	amine	chloride	4	yield ^b
1 ^c			4a	99%
2			4b	72%
3			4c	98%
4			4e	99%
5			4f	82%
6 ^d			4g	99% ^e
7			4h	<5%
8 ^c			4i	97% ^{f,g}
9 ^c			4j	87% ^f
10 ^c			4j	85%
11 ^d			4j	5% ^e
12 ^d			4i	33% ^e
13 ^c			4h	78% ^{f,h}

^aReactions run with 1 mmol of allyl chloride, 2.2 mmol of amine, and 0.01 mmol of **1** (or 0.005 mmol of [Pd(methallyl)Cl]₂, 0.01 mmol of **2**, and 0.01 mmol of AgOTf) in CDCl₃ or CH₂Cl₂ (1M) for 10 minutes at room temperature. ^bIsolated yields. ^cRun for 20 minutes. ^dRun for 4.5 h. ^eInternal standard yield. ^fLinear product only. ^g5:1 *trans/cis*. ^h1.3:1 *trans/cis*. c-hex=cyclohexyl (Chloride reactions by Whitney Walker)

The cyclization reaction occurred to form both 5- and 6-membered heterocycles (**14** and **15** respectively) in good yield. We were also able to synthesize morpholine heterocycles (**16**) using this method.

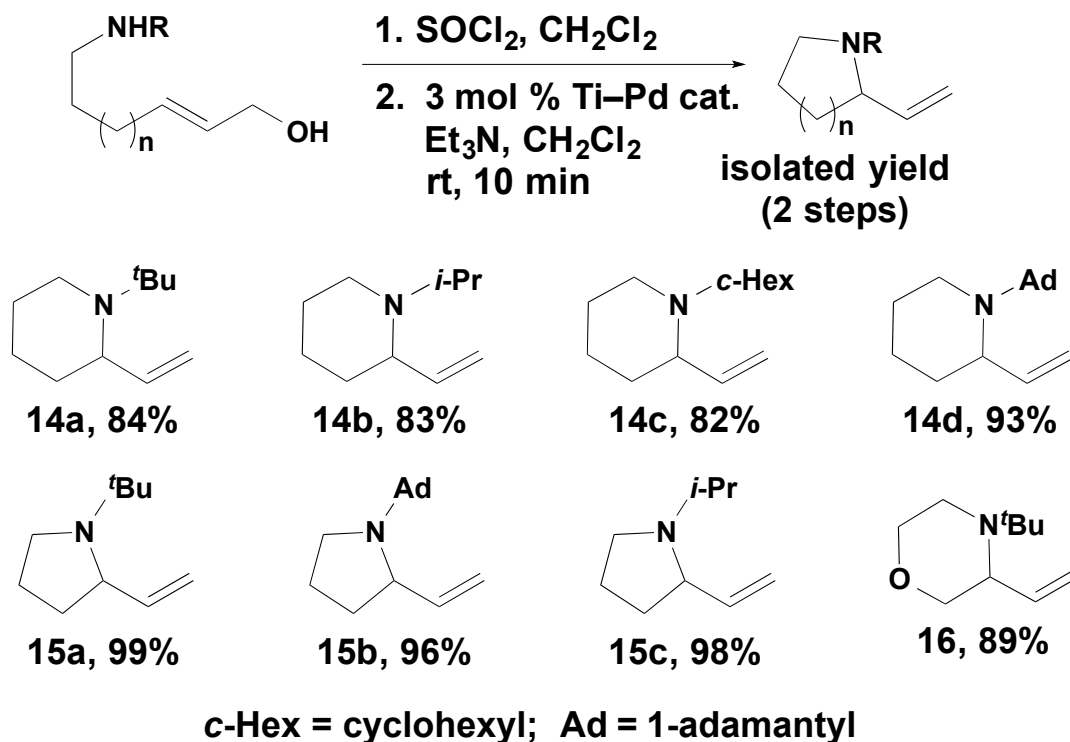


Figure 6: Intramolecular aminations for heterocycle synthesis (with Whitney Walker)

2.3 CONCLUSION

Through these experiments, we concluded that the Pd-Ti heterobimetallic complex proved to be far superior in catalyzing the allylic amination of secondary hindered amines as compared to monometallic palladium catalysts. These types reactions were previously challenging, but the use of a heterobimetallic complex proved to be successful. And even though synthesizing and purifying such complexes can be challenging, often requiring

stringent air-free conditions, we showed that the catalyst could be prepared *in situ*, precluding the need to synthesize and isolate the heterobimetallic complex. This *in situ* catalyst formation strategy was shown to enable fast catalysis with a range of titanium-containing ligands synthesized for the first time in our laboratory. To further demonstrate the utility of this heterobimetallic complex, we explored the substrate scope by varying independently the amine and the allylic electrophile and found nearly all to give moderate to high yields, confirming the versatility of the reactions the complex is able to catalyze. Additionally, we investigated the catalyst's potential to form highly utilized heterocyclic products via intramolecular cyclizations and found them to be successful in these systems as well. These results confirm the potential of metal-metal interactions in heterobimetallic complexes to facilitate unique reactivity in organic synthesis and it is our hope that these principles can guide future catalyst design so that others may tap into the potential that heterobimetallic catalysts have to offer.

2.4 REFERENCES

(1) For reviews, see:

- (a) Cooper, B. G.; Napoline, J. W.; Thomas, C. W. *Catal. Rev.* **2012**, 54, 1.
- (b) Oelkers, B.; Butovskii, M. V.; Kempe, R. *Chem. Eur. J.* **2012**, 18, 13566.
- (c) Mandal, S. K.; Roesky, H. W. *Acc. Chem. Res.* **2010**, 43, 248.
- (d) Ritleng, V.; Chetcuti, M. J. *Chem. Rev.* **2007**, 107, 797.
- (e) Collman, J. P.; Boulatav, R. *Angew. Chem., Int. Ed.* **2002**, 41, 3948.
- (f) Gade, L. H. *Angew. Chem., Int. Ed.* **2000**, 39, 2658.
- (g) Wheatley, N.; Kalck, P. *Chem. Rev.* **1999**, 99, 3379.

(2) For selected recent examples, see:

- (a) Tereniak, S. J.; Carlson, R. K.; Clouston, L. J.; Young, V. G., Jr.; Bill, E.; Maurice, R.; Chen, Y.-S.; Kim, H. J.; Gagliardi, L.; Lu, C. C. *J. Am. Chem. Soc.* **2014**, 136, 1842.
- (b) Clouston, L. J.; Siedschlag, R. B.; Rudd, P. A.; Planas, N.; Hu, S.; Miller, A. D.; Gagliardi, L.; Lu, C. C. *J. Am. Chem. Soc.* **2013**, 135, 13142.
- (c) Cooper, B. G.; Fafard, C. M.; Foxman, B. M.; Thomas, C. M. *Organometallics* **2010**, 29, 5179.
- (d) Greenwood, B. P.; Forman, S. I.; Rowe, G. T.; Chen, C.-H.; Foxman, B. M.; Thomas, C. M. *Inorg. Chem.* **2009**, 48, 6251.
- (e) Nippe, M.; Berry, J. F. *J. Am. Chem. Soc.* **2007**, 129, 12684.
- (f) Nagashima, H.; Sue, T.; Oda, T.; Kanemitsu, A.; Matsumoto, T.; Motoyama, Y.; Sunada, Y. *Organometallics* **2006**, 25, 1987.

(3) (a) Bariwal, J.; Van der Eycken, E. *Chem. Soc. Rev.* **2013**, 42, 9283.

- (b) *Science of Synthesis, Cross Coupling and Heck-Type Reactions*, Vol. 2; Molander, G. A., Wolfe, J. P., Larhed, M., Eds.; Thieme: Stuttgart, **2013**.
- (c) McDonald, R. I.; Liu, G.; Stahl, S. S. *Chem. Rev.* **2011**, 111, 2981.
- (d) Wolfe, J. P. *Top. Heterocycle. Chem.* **2013**, 32, 1.
- (e) Schultz, D. M.; Wolfe, J. P. *Synthesis* **2012**, 44, 351.
- (4) (a) Trost, B. M.; Lee, C. *In Catalytic Asymmetric Synthesis*, 2nd ed.; Ojima, I., Ed.; Wiley-VCH: New York, **2010**; pp 593–649.
- (b) Dieguez, M.; Pa' mies, O. *Acc. Chem. Res.* **2010**, 43, 312.
- (c) Lu, Z.; Ma, S. *Angew. Chem., Int. Ed.* **2008**, 47, 258.
- (d) Trost, B. M.; Machacek, M. R.; Aponick, A. *Acc. Chem. Res.* **2006**, 39, 747.
- (e) Dai, L.-X.; Tu, T.; You, S.-L.; Deng, W.-P.; Hou, X.-L. *Acc. Chem. Res.* **2003**, 36, 659.
- (f) Helmchen, G.; Pfaltz, A. *Acc. Chem. Res.* **2000**, 33, 336.
- (g) Johannsen, M.; Jørgensen, K. A. *Chem. Rev.* **1998**, 98, 1689.
- (5) (a) Tosatti, P.; Nelson, A.; Marsden, S. P. *Org. Biomol. Chem.* **2012**, 10, 3147.
- (b) Milhau, L.; Guiry, P. J. *Top. Organomet. Chem.* **2011**, 38, 95.
- (c) Hartwig, J. F.; Stanley, L. M. *Acc. Chem. Res.* **2010**, 43, 1461.
- (d) Helmchen, G.; Dahnz, A.; Dü bon, P.; Schelwies, M.; Weihofen, R. *Chem. Commun.* **2007**, 675.
- (e) Helmchen, G. *In Asymmetric Synthesis*; Christman, M., Brase, S., Eds.; Wiley-VHC: Weinheim, **2007**; pp 95–99.
- (f) Miyabe, H.; Takemoto, Y. *Synlett* **2005**, 11, 1641.
- (6) For recent selected examples, see:

- (a) Kawatsura, M.; Terasaki, S.; Minakawa, M.; Hirakawa, T.; Ikeda, K.; Itoh, T. *Org. Lett.* **2014**, 16, 2442.
- (b) Kawatsura, M.; Uchida, K.; Terasaki, S.; Tsuji, H.; Minakawa, M.; Itoh, T. *Org. Lett.* **2014**, 16, 1470.
- (c) Boualy, B.; Harrad, M.; El Houssame, S.; El Firdoussi, L.; Ait Ali, M.; Karim, A. *Catal. Commun.* **2012**, 19, 46.
- (d) Touchet, S.; Carreaux, F.; Molander, G. A.; Carboni, B.; Bouillon, A. *Adv. Synth. Catal.* **2011**, 353, 3391.
- (e) Tosatti, P.; Horn, J.; Campbell, A. J.; House, D.; Nelson, A.; Marsden, S. P. *Adv. Synth. Catal.* **2010**, 352, 3153.
- (f) Defieber, C.; Ariger, M. A.; Moriel, P.; Carreira, E. M. *Angew. Chem., Int. Ed.* **2007**, 46, 3139.
- (g) Roggen, M.; Carreira, E. M. *J. Am. Chem. Soc.* **2010**, 132, 11917.
- (h) Pouy, M. J.; Stanley, L. M.; Hartwig, J. F. *J. Am. Chem. Soc.* **2009**, 131, 11312.
- (i) Adak, L. Chattopadhyay, K.; Ranu, B. C. *J. Org. Chem.* **2009**, 74, 3982.
- (j) Nagano, T.; Kobayashi, S. *J. Am. Chem. Soc.* **2009**, 131, 4200.
- (k) Kawatsura, M.; Ata, F.; Hirakawa, T.; Hayase, S.; Itoh, T. *Tetrahedron Lett.* **2008**, 49, 4873.
- (l) Dubovyk, I.; Watson, I. D. G.; Yudin, A. K. *J. Am. Chem. Soc.* **2007**, 129, 14172.
- (m) Takeuchi, R.; Ue, N.; Tanabe, K.; Yamashita, K.; Shiga, N. *J. Am. Chem. Soc.* **2001**, 123, 9525.
- (7) Tsutsumi, H.; Sunada, Y.; Shiota, Y.; Yoshizawa, K.; Nagashima, H. *Organometallics* **2009**, 28, 1988.

- (8) Cationic bis(triphenylphosphine)(η^3 -allyl)palladium complexes are among the most active catalysts for allylic aminations. See: Canovese, L.; Visentin, F.; Levi, C.; Dolmella, A. *Dalton Trans.* **2011**, 40, 966.
- (9) Silver triflate led to faster reaction kinetics in the in situ formation protocol, but its omission still provided full conversion in 1 h.
- (10) ^{31}P NMR of the in situ formed catalyst solution shows a characteristic shift from -17.2 ppm for ligand 2 to $+9.08$ ppm for complex 1.
- (11) (a) Sue, T.; Sunada, Y.; Nagashima, H. *Eur. J. Inorg. Chem.* **2007**, 2897.
- (b) Kühl, O.; Koch, T.; Somoza, F. B., Jr.; Junk, P. C.; HeyHawkins, E.; Plat, D.; Eisen, M. *S. J. Organomet. Chem.* **2000**, 604, 116.
- (12) Olszewska, B.; Kryczka, B.; Zawisza, A. *Tetrahedron* **2013**, 69, 9551.
- (13) Cbc.arizona.edu,. Top Pharmaceuticals Poster | Njarðarson Group
<http://cbc.arizona.edu/njardarson/group/top-pharmaceuticals-poster> (accessed May 21, 2015).

Chapter 3

Origin of Fast Catalysis in Allylic Amination Reactions Catalyzed by Pd–Ti Heterobimetallic complexes

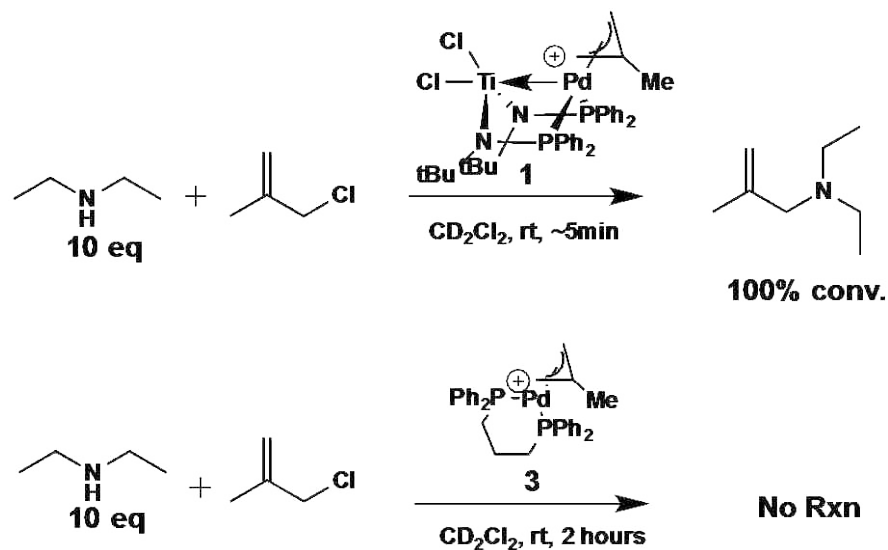
3.1 INTRODUCTION

Heterobimetallic complexes have recently gained much attention for the unique ability of metal–metal communication to alter the electronic properties of the catalytically active metal and influence catalysis. This influence is often achieved by having two electronically disparate metals held in close proximity to each other, allowing the orbitals of each metal to interact.

Although many studies have been conducted with regards to the structure of and bonding in heterobimetallic complexes, there is still a general lack of understanding of how formation of a dative metal-metal interaction can impact catalysis. In continuation of our studies on the allylic amination of allyl chlorides with heterobimetallic Pd–Ti complexes, we sought to better understand and quantify the significance of the Pd–Ti interaction to catalysis. Such understanding could enable the use of heterobimetallic complexes for the design and development of new catalytic processes.

In Nagashima's original report on the reactivity of heterobimetallic complex **1**, the authors demonstrated that the phosphinoamide ligand structure could bring the titanium and palladium centers into close proximity and enable formation of a dative Pd–Ti interaction (Scheme 1). When they tested its catalytic capabilities in the allylic amination of methallyl chloride with diethylamine, they found the reaction went to completion within 5 minutes at

room temperature. They then constructed a control catalyst that lacked the Pd-Ti interaction and found that it yielded no product even after 2 hours under



Scheme 1 A study by Nagashima of allylic aminations using heterobimetallic Pd-Ti complex

the same conditions. This result led them to postulate that the dative interaction between Pd and Ti was responsible for the observed catalysis. However, upon analysis of the control catalyst used, one finds many discrepancies between it and the heterobimetallic complex, some of which may be responsible for the difference in reactivity. These differences include the ligand composition, the geometry and electronic properties of the bidentate phosphine ligand. The heterobimetallic complex **1** has a bidentate phosphonamide scaffold while the control catalyst **3** lacks the amides in the scaffold. Not only does this have implications for the electronics of the backbone of the structure, but the difference in the sterics in complex **3** from the missing *tert*-butyl groups may also impact catalysis.

Additionally, the P-Pd-P angle is different in each of the complexes **1** and **3**, which may also be responsible for enhanced catalytic activity. Due to these discrepancies, we sought to use both experiment and computation to generate a more complete picture of the impact of the Pd-Ti interaction on specific steps in the allylic amination catalytic cycle and its contributions to accelerating catalysis in this system. In so doing, we would be able to better understand the nature of the fast catalysis of the heterobimetallic complex, explore its limitations, and potentially find new applications in which such complexes may be useful.

3.2 RESULTS AND DISCUSSION

3.2.1 A Brief Review of Density Functional Theory

Density functional theory (DFT) provides a quantum-mechanical solution for the electronic structure of atoms and molecules at relatively low computational cost. DFT is usually applied within the Born-Oppenheimer approximation and the Hohenberg and Kohn (HK) postulate provides an avenue for the ground state properties of a many-electron system to be solved using the electron density. The HK theorem allows for the use of functionals of electron density to simplify the many-body N electron problem down to $3N$ spatial coordinates.¹ Density functional theory divides the electronic energy of a system into several terms:

$$E = E^T + E^V + E^J + E^{XC}$$

E^T is the electronic kinetic energy. E^V is the potential energy from nuclear-electron attraction as well as repulsion between nuclei. E^J describes the electron-electron repulsion. E^{XC} is the critical exchange correlation energy. Because the exact exchange-correlation functional is unknown there are several approximations with varying levels of sophistication

and accuracy. For example, the local exchange functional shown below is straightforward, but often very inaccurate:

$$E_{LDA}^X = -\frac{3}{2} \left(\frac{3}{4\pi} \right)^{1/3} \int \rho^{4/3} d^3\mathbf{r}$$

In our study on Pd-Ti heterobimetallic complexes we used the M06 functional. This functional generally performs well for organometallic systems. The M06 functional for exchange is defined as follows:

$$E_X^{M06} = \sum_{\sigma} \int dr [F_{X\sigma}^{PBE}(\rho_{\sigma}, \nabla\rho_{\sigma})f(w_{\sigma}) + \varepsilon_{X\sigma}^{LSDA}h_x(x_{\sigma}, z_{\sigma})]$$

where

$$h_x(x_{\sigma}, z_{\sigma}) = \left(\frac{d_0}{\gamma(x_{\sigma}, z_{\sigma})} + \frac{d_1x_{\sigma}^2 + d_2z_{\sigma}}{\gamma_{\sigma}^2(x_{\sigma}, z_{\sigma})} + \frac{d_3x_{\sigma}^4 + d_4x_{\sigma}^2z_{\sigma} + d_5z_{\sigma}^2}{\gamma_{\sigma}^3(x_{\sigma}, z_{\sigma})} \right)$$

and $F_{X\sigma}^{PBE}(\rho_{\sigma}, \nabla\rho_{\sigma})$ is the exchange density functional of the PBE functional series, $\varepsilon_{X\sigma}^{LSDA}$ is the local spin density approximation for the following:

$$\varepsilon_{X\sigma}^{LSDA} = -3/2 \left(\frac{3}{4\pi} \right)^{1/3} \rho_{\sigma}^{4/3}$$

The $f(w_{\sigma})$ is defined as the spin kinetic-energy density enhancement factor.

In DFT Kohn-Sham molecular orbitals can be expressed as linear combination of one-electron basis functions. Basis functions centered on atomic nuclei, can construct a molecular orbital through:

$$\phi_i = \sum_{\mu=1}^N c_{\mu i} \chi_{\mu}$$

where $c_{\mu i}$ is the molecular orbital expansion coefficient and χ_{μ} refers to an arbitrary basis function. Furthermore, Gaussian-type orbitals follow the general form:

$$g(\alpha, \mathbf{r}) = cx^n y^m z^l e^{-\alpha r^2}$$

where \mathbf{r} is composed of the spatial coordinates x , y , and z ; α is a constant determining the radial extent of the function; and $e^{-\alpha r^2}$ is multiplied by powers of x , y , and z and some normalization constant to satisfy:

$$\int_{all\ space} g^2 = 1$$

Therefore, c is dependent on α , l , m , and n .²

In our study of the Pd-Ti heterobimetallic system geometry optimizations we carried out using the 6-31G(d,p) basis set for all non-metal atoms (small). This basis set includes d functions on all non-metal atoms other than hydrogen and includes p functions on hydrogen atoms. For Pd and Ti we utilized the LANL2DZ basis set. This basis set provides an “effective core potential”.²⁵ Solvent was included using the SMD implicit self-consistent reaction field model for dichloromethane. This provides solvation energy through a continuum dielectric.²⁵ SCF energies were further calculated with the 6-311+G(2d,p)[LANL2TZ] basis set combination $\Delta E_{(large)}$. ΔG values reported correspond to:

$$\Delta G = \Delta E_{(large)} + \Delta G_{solv}(small) + \Delta E_{ZPE}(small) + \Delta H_{(small)} + nRT - T\Delta S_{correction}$$

3.2.2 Computational Assessment of Heterobimetallic Pd-Ti Complex 1 and Mechanism for Allylic Amination

In order to quantify the impact of the metal-metal interaction in heterobimetallic complex **1** on catalysis, we first needed to confirm the mechanism by which the allylic amination was occurring. At the outset, it was unclear whether the heterobimetallic complex followed the established mechanism for palladium-catalyzed allylic aminations, or whether the presence of the second metal enabled a new mechanism. We first used computation to explore several potential mechanisms involving inner-sphere reductive elimination, where the reductive elimination could occur from an amine bound either to titanium or palladium. We also investigated other potential mechanisms, including direct C–Cl bond oxidative insertion, and Lewis acid-catalyzed S_N2 addition. However, we found that the pathway involving outer sphere addition proved to be the lowest in energy. These findings concurred with previous mechanistic studies of Pd and η³-allyl complexes.^{9,10} The mechanism proceeds via an outer-sphere amine addition to the allyl followed by ligand substitution. Subsequent addition of the palladium to the σ* orbital of the C–Cl bond in the allyl chloride re-oxidizes the Pd⁰ to Pd^{II} and regenerates the allyl-palladium intermediate (Figure 1).

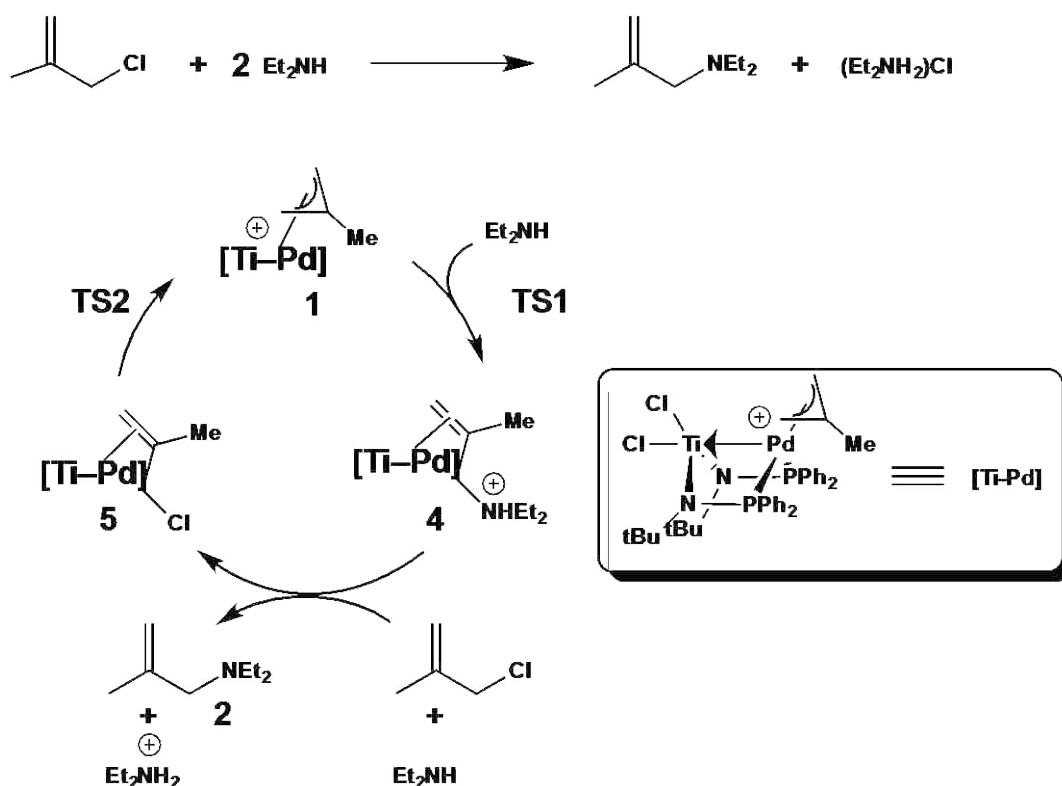
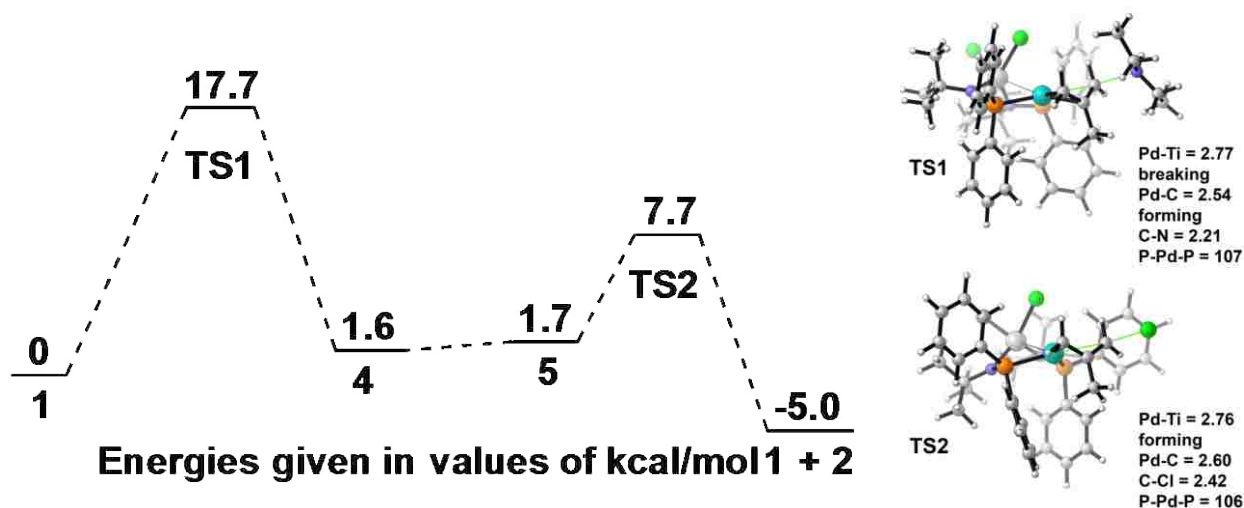


Figure 1: Mechanism for allylic amination catalyzed by **1** (Calculations by Scott Michaelis)

Once the mechanism of the allylic amination with complex **1** was established, we next calculated the free energy required for each step of the cycle and quantitatively analyzed the significance of the Pd-Ti interaction. As described in Figure 1, catalysis initiates with the transition state **TS1** in which the diethylamine nucleophilically attacks the η^3 -allyl at a terminal carbon. This addition reduces Pd^{II} to Pd⁰ and generates complex **4**. This step requires 15.8 kcal/mol and is endergonic by 1.6 kcal/mol, relative to complex **1**, diethylamine and methallyl chloride (Figure 2). It was also observed that as **TS1** proceeded, the Pd-Ti bond distance shortens from 2.88 Å to 2.77 Å, indicating greater interaction between the metals. This observation strongly suggests that stabilization occurs as electron density increases at the palladium during Pd(II) to Pd(0), where titanium is able to form a stronger dative interaction and stabilize the newly forming electron- rich

palladium center. The next step in the catalytic cycle involves replacement of the allyl ammonium intermediate by the methallyl chloride. Our calculations showed this step to be thermoneutral. The active catalyst **1** is then regenerated as the Pd(0) undergoes oxidative addition into the C–Cl bond, ejecting the chloride and reforming the palladium-allyl intermediate (TS2, Figure 2). We initially worried that the presence of the Pd–Ti interaction would make this oxidative process more difficult, and potentially slow catalysis by making the oxidative addition step rate determining.

Figure 2: (a) M06 free energy landscape for Et₂NH reductive addition and methallyl chloride oxidative



addition. ωB97X-D free energy values given in parenthesis. (kcal/mol) (b) Transition-state structures. Bond lengths reported in Å. (Energy barriers calculated with Scott Michaelis and Benjamin Kay)

However, our calculations confirmed that this effect was not significant enough to cause this step to become rate limiting. The free energy barrier of the oxidative addition (TS2) was calculated to be 7.7 kcal/mol, which is approximately 8.1 kcal/mol lower than that of the reductive amine addition step (TS1). We also were concerned that our calculations for the free-energy diagram would not sufficiently take into consideration the entropic

differences between **TS1** and **TS2**. We therefore scaled the entropy values by 50% and found that the ΔG^\ddagger for **TS1** remained about 4 kcal/mol higher than that of **TS2**. This difference in barrier indicated **TS1** to be rate determining, therefore improving catalytic activity hinges on lowering the barrier for the reductive addition.

Our experiments conducted thus far assume that heterobimetallic complex **1** with the metal-- metal dative bond intact is responsible for catalysis. Upon analysis of the reaction conditions, we realized that there exists a possibility in which the catalyst may be transformed into a catalytically active species that does not contain a metal--metal interaction prior to catalysis.

Several potential catalyst structures were considered, and the barriers for the reductive amine addition step were calculated for each of the intermediates considered (Figure 3). We considered that a phosphine ligand could slip to titanium (**1-slip**), generating a more electron-deficient palladium that could enable faster catalysis. We also considered the possibility that chloride, which is generated in high concentrations in the reaction, could coordinate to either the titanium or palladium center (**1-Cl**).

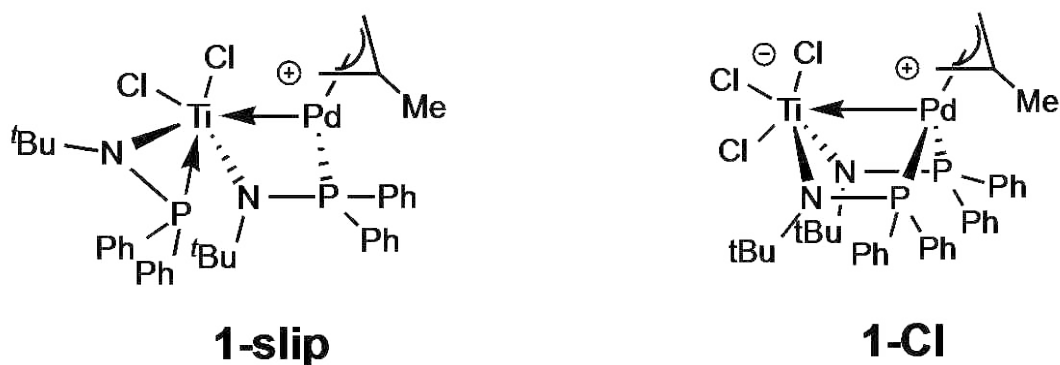


Figure 3. Possible alternative species involved in catalysis.

In our computational studies, we found **1-slip** to be endergonic by 11.5 kcal/mol relative to the **1** and that the barrier for amine addition to **1-slip** was 25.5 kcal/mol. This barrier is substantially higher than that of **TS1** making it an unviable pathway for amine addition. We also explored the possibility that chloride and diethylamine coordinated to Pd after a phosphine ligand slipped from the palladium. However, the ΔG^\ddagger values for amine addition were still larger than that of **TS1**. In consideration of the excess chloride in solution, we also considered the possibility of chloride coordinating to both palladium and titanium centers. We found that chloride coordination to the titanium center severed the Pd-Ti interaction and was endergonic by 0.8 kcal/mol. However the barrier for amine addition of **1-Cl** was calculated to be 22.7 kcal/mol. Comparison to the barrier of **TS1** makes this an unviable pathway as well. This, while we believe large amounts of chloride in solution could lead to formation of **1-Cl**, catalysis can occur only as chloride dissociates from the Ti and allows the Pd-Ti interaction to form and facilitate the reductive addition step. Lastly we explored the possibility of diethylamine replacing a chloride on the titanium, forming $(\text{Cl})(\text{Et}_2\text{N})\text{Ti}(\text{N}^t\text{BuPPh}_2)_2\text{Pd}(\eta^3\text{-CH}_2\text{C}(\text{CH}_3)\text{CH}_2)$. Like in **1-Cl**, the addition of a diethylamine to the titanium severed the Pd-Ti interaction and resulted in a larger transition state barrier.

Having explored various possibilities for catalyst transformation prior to catalysis and having found them all to be non-viable pathways, we moved forward, confident that the complex **1** containing an intact Pd-Ti interaction was the active catalyst for allylic aminations. We next sought to quantify the significance of the Pd-Ti interaction. To this end we performed ADF calculations and determined that there was in fact a weak but direct through space interaction between the Pd and Ti. The Pd d_{yz} and $d_{x^2-y^2}$ orbitals

overlapped with vacant $d_{x^2-y^2}$ and p-orbitals from the TiCl_2 fragment. The orbital contributions were shown to be 35% and 3% from the Pd and Ti respectively. Because of the small contribution from the Ti, NBO analysis proved insufficient to measure orbital contributions, as reported by Nagashima. Although the contribution is small, it still proved significant enough to increase the electrophilicity of the Pd and thereby facilitate fast catalysis. To further quantify this interaction and its impact on catalysis, we designed an analogous catalyst (**1(flat)**) where the Pd–Ti interaction had been severed (Figure 4).

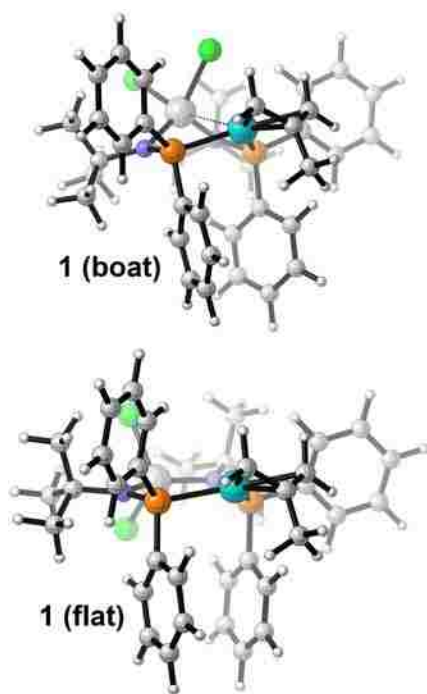


Figure 4. Boat and flat conformations of catalyst 1.

We used this control structure to calculate the energy surface of the same catalytic cycle and compare to the energy surface with that of complex **1** (Figure 5). The barrier for amine addition increased to 20.3 kcal/mol and the barrier for the oxidative substitution of methyl chloride increased to 10.2 kcal/mol, each of which is larger than the respective

barriers calculated using complex **1**. This result suggests that the Pd–Ti interaction is responsible for at least 4.5 kcal/mol stabilization, which translates into a rate enhancement of 10^3 . This enhancement can be attributed to the Pd–Ti interaction serving to stabilize the reduction of Pd^{II} to Pd⁰ as the amine attacks the allyl ligand.

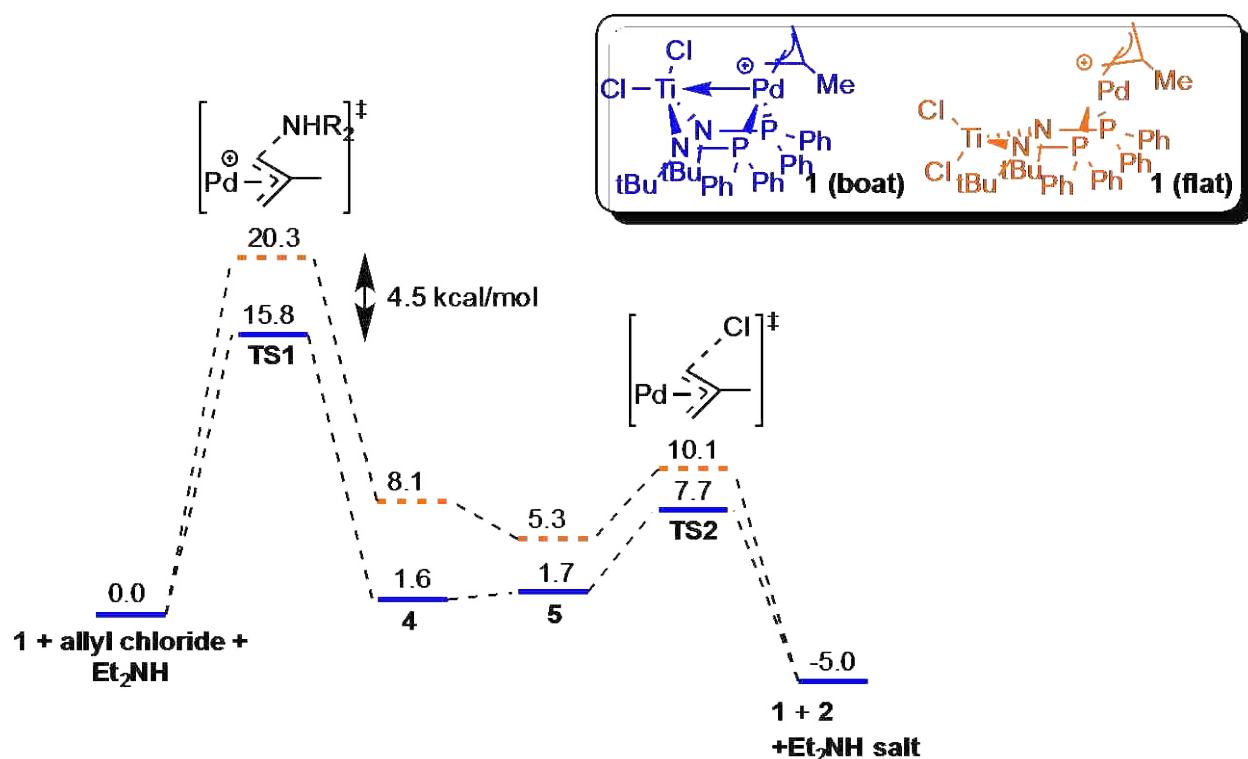


Figure 5: Comparison of allylic amination M06 free energy landscapes catalyzed by **1** (boat) and **1** (flat).
(kcal/mol) (Calculated with Scott Michaelis and Benjamin Kay)

To further substantiate this claim, we analyzed the frontier molecular orbitals and found that the Pd–Ti interaction causes the vacant π^* orbitals on the Pd–C allyl to be lowered by approximately 0.1 eV. This creates a stronger interaction with the HOMO of the incoming diethylamine. Both these models are consistent with Nagashima’s hypothesis that the

proximity of titanium increases the electrophilicity of the palladium and thereby significantly enhances the rate of nucleophilic amine addition.

We next desired to determine if the Pd–Ti interaction formed because it was electronically favorable or if the structure of the ligand framework forced the two metals into close proximity. Therefore, we replaced the *tert*-butyl groups on the nitrogen of the phosphinoamide ligands of **1** with methyl groups (Figure 6). We found that the boat structure was maintained but the Pd–Ti bond distance increased dramatically from 2.88 Å to 3.38 Å, indicating a loss of the Pd–Ti interaction. The boat structure of the methylated phosphinoamide complex was calculated to be 2.4 kcal/mol more stable than **1-flat**. This result shows that the *tert*-butyl groups are critical for the formation of the Pd–Ti interaction, which is also crucial for lowering the reductive addition barrier. We confirmed this by calculating the barrier using the boat and flat methylated species and found a $\Delta\Delta G^\ddagger$ of 0.2 kcal/mol, indicating little difference between **1-flat** and the methylated boat complex. In the calculated transition state for amine addition with the methylated boat complex, the Pd–Ti distance was increased by 0.08 Å compared to the original TS1. This increase in bond distance was enough to nullify the stabilization gained by Pd-Ti interaction and slow down the rate of the amine addition.

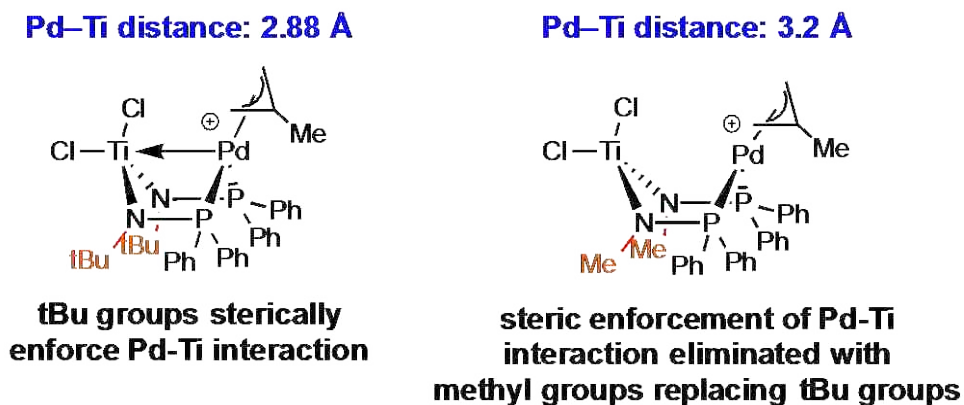


Figure 6: Significance of phosphinoamide ligand to enforcing Pd-Ti interaction and fast catalysis

3.2.3 Experimental and Computational Evaluation of the Impact of Replacing TiCl_2 to Remove the Pd-Ti Interaction

After performing the computations above to determine the impact of the M–M interaction on catalysis, we next desired to confirm our results experimentally by generating a complex that lacked the Pd–Ti interaction. We therefore designed, synthesized and characterized complex **6** (Figure 7). This complex was designed to closely mimic complex **1** in structure and electronics by maintaining the bidentate phosphinoamide scaffold but lacking the titanium. This would allow us to directly quantify the significance of the Pd–Ti interaction experimentally. As seen in Figure 7, X-ray crystallography confirmed that the boat conformation from **1** is maintained in complex **6**. However, the TiCl_2 was replaced with an ethylene group bridging the two N atoms. The crystal structure also reveals the P–Pd–P angle to vary only slightly from **1** (103.8° vs. 104.3° respectively), minimizing catalytic differences caused by variation of this angle.

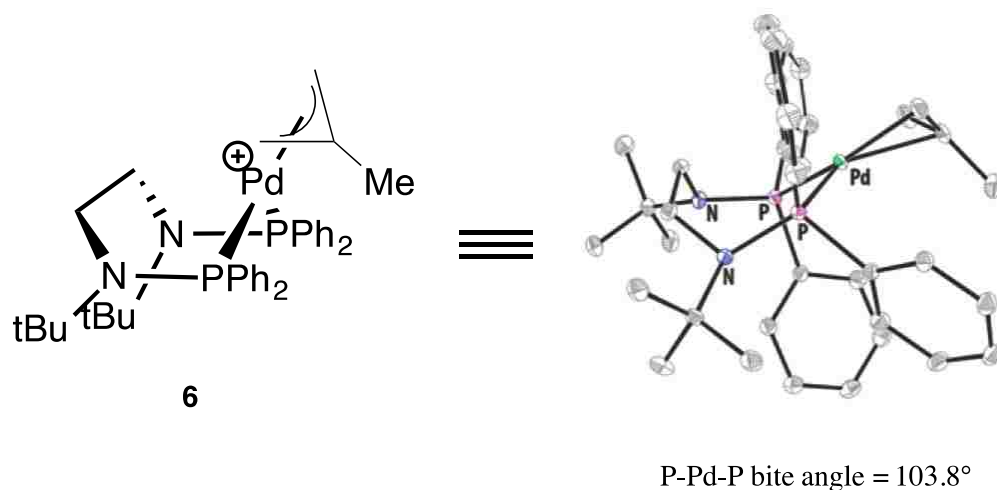


Figure 7: Bidentate phosphinoamine Pd-Ti mimic

Once synthesized, we tested the catalytic abilities of **6** and found it to enable moderate catalytic activity in the allylic amination of diethylamine. In 3 hours, it went to 50% conversion at room temperature (TOF = 17). This is significantly slower catalysis than that observed with complex **1** in which the same reaction went to completion within less than 1 minute (TOF of >1200). This result confirms the necessity of the Pd–Ti interaction to enable fast catalysis.

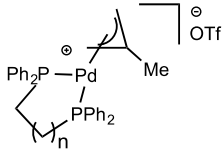
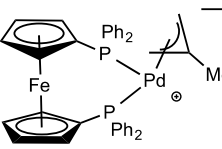
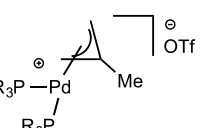
We next supplemented our experimental findings with computational analysis of the catalytic cycle in allylic amination using complex **6**. Our calculations indicated that although the geometries of the transition states with complex **1** and **6** were similar, the ΔG^\ddagger for diethylamine addition to **6** was 23.8 kcal/mol. This is about 8.0 kcal/mol higher than the transition state barrier for **1** and corresponds to a rate decrease of about $\sim 10^5$ with complex **6**.

With these theoretical and experimental results, we concluded that the Pd–Ti interaction in **1** is essential for fast catalysis. Through our computational studies, we confirmed that the barrier for the rate limiting reductive addition is significantly lowered by the stabilizing interaction between palladium and titanium. We also demonstrated that the Pd–Ti interaction in **1** exists not because of favorable electronic overlap but due to steric enforcement from the *tert*-butyl groups on the phosphoramidate scaffold. This forced boat conformation successfully maintains the two metals in close enough proximity for interaction throughout the reaction and allows fast catalysis to occur.

3.2.4 Impact of Coordination Angle and Electronic Effects on Catalysis

Having established the fast reactivity achieved by heterobimetallic complex **1**, we next sought to determine if other monometallic systems could achieve similar reaction rates. In Nagashima's study, he used complex **3** as a control catalyst to gauge the value of having a second metal present. However, several differences in the ligand structure and geometry between **1** and **3** bring into question the actual contributions by the second metal independent from ligand structural changes. Therefore, our next study sought to verify the impact of structural and electronic properties of the ligand on the rate of catalysis in allylic aminations. To this end, we designed and synthesized several monometallic Pd catalysts containing bisphosphine ligands that varied in coordination angle, ligand structure, and electronic properties (Table 1).

Table 1: Reactivity comparison for monometallic Pd catalyzed allylic aminations

	n = 0, 7a, dppm	entry	complex	P-Pd-P angle	time	% conv	~TOF
	1, 7b, dppe	1	1	104.3°	< 1 min	100	>1200
	2, 7c, dppp	2	7a	72°	1 min	48	576
	3, 7d, dppb	3	7b	85.8°	12 h	45	0.75
	7e, dppf	4	7c	95°	12 h	73	1.2
		5	7d	99°	1 h	46	9.1
		6	7e	101.2°	6 h	78	2.6
	8 PPh₃	7	8	-	< 1 min	100	>1200
	9 P(4-CF₃C₆H₄)₃	8	9	-	< 1 min	100	>1200
	10 P(OEt)₃	9	10	-	15 min	71	57
	11 t-BuNHPPH₂	10	11	-	3 h	50	3.3

^a Reactions performed using 1 mmol of methallyl chloride, 10 equiv of diethyl amine and 0.05 mmol of the indicated preformed allyl complex in CDCl₃ (1M) for indicated time. ^bDetermined by ¹HNMR analysis of the crude reaction mixture. ^cReported in (mmol product/mmol catalyst)/hr

Each of these complexes was tested for catalytic activity in the allylic amination of diethylamine and methallyl chloride. Heterobimetallic complex **1** was able to efficiently catalyze the reaction to completion in less than 1 minute. In testing other bis(phosphine) allyl complexes, we found several to be catalytically active, but most were not nearly as efficient as the bimetallic system. The bis(diphenylphosphino)methane catalyst **7a** had the smallest coordination angle of the bis(phosphine) allyl complexes and also corresponded to the highest activity of the group with a TOF of 576. The other bis(phosphine) complexes had TOFs of less than 10. This result further confirmed the importance of coordination angle to catalytic activity in this particular system.^{14,15} Additionally, we explored the catalytic activity of bis(monophosphine) palladium complexes to better understand the impact of electronics on catalysis. We tested several Pd catalysts with varying electron

donating/withdrawing groups to see how they would affect reactivity (Table 1, entries 8-11). With complexes **8** and **9**, reactivity was comparable to that of complex **1** making it difficult to pinpoint the reason for fast catalysis in this system.

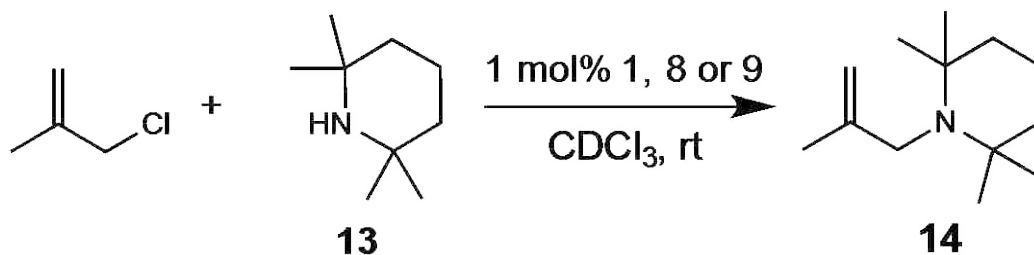
We next performed additional experiments with complex **8** to further investigate its high catalytic activity. The reported coordination angle of **8** is quite close to that of **1** (105.4° and 104.3° respectively). This lead us to believe that there may be an optimal P–Pd–P coordination angle that has a significant impact on catalytic activity in this system. We first calculated the activation barrier for the reductive amine addition using complex **8** and found a ΔG^\ddagger of 21.3 kcal/mol, which is substantially higher than that of complex **1**. We therefore concluded that the similar reactivity observed between **1** and **8** was simply due to our inability to measure fast reaction kinetics. We then tested catalyst **1** and **8** in the same system but using only 1 mol% catalyst loading, rather than the 5 mol% previously used. Catalyst **1** was still able to catalyze the reaction to completion in less than a minute, however, catalyst **8** only gave 28% yield in 3 minutes. We were therefore able to confirm complex **1**'s catalytic superiority as reflected by our calculations. We attribute the exceptional reactivity of complexes **8** and **9** to having an optimal P–Pd–P coordination angle that facilitates catalysis efficiently in this system by increasing the electrophilicity of the Pd-methallyl fragment. However we also recognized that fast catalysis by these complexes may have also occurred because of phosphine dissociation, opening up a coordination site on the Pd and increasing its electrophilicity. In order to test this, we calculated the activation barriers and thermodynamics of $(\text{PPh}_3)\text{Pd}(\eta^3\text{-CH}_2\text{C}(\text{CH}_3)\text{CH}_2)$, $(\text{X}_2)\text{Pd}(\eta^3\text{-CH}_2\text{C}(\text{CH}_3)\text{CH}_2)$ where X=chloride or diethylamine, and others. Our calculations showed that the thermodynamics for these complexes were all viable but they

all had higher transition state barriers than that calculated for **8**, making them unviable alternative pathways.

3.2.5 Testing the Limits of The Pd-Ti Interaction

In our previous studies of this system, we reported that complex **1** is able to catalyze the allylic amination of sterically hindered secondary amines, a reaction previously difficult to achieve.¹⁸ We therefore sought to test the reactivity of complexes **8** and **9** in a more challenging system and compare the results to those obtained by **1**. We tested **8** and **9** in the allylic amination of methallyl chloride using 2,2,6,6-tetramethylpiperidine (TMP) (**13**) in the hope that the steric strain of this amine would distinguish the reactivity of these complexes from that of **1**. In agreement with our previous studies, complex **1** catalyzed the amination reaction to 85% conversion within 15 minutes at room temperature (Table 2). To our delight, catalyst **8** produced no product even after 24 hours. We then heated the reaction to 90° C and found that the reaction had proceeded to 17% conversion after 24 hrs. Similarly, complex **9** only showed 6% conversion after 24 hours at 90° C.

Table 2. Reactivity of sterically-hindered amine **13**



entry	complex	Time ^a	Yield ^b	Rate ^c	Ar ^e
1	1	24 hr	100%	1.0	H
2	8	24 hr	100%	1.0	H
3	8	24 hr	100%	1.0	H
4	9	24 hr	100%	1.0	H

^aReactions performed using 1 mmol allyl chloride, 2.2 equiv of amine, and 0.01 mmol of the indicated preformed allyl complex in CDCl_3 (0.1 M). ^bDetermined by ^1H NMR analysis. ^cReported in (mmol product/mmol catalyst)/hr. ^dReaction run at 90 °C in a sealed vial. ^eAr = 4-CF₃C₆H₄

(Reactions performed with Whitney Walker)

We also calculated the activation barrier for TMP addition to **1** to be 18.5 kcal/mol, which is only ~2.7 kcal/mol higher than that calculated using diethylamine in **TS1**. However, the ΔG^\ddagger for complex **8** in this system was calculated to be 26.0 kcal/mol which is almost 4 kcal/mol higher than the corresponding barrier with diethylamine and 7.5 kcal/mol higher than complex **1**. These results lead us to conclude that the Pd–Ti interaction generates a more electrophilic allyl species and stabilizes the Pd⁰ intermediate. By lowering the activation barrier in this fashion, complex **1** is less susceptible to slowed reactivity expected by sterically hindered substrates. This unique reactivity may serve as a guiding principle in future heterobimetallic catalyst design.

In our previous synthetic studies on allylic amination with **1** presented in chapter 2 of this work, we found that allylic acetates are poor substrates for catalysis. One foreseeable challenge is the formation of Lewis-basic acetate byproducts that decompose/deactivate the active catalyst when they coordinate to titanium. An alternative explanation for poor catalysis is that the activation barrier for oxidative addition into the allylic acetate via **TS2** is significantly higher for allylic acetates, and has become rate limiting in this example. The higher barrier for oxidative addition into allylic acetates is due to the fact that acetates are poorer leaving groups than chlorides. In addition, formation of the Pd–Ti interaction could make this oxidative addition barrier potentially higher than with monometallic palladium complexes. In our experiments, we found that the allylic amination of methallyl acetate with **13** the reaction proceeded to 16% completion before stalling (Figure 8). This confirmed that the catalyst was decomposing or deactivating before the reaction could go to completion.

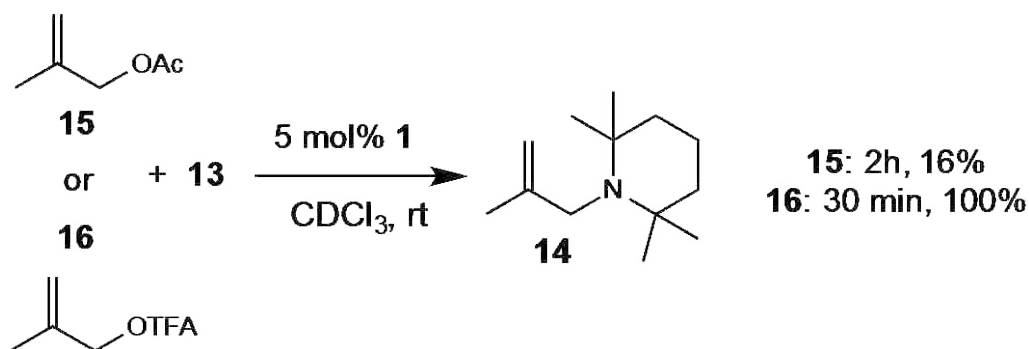


Figure 8: Allylic amination using allyl acetates and **13** catalyzed by **1**

(Reactions performed with Whitney Walker; Calculations performed with Benjamin Kay)

We then calculated the activation barrier for the oxidation of Pd⁰ in this system and found that it increased by 16.8 kcal/mol as compared to methallyl chloride and therefore became

the rate determining step. For this reason, as well as probable catalyst decomposition, complex **1** was not an effective catalyst for allylic aminations with allyl acetates.

3.3 CONCLUSION

Our computational and experimental analysis of allylic aminations using Pd–Ti heterobimetallic complex **1** indicate that the fast catalysis is largely due to a dative interaction between the palladium and titanium. The electron deficient titanium is able to withdraw electron density from the palladium and thereby increase its electrophilicity. This in turn lowers the activation barrier for the rate-determining step of reductive addition of the amine to the methallyl fragment. The Pd–Ti interaction is made possible by the steric enforcement provided by the *tert*-butyl groups on the phosphoramidate scaffold. By studying the boat and flat conformations of the catalyst, calculating the respective transition state barriers, and analyzing barriers for control complexes **6** and **8**, we found that catalysis was accelerated by $\sim 10^3$ - 10^5 when the Pd–Ti interaction was intact. The Pd–Ti interaction facilitates catalysis with sterically hindered secondary amines in mild conditions.

These results show the potential of heterobimetallic complexes to facilitate novel catalysis by lowering the barriers to specific steps in a catalytic cycle. This catalysis is achieved by using two transition metals in close proximity to each other in order to tune the reactivity of the catalytically active metal. Although this did not prove to be an effective approach in the amination of allylic acetates, it was very effective in the amination of allyl chlorides. The use of a bimetallic system serves as a viable alternative for altering the electronics of transition metal catalysts

3.4 REFERENCES

(1) (a) Cooper, B. G.; Napoline, J. W.; Thomas, C. M. *Catal. Rev. Sci. Eng.* **2012**, *54*, 1.

(b) Thomas, C. M. *Comments Inorg. Chem.* **2011**, *32*, 14.

(2) For reviews see:

(a) Oelkers, B.; Butovskii, M. V.; Kempe, R. *Chem. Eur. J.* **2012**, *18*, 13566.

(b) Mandal, S. K.; Roesky, H. W. *Acc. Chem. Res.* **2010**, *43*, 248.

(c) Ritleng, V.; Chetcuti, M. J. *Chem Rev.* **2007**, *107*, 797.

(d) Collman, J. P.; Boulatav, R. *Angew. Chem. Int. Ed.* **2002**, *41*, 3948.

(e) Gade, L. H. *Angew. Chem. Int. Ed.* **2000**, *39*, 2658.

(f) Wheatley, N.; Kalck, P. *Chem. Rev.* **1999**, *99*, 3379.

(g) Stephan, D. W. *Coord. Chem. Rev.* **1989**, *95*, 41.

(h) Zhang, Y.; Roberts, S. P.; Bergman, R. G.; Ess, D. H. *ACS Catal.* **2015**, *5*, 1840.

(3) For selected recent examples, see:

(a) Kuppuswamy, S.; Cass, T. R.; Bezpalko, M. W.; Foxman, B. M.; Thomas, C. M. *Inorg. Chim. Acta* **2014**, *424*, 167.

(b) Tereniak, S. J.; Carlson, R. K.; Clouston, L. J.; Young Jr., V. G.; Bill, E.; Maurice, R.; Chen, Y.-S.; Kim, H. J.; Gagliardi, L.; Lu, C. C. *J. Am. Chem. Soc.* **2014**, *136*, 1842.

(c) Clouston, L. J.; Siedschlag, R. B.; Rudd, P. A.; Planas, N.; Hu, S.; Miller, A. D.; Gagliardi, L.; Lu, C. C. *J. Am. Chem. Soc.* **2013**, *135*, 13142.

(d) Cooper, B. G.; Fafard, C. M.; Foxman, B. M.; Thomas, C. M. *Organometallics* **2010**, *29*, 5179.

- (e) Greenwood, B. P.; Forman, S. I.; Rowe, G. T.; Chen, C.- H.; Foxman, B. M.; Thomas, C. M. *Inorg. Chem.* **2009**, *48*, 6251.
- (f) Nippe, M.; Berry, J. F. *J. Am. Chem. Soc.* **2007**, *129*, 12684.
- (g) Nagashima, H.; Sue, T.; Oda, T.; Kanemitsu, A.; Matsumoto, T.; Motoyama, Y.; Sunada, Y. *Organometallics* **2006**, *25*, 1987.
- (h) Uyeda, C.; Peters, J. *Chem. Sci.* **2013**, *4*, 157.
- (i) Curley J.J.; Bergman, R.G.; Tilley T.D. *Dalton Trans.* **2012**, *41*, 192–200.
- (j) Hansen, J.; Li, B.; Dikarev, E.; Autschbach, J.; Davies, H. M. L. *J. Org. Chem.* **2009**, *74*, 6564.
- (k) Hostetler, M. J.; Bergman, R. G. *J. Am. Chem. Soc.* **1990**, *112*, 8621– 8623.
- (l) Baxter, S. M.; Ferguson, G. S.; Wolczanski, P. T. *J. Am. Chem. Soc.* **1988**, *110*, 4231.
- (m) Casey, C. P.; Rutter, E. W.; Haller, K. J. *J. Am. Chem. Soc.* **1987**, *109*, 6886–6887.
- (4) (a) Zhou, W.; Saper, N. I.; Krogman, J. P.; Foxman, B. M.; Thomas, C. M. *Dalton Trans.* **2014**, *43*, 1984.
- (b) Zhou, W.; Marquard, S. L.; Bezpalko, M. W.; Foxman, B. M.; Thomas, C. M. *Organometallics* **2013**, *32*, 1766.
- (c) Zhou, W.; Napoline, J. W.; Thomas, C. M. *Eur. J. Inorg. Chem.* **2011**, 2029.
- (5) (a) Trost, B. M.; Lee, C. In *Catalytic Asymmetric Synthesis*; Ojima, I., Ed.; Wiley-VCH: New York, 2010; pp. 593–649.
- (b) Diéguez, M.; Pàmies, O. *Acc. Chem. Res.* **2010**, *43*, 312.
- (c) Lu, Z.; Ma, S. *Angew. Chem. Int. Ed.* **2008**, *47*, 258.
- (d) Trost, B. M.; Machacek, M. R.; Aponick, A. *Acc. Chem. Res.* **2006**, *39*, 747.

- (e) Dai, L.-X.; Tu, T.; You, S.-L.; Deng, W.-P.; Hou, X.-L. *Acc. Chem. Res.* **2003**, *36*, 659.
- (f) Helmchen, G.; Pfaltz, A. *Acc. Chem. Res.* **2000**, *33*, 336.
- (g) Johannsen, M.; Jørgensen, K. A. *Chem. Rev.* **1998**, *98*, 1689. Tsutsumi, H.; Sunada, Y.; Shiota, Y.; Yoshizawa, K.; Nagashima, H. *Organometallics* **2009**, *28*, 1988.
- (6) (a) Tolman, C. A. *Chem. Rev.* **1977**, *77*, 313.
- (b) van Leeuwen, P. W. N. M.; Kamer, P. C. J.; Reek, J. N. H.; Dierkes, P. *Chem Rev.* **2000**, *100*, 2741.
- (c) Canovese, L.; Visentin, F.; Levi, C.; Dolmella, A. *Dalton Trans.* **2011**, *40*, 966.
- (7) For reports of amine addition transition states to Pd allyl complexes see:
- (a) Blöchl, P. E.; Togni, A. *Organometallics* **1996**, *15*, 4125.
- (b) Hagelin, H.; Åkermark, B.; Norrby, P.-O. *Chem. Eur. J.* **1999**, *5*, 902.
- (c) Macsári, I. Szabó, K. J. *Organometallics* **1999**, *18*, 701.
- (d) Branchadell, V.; Moreno-Mañas, M.; Pajuelo, F.; Pleixats, R. *Organometallics* **1999**, *18*, 4934.
- (e) Delbecq, F.; Lapouge, C. *Organometallics* **2000**, *19*, 2716.
- (f) Branchadell, V.; Moreno-Mañas, M.; Pleixats, R. *Organometallics* **2002**, *21*, 2407.
- (g) Piechaczyk, O.; Thoumazet, C.; Jean, Y.; le Floch, P. *J. Am. Chem. Soc.* **2006**, *128*, 14306.
- (h) De luliis, M. Z.; Watson, I. D. G.; Yudin, A. K.; Morris, R. H. *Can. J. Chem.* **2009**, *87*, 54.
- (8) For general computational reports of nucleophile addition to Pd allyl complexes see:
- (a) Schilling, B. E. R.; Hoffmann, R.; Faller, J. W. *J. Am. Chem. Soc.* **1979**, *101*, 592.

- (b) Sakaki, S.; Nishikawa, M.; Ohyoshi, A. *J. Am. Chem. Soc.* **1980**, *102*, 4062.
- (c) Curtis, M. D.; Eisenstein, O. *Organometallics* **1984**, *3*, 887.
- (d) Bigot, B.; Delbecq, F. *New J. Chem.* **1990**, *14*, 659.
- (e) Sjögern, M.; Hansson, S.; Norrby, P.-O.; Åkermark, B.; Cucciolito, M. E.; Vitagliano, A. *Organometallics*, **1992**, *11*, 3954.
- (f) Blöchl, P. E.; Togni, A. *Organometallics* **1996**, *15*, 4125.
- (g) Ward, T. R. *Organometallics* **1996**, *15*, 2836.
- (h) Sakaki, S.; Takeuchi, K.; Sugimoto, M. *Organometallics* **1997**, *16*, 2995.
- (i) Lloyd-Jones, G. C.; Stephen, S. C. *Chem. Eur. J.* **1998**, *4*, 2539.
- (j) Dedieu, A. *Chem. Rev.* **2000**, *100*, 543. (k) Solin, N.; Szabó, K. *J. Organometallics* **2001**, *20*, 5464.
- (l) Szabó, K. *J. Chem. Soc. Rev.* **2001**, *30*, 136.
- (m) Fristrup, P.; Jensen, T.; Hoppe, J.; Norrby, P.-O. *Chem. Eur. J.* **2006**, *12*, 5352.
- (n) Ariafard, A.; Lin, Z. *J. Am. Chem. Soc.* **2006**, *128*, 13010.
- (o) Fristrup, P.; Ahlquist, M.; Tanner, D.; Norrby, P.-O. *J. Phys. Chem. A* **2008**, *112*, 12862.
- (p) Kazmaier, U.; Stolz, D.; Kraemer, K.; Zumpe, F. L. *Chem. Eur. J.* **2008**, *14*, 1322.
- (q) Marinho, V. R.; Ramalho, J. P. P.; Rodrigues, A. I.; Burke, A. J. *Eur. J. Org. Chem.* **2009**, 6311.
- (r) Kleimark, J.; Johansson, C.; Olsson, S.; Håkansson, M.; Hansson, S.; Åkermark, B.; Norrby, P.-O. *Organometallics* **2011**, *30*, 230.
- (s) Ortiz, D.; Blug, M.; Le Goff, X.-F.; Le Floch, P.; Mézailles, N.; Maître, P. *Organometallics* **2012**, *31*, 5975.

(9) Indeed, when tetrabutylammonium chloride is added to catalyst **1**, a new species is seen to reversibly form, as observed by ^{31}P NMR. (See supporting information).

(10) When exogenous chloride is added to of the reaction, the rate of catalysis decreases, as suggested by this study (see supporting information).

(11) (a) Birkholz, M.-N.; Freixa, Z.; van Leeuwen, P. W. N. M. *Chem Soc. Rev.* **2009**, *38*, 1099.

(b) Jones, A. M.; Tye, J. W.; Hartwig, J. F. *J. Am. Chem. Soc.* **2006**, *128*, 16010.

Hughes, A. N. *ACS Symp. Ser.* **1992**, *486*, 173.

(12) General phosphine bite angle references:

(a) Dierkes, P.; van Leeuwen, P. W. N. M. *J. Chem. Soc., Dalton Trans.* **1999**, 1519.

(b) Van Leeuwen, P. W. N. M.; Kamer, P. C. J.; Reek, J. N. H.; Dierkes, P. *Chem. Rev.* **2000**, *100*, 2741.

(13) Specific phosphine of bite angle references for Pd complexes:

(a) Sjorgen, M. P. T.; Hansson, S.; Åkermark, B.; Vitagliano, A. *Organometallics* **1994**, *13*, 1963.

(b) Szabó, K. J. *Organometallics* **1996**, *15*, 1128.

(c) Aranyos, A.; Szabó, K. J.; Castaño, A. M.; Bäckvall, J.-E. *Organometallics* **1997**, *16*, 1058.

(d) van Haaren, R. J.; Oevering, H.; Coussens, B.; van Strijdonck, G. P. F.; Reek, J. N. H.; Kamer, P. C. J.; van Leeuwen, P. W. N. M. *Eur. J. Inorg. Chem.* **1999**, 1237.

(e) van Haaren, R. J.; Druijven, C. J. M.; van Strijdonck, G. P. F.; Oevering, H.; Reek, J. N. H.; Kamer, P. J. C.; van Leeuwen, P. W. N. M. *J. Chem. Soc., Dalton Trans.* **2000**, *10*, 1549.

- (f) Delbecq, F.; Lapouge, C. *Organometallics* **2000**, *19*, 2716.
- (g) van Haaren, R. J.; Goubitz, K.; Fraanje, J.; van Strijdonck, G. P. F.; Oevering, H.; Coussens, B.; Reek, J. N. H.; Kamer, P. C. J.; van Leeuwen, P. W. N. M. *Inorg. Chem.* **2001**, *40*, 3363.
- (h) Tromp, M.; van Bokhoven, J. A.; van Haaren, R. J.; van Strijdonck, G. P. F.; van der Eerden, A. M. J.; van Leeuwen, P. W. N. M.; Koningsberger, D. C. *J. Am. Chem. Soc.* **2002**, *124*, 14814
- (14) Walker, W. K.; Anderson, D. L.; Stokes, R. W.; Smith, S. J.; Michaelis, D. J. *Org. Lett.* **2015**, *17*, 752.
- (15) These results are consistent with the reported rates of allylic amination of **13** with *in situ* generated complexes **8** and **9**. See reference 16.
- (16) Gaussian 09, Revision B.01, Frisch, M. J.; Trucks, G. W.; Schlegel, H. B.; Scuseria, G. E.; Robb, M. A.; Cheeseman, J. R.; Scalmani, G.; Barone, V.; Mennucci, B.; Petersson, G. A.; Nakatsuji, H.; Caricato, M.; Li, X.; Hratchian, H. P.; Izmaylov, A. F.; Bloino, J.; Zheng, G.; Sonnenberg, J. L.; Hada, M.; Ehara, M.; Toyota, K.; Fukuda, R.; Hasegawa, J.; Ishida, M.; Nakajima, T.; Honda, Y.; Kitao, O.; Nakai, H.; Vreven, T.; Montgomery, J. A., Jr.; Peralta, J. E.; Ogliaro, F.; Bearpark, M.; Heyd, J. J.; Brothers, E.; Kudin, K. N.; Staroverov, V. N.; Kobayashi, R.; Normand, J.; Raghavachari, K.; Rendell, A.; Burant, J. C.; Iyengar, S. S.; Tomasi, J.; Cossi, M.; Rega, N.; Millam, M. J.; Klene, M.; Knox, J. E.; Cross, J. B.; Bakken, V.; Adamo, C.; Jaramillo, J.; Gomperts, R.; Stratmann, R. E.; Yazyev, O.; Austin, A. J.; Cammi, R.; Pomelli, C.; Ochterski, J. W.; Martin, R. L.; Morokuma, K.; Zakrzewski, V. G.; Voth, G. A.; Salvador, P.; Dannenberg, J. J.; Dapprich, S.; Daniels, A.

D.; Farkas, Ö.; Foresman, J. B.; Ortiz, J. V.; Cioslowski, J.; Fox, D. J. Gaussian, Inc., Wallingford CT, 2009.

(17) Zhao, Y.; Truhlar, D. G. *Theor. Chem. Acc.* **2008**, *120*, 215.

(18) (a) Ditchfield, R.; Hehre, W. J.; Pople, J. A. *J. Chem. Phys.* **1971**, *54*, 724.

(b) Hehre, W. J.; Ditchfield, R.; Pople, J. A. *J. Chem. Phys.* **1972**, *56*, 2257.

(c) Francel, M. M.; Pietro, W. J.; Hehre, W. J.; Binkley, J. S.; Gordon, M. S.; DeFrees, D. J.; Pople, J. A. *J. Chem. Phys.* **1982**, *77*, 3654.

(d) Frisch, M. J.; Pople, J. A.; Binkley, J. S. *J. Chem. Phys.* **1984**, *80*, 3265.

(e) Rassolov, V. A.; Pople, J. A.; Ratner, M. A.; Windus, T. L. *J. Chem. Phys.* **1998**, *109*, 1223.

(f) Rassolov, V. A.; Ratner, M. A.; Pople, J. A.; Redfern, P. C.; Curtiss, L. A. *J. Comp. Chem.* **2001**, *22*, 976.

(19) (a) Dunning, T. H., Jr.; Hay, P. J. in *Modern Theoretical Chemistry*, Ed. H. F. Schaefer III, Vol. 3 (Plenum, New York, 1977) 1-28.

(b) Hay P. J.; Wadt, W. R. "*J. Chem. Phys.* **1985**, *82*, 270.

(c) Wadt, W. R.; Hay, P. J. *J. Chem. Phys.* **1985**, *82*, 284.

(d) Hay P. J.; Wadt, W. R. *J. Chem. Phys.* **1985**, *82*, 299.

(20) Marenich, A. V.; Cramer, C. J.; Truhlar, D. G. *J. Phys. Chem. B* **2009**, *113*, 6378.

(21) The LANL2TZ(f) basis set for Pd and Ti was obtained from the EMSL Basis Set Exchange. See: <https://bse.pnl.gov/bse/portal>

(22) Wikipedia: Density Functional Theory,

https://en.wikipedia.org/wiki/Density_functional_theory. (accessed June 13, 2015).

(23) Foresman, James B., Frisch, Aileen *Exploring Chemistry with Electronic Structure Methods*. Gaussian Inc. 1996

(24) Wikipedia: Basis Sets [https://en.wikipedia.org/wiki/Basis_set_\(chemistry\)](https://en.wikipedia.org/wiki/Basis_set_(chemistry)). (accessed June 13, 2015).

Chapter 4

Supporting Information

4.1 Supporting Information for Chapter 2

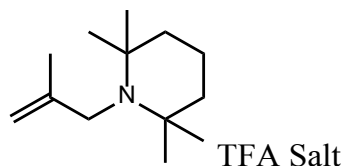
4.1.1 General Information

All reactions were carried out in oven-dried glassware with magnetic stirring, unless otherwise indicated. All the reagents were used as obtained unless otherwise noted. All commercially available amines were distilled from calcium hydride under nitrogen and stored over 4Å molecular sieves for at least 12 h before use. Reactions requiring a moisture-free environment were conducted in a nitrogen atmosphere glove box (Innovative Technology, PureLab HE system, double glove box). Analytical thin-layer chromatography was performed with 0.25 mm coated commercial silica gel plates (E. Merck, DC-Plastikfolien, kieselgel 60 F254). Flash Chromatography was performed with EM Science silica gel (0.040-0.063µm grade) Proton nuclear magnetic resonance (¹H NMR) data were acquired on a Inova 300 (300 MHz) or on a Inova-500 (500 MHz) spectrometer. Chemical shifts are reported in delta (δ) units, in parts per million (ppm) downfield from tetramethylsilane. Carbon-13 nuclear magnetic resonance (¹³C-NMR) data were acquired on a Inova 500 at 125 MHz. Signals are reported as follows: s (singlet), d (doublet), t (triplet), q (quartet), dd (doublet of doublets), qd (quartet of doublets), brs (broad singlet), m (multiplet). Coupling constants are reported in hertz (Hz). Chemical shifts are reported in ppm relative to the center line of a triplet at 77.0 ppm for chloroform-d. Mass spectral data were obtained using ESI techniques (Agilent, 6210 TOF). Commercially available ligands 5–8, 10a–10d, and 11 were used as obtained.

Heterobimetallic complex 1¹ and titanium-ligand 2² were synthesized as previously described.

DCM= dichloromethane (CH₂Cl₂)

II. Intramolecular Allylic Aminations with Ti–Pd complex 1

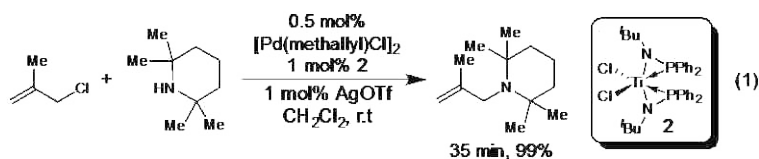


General Procedure I: Intermolecular allylic aminations:

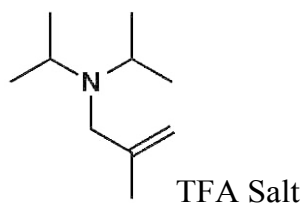
2,2,6,6-tetramethyl-1-(2-methylallyl)piperidine TFA Salt (4a): In a glove box, 9.4 mg (0.01 mmol, 1 mol%) 1 was added to a 25 ml vial and 1 ml of DCM added. 2,2,6,6-tetramethylpiperidine (311 mg, 2.2 mmol, 2.2 equiv) was then added, followed by methylallyl chloride (91 mg, 1.0 mmol). The reaction was allowed to stir for 10 minutes, removed from the glove box, diluted with 1 ml DCM and loaded directly onto a column of silica gel and eluted with 10% MeOH in DCM. Due to the volatility of the products, the fractions containing the product were combined, treated with TFA (1 equiv) and the solvent removed *in vacuo*. The product TFA salt was isolated as a pale yellow oil (318mg, >99% yield). IR (film): ν = 3408, 2956, 1736, 1687, 1462, 1410, 1394, 1200, 1173, 1129; ¹H-NMR (500 MHz, CDCl₃): δ (ppm) = 7.50 (bs, 1H), 5.35 (s, 1H), 5.20 (s, 1H), 3.68 (s, 2H), 2.36 (td, J=3.97 Hz, J=13.58 Hz, 2H), 1.96 (s, 3H), 1.82-1.61 (m, 4H) 1.54 (s, 6H) 1.45 (s, 6H); ¹³C-NMR (500 MHz, CDCl₃): δ (ppm) = 15.7, 21.2, 21.4, 29.9, 37.2, 53.0, 67.9, 119.1, 137.6, 160.2 (q, TFA). HRMS (ESI): C₁₃H₂₅N (M+H) calculated: 196.2065, found 196.2089.

¹ Tsutsumi, H.; Sunada, Y.; Shiota, Y.; Yoshizawa, K.; Nagashima, H. *Organometallics* **2009**, *28*, 1988–1991.

² Nagashima, H.; Sue, T.; Oda, T.; Kanemitsu, A.; Matsumoto, T.; Motoyama, Y.; Sunada, Y. *Organometallics* **2006**, *25*, 1987–1994.

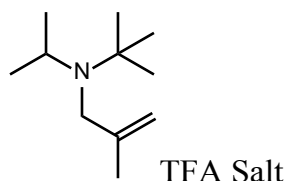


General Procedure for *in situ* formation of active bimetallic catalyst: In a glove box, into a 3 dram vial with a stil bar was weighed ligand 2 (6.3 mg, 0.01 mmol) followed by [Pd(methallyl)Cl]₂ (2.0 mg, 0.005 mmol), and silver triflate (2.6 mg, 0.01 mmol). The mixture was then dissolved in DCM and allowed to stir for 30 minutes. 2,2,6,6-Tetramethylpiperidine (.371 ml, 2.2 mmol), followed by methallyl chloride (0.10 ml, 1.0 mmol) were then added and the reaction progress was monitored by removing a small aliquot from each reaction vial, diluting in 0.7 ml of CDCl₃, and then by ¹H NMR analysis of the crude reaction mixture. Complete conversion to product was observed after 20 minutes.

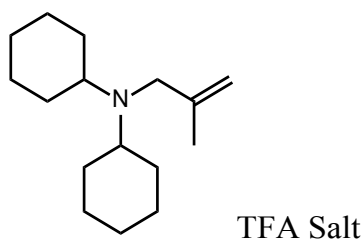


N,N-diisopropyl-2-methylprop-2-en-1-amine TFA Salt (4b): Synthesized according to general procedure I using 91 mg (1.0mmol) methallyl chloride, 223 mg (2.2mmol, 2.2 equiv) of diisopropylamine, and 9.4 mg (0.01 mmol, 1mol %) 1 and purified on silica gel with 10% MeOH in DCM as eluent. The product thus obtained was treated with TFA (1 equiv) and isolated and characterized as the TFA salt. The product was obtained as a yellow oil (161mg, 72% yield). IR (film): $\nu = 2995, 1780, 1738, 1674, 1402, 1174$; ¹H-NMR (500 MHz, CDCl₃): δ (ppm) = 7.80 (bs, 1H), 5.28 (s, 1H), 5.23 (s, 1H), 3.81-3.72 (m, 1H), 3.62 (d, J=4.93 Hz, 2H), 1.89 (s, 3H), 1.41 (t, J=7.48 Hz, 12H); ¹³C-NMR (500 MHz, CDCl₃): δ (ppm) = 17.1, 18.4, 20.6, 53.3, 56.4, 119.3, 135.8, 160.3 (q, TFA). HRMS (ESI): C₁₀H₂₁H (M+H) calculated: 156.1752, found 156.1967.

When performed using the in situ catalyst preparation method, 100% conversion to the desired product was also observed in <10 min. Spectral data matched reported values.

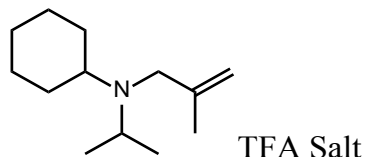


N-(*tert*-butyl)-N-isopropyl-2-methylprop-2-en-1-amine TFA Salt (4c): Synthesized according to general procedure I using 91 mg (1.0 mmol) methallyl chloride, 253 mg (2.2 mmol, 2.2 equiv) of N-isopropyl-*tert*-butylamine and 9.4 mg (0.01 mmol, 1 mol%) 1 and purified on silica gel with 10% MeOH in DCM as eluent. The product thus obtained was treated with TFA (1 equiv) and isolated and characterized as the TFA salt. The product was obtained as a yellow oil (248 mg, 98% yield). IR (film): ν = 3405, 2980, 2696, 1648, 1460, 1412, 1394, 1175, 1129; $^1\text{H-NMR}$ (500 MHz, CDCl_3): δ (ppm) = 9.91 (bs, 1H), 5.46 (s, 1H), 5.22 (s, 1H), 4.28-4.17 (m, 1H), 3.68-3.52 (m, 2H), 2.20 (s, 3H), 1.74-1.38 (m, 15 H); $^{13}\text{C-NMR}$ (500 MHz, CDCl_3): δ (ppm) = 17.3, 22.1, 26.9, 50.9, 55.8, 67.9, 119.8, 138.1. HRMS (ESI): $\text{C}_{13}\text{H}_{25}\text{N}$ (M+H) calculated: 170.1903, found 170.1910.

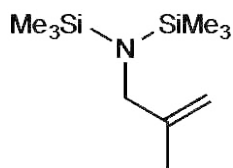


N-cyclohexyl-N-(2-methylallyl)cyclohexanamine TFA Salt (4d): Synthesized according to general procedure I using 91 mg (1.0 mmol) methallyl chloride, 400 mg (2.2 mmol, 2.2 equiv) of dicyclohexylamine, and 9.4 mg (0.01 mmol, 1 mol%) 1 and purified on silica gel with 10% MeOH in DCM as eluent. The product thus obtained was treated with TFA (1 equiv) and isolated and characterized as the TFA salt. The product was obtained as an orange oil (391

mg, 98% yield). IR (film): $\nu = 3405, 2935, 2858, 1454, 1270, 1031, 909$; $^1\text{H-NMR}$ (500 MHz, CDCl_3): δ (ppm) = 10.32 (bs, 1H), 5.48 (s, 1H), 5.27 (s, 1H), 3.55 (d, $J=67.27$ Hz, 2H), 2.47 (bs, 2H), 2.32-2.10 (m, 5H), 1.99-1.64 (m, 11H), 1.38-1.18 (m, 7H); $^{13}\text{C-NMR}$ (500 MHz, CDCl_3): δ (ppm) = 25.5, 27.8, 29.0, 63.9, 120.7, 138.9. HRMS (ESI): $\text{C}_{16}\text{H}_{29}\text{N}$ (M+H) calculated: 236.2373, found 236.2400.

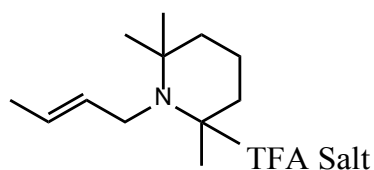


N-isopropyl-N-(2-methylallyl)cyclohexanamine TFA Salt (4e): Synthesized according to general procedure I using 91 mg (1.0 mmol) methallyl chloride, 310 mg (2.2 mmol, 2.2 equiv) of cyclohexylisopropylamine, and 9.4 mg (0.01 mmol, 1 mol%) 1 and purified on silica gel with 10% MeOH in DCM as eluent. The product thus obtained was treated with TFA (1 equiv) and isolated and characterized as the TFA salt. The product was obtained as a yellow oil (338 mg, >99% yield). IR (film): $\nu = 3406, 2933, 2858, 1445, 1119, 1031, 911$; $^1\text{H-NMR}$ (500 MHz, CDCl_3): δ (ppm) = 10.53 (bs, 1H), 5.43 (s, 1H), 5.24 (s, 1H), 3.87-3.77 (m, 1H), 3.62-3.52 (m, 2H), 3.35-3.26 (m, 1H), 2.41 (d, $J=11.92$ Hz, 1H), 2.25 (d, $J=11.93$ Hz, 1H), 2.11 (s, 3H), 1.98-1.88 (m, 1H), 1.83-1.67 (m, 3H), 1.62-1.55 (m, 6H), 1.47 (d, $J=8.52$ Hz, 3H); $^{13}\text{C-NMR}$ (500 MHz, CDCl_3): δ (ppm) = 17.5, 19.3, 22.4, 25.0, 25.5, 25.6, 27.7, 28.5, 53.6, 55.3, 64.2, 120.3, 136.7. HRMS (ESI): $\text{C}_{13}\text{H}_{25}\text{N}$ (M+H) calculated: 196.2060, found 196.2064.



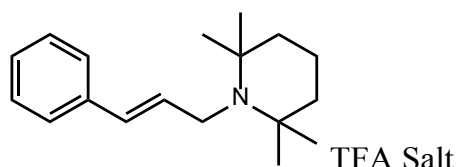
1, 1, 1-trimethyl-N-(2-methylallyl)-N-(trimethylsilyl)silanamine TFA Salt (4f): Synthesized according to general procedure I using 91 mg (1.0mmol) methallyl chloride, 474 mg

(2.2mmol, 2.2 equiv) of bis(trimethylsilyl)amine, and 9.4 mg (0.01 mmol, 1mol %) 1. Yield obtained by comparison with an internal standard (mesitylene) was >99%. The product was not isolated due to the instability of TMS-amides to moisture and silica gel chromatography. Spectral data matched reported values.³ ¹H-NMR (500 MHz, CDCl₃): δ (ppm) = 4.92 (s, 1H), 4.84 (s, 1H), 2.81 (s, 2H), 1.76 (s, 3H), 0.079 (s, 18H); ¹³C-NMR (500 MHz, CDCl₃): δ (ppm) = 2.4, 20.6, 60.6, 112.5, 144.0.

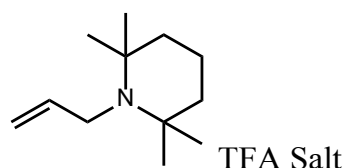


1-(but-2-en-1-yl)-2,2,6,6-tetramethylpiperidine TFA Salt (4h): Synthesized according to general procedure I using 91 mg (1.0 mmol) crotyl chloride, 311 mg (2.2 mmol, 2.2 equiv) of 2,2,6,6-tetramethylpiperidine, and 9.4 mg (0.01 mmol, 1 mol%) 1 and purified on silica gel with 10% MeOH in DCM as eluent. The product thus obtained was treated with TFA (1 equiv) and isolated and characterized as the TFA salt. The product TFA salt was isolated as a pale yellow oil (316mg, 97% yield). The product consisted of ~5:1 mixture of cis/trans isomers as reflected from the same ratio of isomers in the chloride starting material. IR (film): ν = 3363, 2949, 2748, 2621, 1777, 1740, 1687, 1462, 1434, 1395, 1199, 1172, 1143; ¹H-NMR (500 MHz, CDCl₃): δ (ppm) = 8.89 (bs, 1H), 5.91 (m, 1H), 5.76 (m, 1H), 3.67 (m, 2H), 2.42 (td, J=3.01 Hz, J=13.99 Hz, 2H), 1.82-1.63 (m, 7H), 1.56 (s, 6H), 1.35 (s, 6H); ¹³C-NMR (500 MHz, CDCl₃): δ (ppm) = 15.9, 17.6, 21.3, 29.3, 36.7, 49.2, 65.9, 123.9, 132.9, 160.0 (q, TFA). HRMS (ESI): C₁₃H₂₅N (M+H) calculated: 196.2065, found 196.2091.

³ Paulini, K.; Reissig, H.-U. *Liebigs Annalen der Chemie* **1991**, *5*, 455.

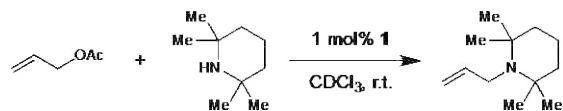


1-cinnamyl-2,2,6,6-tetramethylpiperidine TFA Salt (4i): Synthesized according to the general procedure I using 153 mg (1.0 mmol) cinnamyl chloride, 311 mg (2.2 mmol, 2.2 equiv) of 2,2,6,6-tetramethylpiperidine, and 9.4 mg (0.01 mmol, 1 mol%) 1 and purified on silica gel with 10% MeOH in DCM as eluent. The product thus obtained was treated with TFA (1 equiv) and isolated and characterized as the TFA salt. The product TFA salt was isolated as an orange oil (325mg, 87% yield). IR (film): ν = 3026, 2952, 1775, 1736, 1685, 1670, 1460, 1396, 1201; $^1\text{H-NMR}$ (500 MHz, CDCl_3): δ (ppm) = 8.12 (bs, 1H), 7.42-7.28 (m, 5H), 6.64 (d, $J=15.63$ Hz, 1H), 6.50-6.43 (m, 1H), 3.92-3.89 (m, 2H), 2.19 (t, $J=13.30$ Hz, 2H), 1.85-1.66 (m, 4H), 1.57 (s, 6H), 1.45 (s, 6H); $^{13}\text{C-NMR}$ (500 MHz, CDCl_3): δ (ppm) = 15.7, 21.2, 29.6, 37.1, 49.7, 66.4, 120.8, 126.9, 128.8, 128.9, 134.8, 136.6, 160.1 (q, TFA). HRMS (ESI): $\text{C}_{18}\text{H}_{27}\text{N}$ (M+H) calculated: 258.222, found 258.2247.

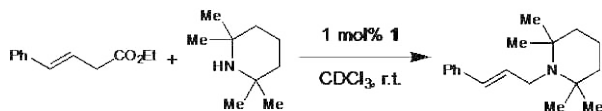


1-allyl-2,2,6,6-tetramethylpiperidine TFA Salt (4j): Synthesized according to general procedure I using 77 mg (1.0 mmol) allyl chloride, 311 mg (2.2 mmol, 2.2 equiv) of 2,2,6,6-tetramethylpiperidine, and 9.4 mg (0.01 mmol, 1 mol%) 1 and purified on silica gel with 10% MeOH in DCM as eluent. The product thus obtained was treated with TFA (1 equiv) and isolated and characterized as the TFA salt. The product TFA salt was isolated as an orange oil (247mg, 85% yield). IR (film): ν = 3407, 2987, 2953, 1736, 1686, 1671, 1461, 1437, 1396, 1200, 1141; $^1\text{H-NMR}$ (500 MHz, CDCl_3): δ (ppm) = 8.09 (bs, 1H), 6.17-6.06 (m, 1H), 5.39

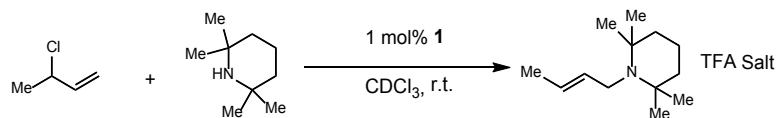
(d, $J=4.77$ Hz, 1H), 5.37 (s, 1H), 3.75-3.71 (m, 2H), 2.17 (td, $J=3.18$ Hz, $J=13.87$ Hz, 2H), 1.84-1.63 (m, 4H), 1.49 (s, 6H), 1.40 (s, 6H); ^{13}C -NMR (500 MHz, CDCl_3): δ (ppm) = 15.7, 21.0, 29.3, 36.8, 49.7, 66.3, 121.9, 130.6, 160.2 (q, TFA). HRMS (ESI): $\text{C}_{12}\text{H}_{23}\text{N}$ ($\text{M}+\text{H}$) calculated: 182.1909, found 182.1918.



1-allyl-2,2,6,6-tetramethylpiperidine 4j (Table 2, entry 11): Prepared according to general Procedure I using allyl acetate (0.10 g, 1 mmol), catalyst 1 (0.0093 g, 0.01 mmol), 2,2,6,6-tetramethylpiperidine (371 μL , 2.2 mmol, 2.2 equiv), and mesitylene (internal standard, 46 μL) in 1 mL CDCl_3 . The reaction was run at ambient temperature for 4.5 h and the yield (5.0%) determined by ^1H NMR analysis by comparison to an internal standard.



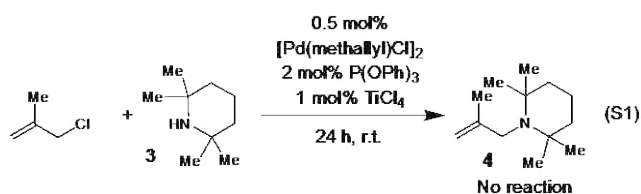
1-cinnamyl-2,2,6,6-tetramethylpiperidine 4i (Table 2, entry 12): Prepared according to general Procedure I using ethyl cinnamylcarbonate (0.206 g, 1 mmol), catalyst 1 (0.0093 g, 0.01 mmol), 2,2,6,6-tetramethylpiperidine (371 μL , 2.2 mmol, 2.2 equiv), and mesitylene (internal standard, 46 μL) in 1 mL CDCl_3 . The reaction was run at ambient temperature for 4.5 h and the yield (33.0%) determined by ^1H NMR analysis by comparison to an internal standard.



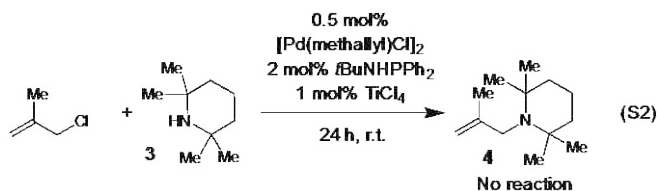
1-(but-2-en-1-yl)-2,2,6,6-tetramethylpiperidine TFA Salt (Table 2, Entry 13): Synthesized according to general procedure I using 91 mg (1.0 mmol) 3-chloro-1-butene, 311 mg (2.2

mmol, 2.2 equiv) of 2,2,6,6-tetramethylpiperidine, and 9.4 mg (0.01 mmol, 1 mol%) 1 and purified on silica gel with 10% MeOH in DCM as eluent. The product thus obtained was treated with TFA (1 equiv) and isolated and characterized as the TFA salt. The product TFA salt was isolated as a pale yellow oil (78% yield by internal standard). The product consisted of ~1.3:1 mixture of trans/cis isomers. The product obtained was the same as in reaction 4h.

III. Control Studies:

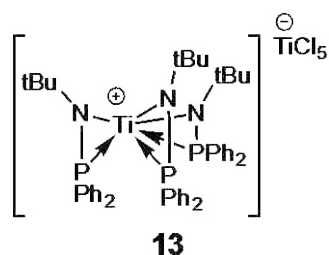


Control Study with P(OPh)₃ + TiCl₄ (Eq. S2): In a glove box, into a 3 dram vial was placed [Pd(methallyl)Cl]₂ (2.0 mg, 0.005 mmol), AgOTf (2.6 mg, 0.01 mmol), and triphenylphosphite (6.2 mg, 0.02 mmol). The mixture was dissolved in 1 ml CDCl₃, and the reaction stirred 20 min. Titanium tetrachloride (1.7 mg, 0.01 mmol) was then added and the mixture allowed to stir 5 minutes. 2,2,6,6-Tetramethylpiperidine (310 mg, 2.2 mmol) was then added, followed by methallyl chloride (92.5 mg, 1.0 mmol). The reaction mixture was then transferred to an NMR tube and the reaction progress monitored by ¹H NMR. The reaction proceeded to 22% conversion after 2 hrs and then conversion stalled, leading to no further conversion after 24 hrs.



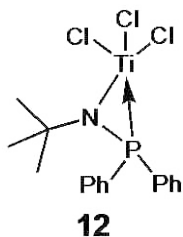
Control Study with *t*-BuNHPPH₂ + TiCl₄: In a glove box, into a 3 dram vial was placed [Pd(methallyl)Cl]₂ (2.0 mg, 0.005 mmol), AgOTf (2.6 mg, 0.01 mmol), and *N*-*tert*-butyldiphenylphosphinoamine (2.6 mg, 0.02 mmol). The mixture was dissolved in 1 ml CDCl₃, and the reaction stirred 20 min. Titanium tetrachloride (1.7 mg, 0.01 mmol) was then added and the mixture allowed to stir 5 minutes. 2,2,6,6-Tetramethylpiperidine (310 mg, 2.2 mmol) was then added, followed by methallyl chloride (92.5 mg, 1.0 mmol). The reaction mixture was then transferred to an NMR tube and the reaction progress monitored by ¹H NMR. No product formation was observed, even after 24 hrs.

IV. Synthesis of Titanium-containing ligands 12 and 13.



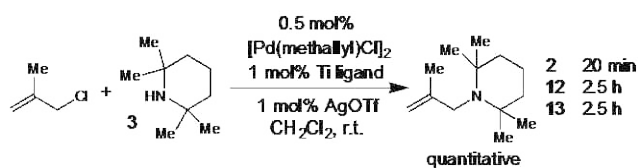
Titanium Tris(*N*-*tert*-butyl(diphosphino)amide) pentachlorotitanate (13): In a dry 100 ml round bottom flask 1.33 g (5.0 mmol) of phosphinoamine (Ph₂PNHtBu) was dissolved in 90 ml dry Et₂O. A hexane solution of 1.6 M *n*-BuLi (2.5 ml) was added dropwise at -78 C. The solution was warmed to room temperature and stirred for two hours. TiCl₄ (0.23 ml, 2.09 mmol) was slowly added dropwise, which caused precipitation of an orange/yellow solid. The reaction was taken into a glove box and filtered under air and moisture free conditions. The precipitate was filtered off, dissolved in 15 ml DCM in a 5 dram vial, and placed in a larger vial containing hexanes. The product was allowed to crystallize from the solution via slow vapor deposition. This process afforded the desired titanium tris(*N*-*tert*-butyl(diphosphino)amide) as the titanium pentachloride salt. Red solid, 0.280 g, 31%

yield. ^1H NMR (300 MHz, CDCl_3): δ (ppm) 7.474-7.272 (m, 9H), 7.262-7.037 (m, 9H), 6.809-6.699 (m, 6H), 6.581-6.485 (m, 6H), 1.613 (s, 27H); ^{13}C NMR (300 MHz, CDCl_3): δ (ppm) 136.393, 134.051, 132.235, 129.068, 128.084, 127.107, 126.684, 62.570, 62.422, 33.873; ^{31}P NMR (300 MHz, CDCl_3): δ (ppm) -15.919. Structure was confirmed by single Crystal X-ray analysis.



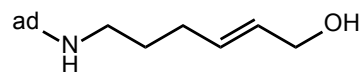
Trichlorotitanium *N-tert*-butyl(diphenylphosphino)amide (12): The red ether filtrate obtained after removal of the yellow solids above was next concentrated under vacuum in the glove box. Toluene (~50 ml) was then added to the resulting red solid, and any insoluble materials were filtered off. The toluene solution was concentrated until the volume reached about 5–7 ml. It was then layered with hexanes and placed in a -40 °C freezer for about 24hrs. The dark red crystals thus obtained were collected and dried under vacuum, affording trichlorotitanium *N-tert*-butyl(diphenylphosphino)amide, 0.120 g, 14% yield (45% total yield of both ligands). ^1H NMR (300 MHz, CDCl_3): δ (ppm) 7.94-7.74 (m, 4H), 7.67-7.47 (m, 6H), 1.59 (s, 9H); ^{13}C NMR (300 MHz, CDCl_3) δ (ppm) 133.738, 133.566, 132.120, 132.078, 129.270, 129.114, 32.576, 32.541; ^{31}P NMR (300 MHz, CDCl_3): δ (ppm) -10.994. Structure was confirmed by single Crystal X-ray analysis.

Scheme 1. Procedure:



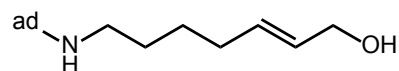
Procedure for *in situ* formation of bimetallic catalysts with ligands 2, 12, and 13. In a glove box, into a 3 dram vial with a stir bar was weighed ligand 2 (6.3 mg, 0.01 mmol) , 12 (8.2 mg, 0.02 mmol) or 13 (10.4 mg, 0.01 mmol), followed by [Pd(methallyl)Cl]₂ (2.0 mg, 0.005 mmol), and silver triflate (2.6 mg, 0.01 mmol). The mixture was then dissolved in DCM and allowed to stir for 30 minutes. 2,2,6,6-Tetramethylpiperidine (.371 ml, 2.2 mmol), followed by methallyl chloride (0.10 ml, 1.0 mmol) were then added and the reaction progress was monitored by removing a small aliquot from each reaction vial, diluting in 0.7 ml of CDCl₃, and then by ¹H NMR analysis of the crude reaction mixture. Complete conversion to the product was observed in 20 min, 2.5 h, and 2.5 h for ligands 1, 12, and 13 respectively.

V. Synthesis of alcohol substrates for Intramolecular Aminations

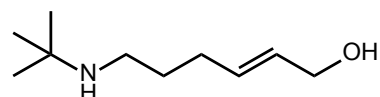


6-((adamantan-2-yl)amino)hex-2-en-1-ol (S1): General Procedure A: Into a 100 ml round bottom flask was placed 6-bromohex-2-en-1-ol (500 mg, 2.8 mmol) in 20 ml DMF. Diisopropylethylamine (1.46 ml, 8.4 mmol, 3 equiv) and 1-adamantylamine (210 mg, 14.0 mmol, 5 equiv) were then added. After stirring at room temperature for 40 hours, the solvent was removed, and the product purified on a column of silica gel. The product was eluted with 5% MeOH in DCM saturated with NH₃, and isolated as a white solid (0.335 mg, 48% yield). Melting Point: 75-80°C. IR (film): ν = 3246, 2902, 1451, 1024; ¹H-NMR (500 MHz, CDCl₃): δ (ppm) = 5.72-5.61 (m, 2H), 4.07 (d, J=4.80 Hz, 2H), 2.58 (t, J=7.32, 2H), 2.12-2.03 (m, 5H), 1.69-1.51 (m, 16H); ¹³C-NMR (500 MHz, CDCl₃): δ (ppm) = 29.6, 30.2, 30.5, 36.7, 39.9,

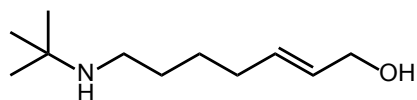
42.7, 50.5, 63.4, 129.4, 132.5. HRMS (ESI): C₁₆H₂₇NO (M+H) calculated: 250.2171, found 250.2181.



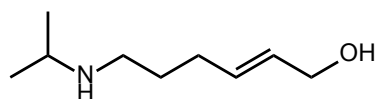
7-((adamantan-2-yl)amino)hex-2-en-1-ol (S2): Synthesized according to general procedure A using 1.5 g (7.77 mmol) 7-bromohept-2-en-1-ol, 4.06 ml (23.3 mmol, 3 equiv) of diisopropylethylamine, and 5.88 g (38.8 mmol, 5 equiv) 1-adamantylamine and purified on silica gel with 5% MeOH in DCM saturated with NH₃ as eluent. The product was isolated as a yellow solid, 1.15 g (56% yield). (Melting Point: 69-71 °C). IR (film): ν = 2905, 2848, 1452, 1098; ¹H-NMR (500 MHz, CDCl₃): δ (ppm) = 5.72-5.60 (m, 2H), 4.08 (d, J=5.07 Hz, 2H), 2.57 (t, J=7.20 Hz, 2H), 2.09-2.04 (m, 5H), 1.70-1.58 (m, 12H), 1.50, 1.38 (m, 4H); ¹³C-NMR (500 MHz, CDCl₃): δ (ppm) = 27.0, 29.6, 30.5, 32.1, 36.8, 40.2, 42.6, 42.7, 50.4, 63.6, 129.4, 132.9. HRMS (ESI): C₁₇H₂₉NO (M+H) calculated: 264.2327, found 264.2320.



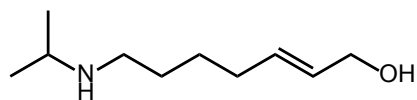
6-(*tert*-butylamino)hex-2-en-1-ol (S3): Synthesized according to general procedure using 1.39 g (7.77 mmol) 6-bromohex-2-en-1-ol, 4.06 ml (23.3 mmol, 3 equiv) of diisopropylethylamine, and 2.84 ml (38.8 mmol, 5 equiv) *tert*-butylamine and purified on silica gel with 5% MeOH in DCM saturated with NH₃ as eluent. The product was isolated as an orange oil (1.134 g, 85.3% yield). IR (film): ν = 3273, 2966, 2931, 2856, 1456, 1364, 1215, 1092, 1020, 967; ¹H-NMR (500 MHz, CDCl₃): δ (ppm) = 5.75-5.62 (m, 2H), 4.09 (d, J=5.12 Hz, 2H), 2.55 (t, J=7.28 Hz, 2H), 2.10 (q, J=6.96 Hz, 2H), 1.55 (p, J=7.55 Hz, 2H), 1.10 (s, 9H); ¹³C-NMR (500 MHz, CDCl₃): δ (ppm) = 29.0, 30.2, 30.4, 42.1, 50.3, 63.6, 129.4, 132.6. HRMS (ESI): C₁₀H₂₁NO (M+H) calculated: 172.1701, found 172.1728.



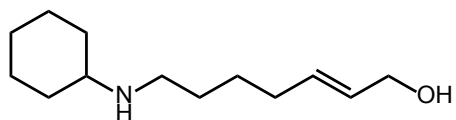
7-(*tert*-butylamino)hept-2-en-1-ol (S4): Synthesized according to general procedure using 500 mg (2.6 mmol) 7-bromohept-2-en-1-ol, 1.4 ml (7.8 mmol, 3 equiv) of diisopropylethylamine, and 1.28 ml (13.0 mmol, 5 equiv) *tert*-butylamine and purified on silica gel with 5% MeOH in DCM saturated with NH₃ as eluent. The product was isolated as a orange oil (414 mg, 86% yield) IR (film): ν = 3275, 2965, 2928, 2855, 1440, 1363, 1231, 1020, 970; ¹H-NMR (500 MHz, CDCl₃): δ (ppm) = 5.70-5.59 (m, 2H), 4.06 (d, J=4.37 Hz, 2H), 2.56 (t, J=7.36 Hz, 2H), 2.52-2.35 (bs, 1H), 2.06 (q, J=6.33 Hz, 2H), 1.54-1.46 (m, 2H), 1.46-1.38 (m, 2H), 1.12 (s, 9H); ¹³C-NMR (500 MHz, CDCl₃): δ (ppm) = 26.9, 28.6, 29.9, 32.0, 42.2, 50.9, 63.4, 129.7, 132.5. HRMS (ESI): C₁₁H₂₃NO (M+H) calculated: 186.1858, found 186.1890.



6-(isopropylamino)hex-2-en-1-ol (S5): Synthesized according to general procedure A using 1.39 g (7.77 mmol) 6-bromohex-2-en-1-ol, 4.06 ml (23.3 mmol, 3 equiv) of diisopropylethylamine, and 2.3 ml (38.8 mmol, 5 equiv) isopropylamine and purified on silica gel with 5% MeOH in DCM saturated with NH₃ as eluent. The product was isolated as a white solid (1.033 g, 85% yield). Melting Point: 28-32°C. IR (film): ν = 3273, 2931, 2847, 1471, 1382, 1175, 1092, 1017, 970; ¹H-NMR (500 MHz, CDCl₃): δ (ppm) = 5.71-5.60 (m, 2H), 4.05 (d, J=4.32 Hz, 2H), 2.78 (sept, J=6.25 Hz, 1H), 2.59 (t, J=7.48 Hz, 2H), 2.08 (q, J=6.78 Hz, 2H), 1.57 (p, J=7.29 Hz, 2H), 1.05 (d, J=6.29 Hz, 6H); ¹³C-NMR (500 Mhz, CDCl₃): δ (ppm) = 22.8, 29.6, 30.1, 46.9, 48.7, 62.8, 130.0, 131.5. HRMS (ESI): C₉H₁₉NO (M+H) calculated: 158.1545, found 158.1568.



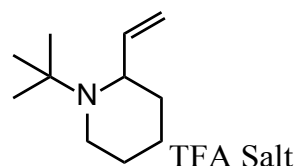
7-(isopropylamino)hept-2-en-1-ol (S6): Synthesized according to general procedure A using 500 mg (2.6 mmol) 7-bromohept-2-en-1-ol, 1.4 ml (7.8 mmol, 3 equiv) of diisopropylethylamine, and 1.12 ml (13.0 mmol, 5 equiv) isopropylamine and purified on silica gel with 5% MeOH in DCM saturated with NH_3 as eluent. The product was isolated as a white solid (395 mg, 89% yield, Melting Point: 46-48°C). IR (film): $\nu = 3273, 2965, 2929, 2854, 1458, 1382, 1339, 1174, 1088, 1015, 970$; $^1\text{H-NMR}$ (500 MHz, CDCl_3): δ (ppm) = 5.69-5.58 (m, 2H), 4.03 (d, $J=4.37$ Hz, 2H), 2.78 (sept, $J=6.21$ Hz, 1H), 2.57 (t, $J=7.42$ Hz, 2H), 2.05 (q, $J=6.27$ Hz, 2H), 1.53-1.45 (m, 2H), 1.45-1.37 (m, 2H), 1.05 (d, $J=6.35$, 6H); $^{13}\text{C-NMR}$ (500 MHz, CDCl_3): δ (ppm) = 22.7, 26.8, 29.5, 32.0, 47.1, 48.6, 62.7, 129.9, 131.7. HRMS (ESI): $\text{C}_{10}\text{H}_{21}\text{NO}$ (M+H) calculated: 172.1701, found 172.1728.



7-(cyclohexylamino)hept-2-en-1-ol (S7): Synthesized according to general procedure A using 500 mg (2.6 mmol) 7-bromohept-2-en-1-ol, 1.4 ml (7.8 mmol, 3 equiv) of diisopropylethylamine, and 1.49 ml (13.0 mmol, 5 equiv) cyclohexylamine and purified on silica gel with 5% MeOH in DCM saturated with NH_3 as eluent. The product was isolated as a white solid (519 mg, 95% yield, Melting Point: 66-69°C). IR (film): $\nu = 3255, 2963, 2928, 1260, 1090, 1021, 799$; $^1\text{H-NMR}$ (500 MHz, CDCl_3): δ (ppm) = 5.70-5.59 (m, 2H), 4.06 (d, $J=4.83$ Hz, 2H), 2.60 (t, $J=7.39$ Hz, 2H), 2.42-2.35 (m, 1H), 2.05 (q, $J=7.04$ Hz, 2H), 1.86 (d, $J=12.53$ Hz, 2H), 1.75-1.68 (m, 2H), 1.65-1.57 (m, 1H), 1.52-1.36 (m, 4H), 1.30-0.99 (m,

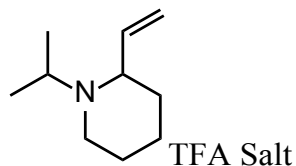
5H); ^{13}C -NMR (500 MHz, CDCl_3): δ (ppm) = 25.3, 26.3, 27.1, 30.1, 32.2, 33.8, 46.9, 57.1, 63.6, 129.7, 132.8. HRMS (ESI): $\text{C}_{13}\text{H}_{25}\text{NO}$ ($\text{M}+\text{H}$) calculated: 212.2014, found 212.2045.

VI. Intramolecular Amination Reaction



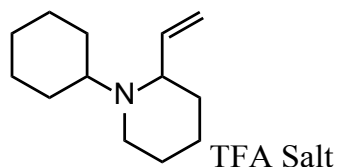
1-(*tert*-butyl)-2-vinylpiperidine TFA Salt (14a): General Procedure B. Into a 3 dram vial was containing a stir bar was placed 60 mg (0.32 mmol) 7-(*tert*-butylamino)hept-2-en-1-ol in 2 ml DCM. Thionyl chloride (0.03 ml, 0.38 mmol, 1 equiv) was slowly added at 0 °C. After stirring at room temperature for 1 hour, the solvent was removed and the resulting chloride was azeotroped with benzene by adding 2 ml benzene and then removing the solvent on the rotary evaporator. The vial containing the chloride was then taken into a glovebox. Next, 8.9 mg (0.009 mmol, 3 mol%) **1** was added and the reaction mixture dissolved in 1 ml DCM. Triethylamine (0.09 ml, 0.64 mmol, 2 equiv) was then added, the reaction was allowed to stir for 10 minutes, removed from the glove box, diluted with 1 ml DCM and loaded directly onto a column of silica gel and eluted with 10% MeOH:H₂O (10:1) in DCM. Due to the volatility of the products, the fractions containing the product were combined, treated with TFA (5 equiv) and the solvent removed *in vacuo*. The product TFA salt was isolated as a yellow oil as a hydrate/TFA adduct 131 mg. The yield was determined by addition of an internal standard (mesitylene) and then via analysis of the ^1H NMR spectrum. 84% yield. IR (film): ν = 2962, 1672, 1260, 1091, 1021, 799; ^1H -NMR (500 MHz, CDCl_3): δ (ppm) = 8.98 (bs, 1H),

6.37-6.27 (m, 1H), 5.51-5.44 (m, 2H), 4.48 (d, J=8.17 Hz, 1H), 3.46 (d, J=12.10 Hz, 1H), 3.10 (q, J=12.22 Hz, 1H), 2.51 (tt, J=4.33 Hz, J=14.18 Hz, 1H), 2.20-2.06 (m, 1H), 1.97 (d, J=14.48 Hz, 1H), 1.77-1.55 (m, 3H), 1.45 (s, 9H); ^{13}C -NMR (500 MHz, CDCl_3): δ (ppm) = 17.3, 23.5, 25.4, 32.1, 43.1, 60.8, 65.6, 121.9, 130.4. HRMS (ESI): $\text{C}_{11}\text{H}_{21}\text{N}$ (M+H) calculated: 168.1752, found 168.1776.



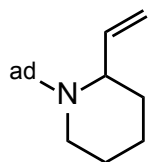
1-isopropyl-2-vinylpiperidine TFA Salt (14b): Synthesized according to general procedure B using 60 mg (0.35 mmol) 7-(isopropylamino)hept-2-en-1-ol, 0.03 ml (0.35 mmol, 1 equiv) thionyl chloride, 8.9 mg (.009 mmol, 3 mol%) of 1, and 0.09 ml (0.63 mmol, 2 equiv) triethylamine and purified on silica gel with 9:1 MeOH:H₂O in DCM. Due to the volatility of the products, the fractions containing the product were combined, treated with TFA (5 equiv) and the solvent removed *in vacuo*. The product TFA salt was isolated as a yellow oil as a hydrate/TFA adduct 168 mg. The yield was determined by addition of an internal standard (mesitylene) and then via analysis of the ^1H NMR spectrum. 83% yield. IR (film): ν = 2992, 2953, 1739, 1671, 1201, 1173, 1142; ^1H -NMR (500 MHz, CDCl_3): δ (ppm) = 13.60 (bs, 1H), 10.24 (bs, 1H), 6.20-6.09 (m, 1H), 5.42-5.35 (m, 2H), 3.83 (p, J=6.51 Hz, 1H), 3.53-3.37 (m, 2H), 2.62 (q, J=11.18 Hz, 1H), 2.17-2.05 (m, 2H), 1.97-1.88 (m, 2H), 1.84 (d, J=14.37 Hz, 1H), 1.54-1.44 (m, 1H), 1.41 (d, J=6.63 Hz, 3H), 1.17 (d, J=6.70 Hz, 3H); ^{13}C -NMR (500 MHz, CDCl_3): δ (ppm) = 13.2, 18.1, 22.5, 22.5, 30.7, 44.8, 53.6, 66.8, 121.4, 133.2. HRMS (ESI): $\text{C}_{10}\text{H}_{19}\text{N}$ (M+H) calculated: 154.1596, found 154.1614.

When this same reaction protocol was performed with the *in situ* generated catalyst, complete consumption of the starting material was also observed in <10 min.



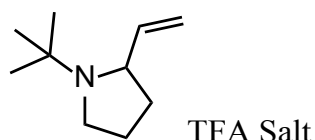
1-cyclohexyl-2-vinylpiperidine TFA Salt (14c): Synthesized according to general procedure B using 60 mg (0.28 mmol) 7-(cyclohexylamino)hept-2-en-1-ol, 0.02 ml (0.28 mmol, 1 equiv) thionyl chloride, 7.4 mg (.008 mmol, 3 mol%) of 1, and 0.07 ml (0.52 mmol, 2 equiv) triethylamine and purified on silica gel with 9:1 MeOH:H₂O in DCM. Due to the volatility of the products, the fractions containing the product were combined, treated with TFA (5 equiv) and the solvent removed *in vacuo*. The product TFA salt was isolated as a yellow oil as a hydrate/TFA adduct 125 mg. The yield was determined by addition of an internal standard (mesitylene) and then via analysis of the ¹H NMR spectrum. 82% yield. IR (film): ν = 2945, 2863, 1670, 1456, 1200, 1177, 1142, 910, 733; ¹H-NMR (500 MHz, CDCl₃): δ (ppm) = 10.07 (bs, 1H), 6.21-6.12 (m, 1H), 5.43-5.32 (m, 2H), 3.60-3.39 (m, 3H), 2.65 (q, J=11.91 Hz, 1H), 2.22-2.08 (m, 3H), 1.92-1.86 (m, 4H), 1.70 (d, J=13.29 Hz, 1H), 1.53-1.09 (m, 8H); ¹³C-NMR (500 MHz, CDCl₃): δ (ppm) = 22.5, 22.7, 23.8, 25.0, 25.3, 28.1, 30.7, 46.8, 61.9, 66.3, 121.3, 133.4. HRMS (ESI): C₁₃H₂₃N (M+H) calculated: 194.1909, found 194.1924.

When this same reaction protocol was performed with the *in situ* generated catalyst, complete consumption of the starting material was also observed in <10 min.



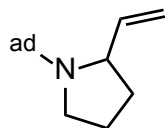
1-(adamantan-2-yl)-2-vinylpiperidine (14d): Synthesized according to general procedure C (see below) using 130 mg (0.50 mmol) 7-((adamantan-2-yl)amino)hex-2-en-1-ol, 0.04 ml (0.50 mmol, 1 equiv) thionyl chloride, 8.5 mg (.009 mmol, 2 mol%) of 1, and 0.13 ml (0.92

mmol, 2 equiv) triethylamine and purified on silica gel with 5% MeOH in DCM saturated with NH₃ as eluent. The product was isolated as an orange solid (106 mg, 93% yield. When this same reaction protocol was performed with the *in situ* generated catalyst, complete consumption of the starting material was also observed in <10 min. Melting Point: 61-65°C). IR (film): ν = 2929, 2905, 2849, 1260, 1099, 1021; ¹H-NMR (500 MHz, CDCl₃): δ (ppm) = 6.55-6.46 (m, 1H), 5.08-5.00 (m, 2H), 3.86-3.81 (m, 1H), 2.87 (d, J=12.12, 1H), 2.69-2.62 (m, 1H), 2.03 (s, 3H), 1.87-1.41 (m, 18H); ¹³C-NMR (500 MHz, CDCl₃): δ (ppm) = 20.5, 27.4, 29.9, 34.8, 36.9, 39.0, 40.1, 54.7, 55.7, 113.3, 140.1. HRMS (ESI): C₁₇H₂₇N (M+H) calculated: 246.2222, found 246.2238.

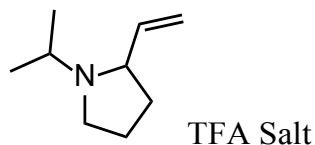


1-(*tert*-butyl)-2-vinylpyrrolidine TFA Salt (15a): Synthesized according to general procedure B using 60 mg (0.35 mmol) 6-(*tert*-butylamino)hex-2-en-1-ol, 0.03 ml (0.35 mmol, 1 equiv) thionyl chloride, 8.9 mg (.009 mmol, 3 mol%) of 1, and 0.09 ml (0.63 mmol, 2 equiv) triethylamine and purified on silica gel with 9:1 MeOH:H₂O in DCM. Due to the volatility of the product, the fractions containing the product were combined, treated with TFA (5 equiv) and the solvent removed *in vacuo*. The product TFA salt was isolated as a yellow oil as a hydrate/TFA adduct 158 mg. The yield was determined by addition of an internal standard (mesitylene) and then via analysis of the ¹H NMR spectrum. : 99% yield. IR (film): ν = 2963, 1673, 1260, 1092, 1020, 799; ¹H-NMR (500 MHz, CDCl₃): δ (ppm) = 13.24 (bs, 1H), 10.47 (bs, 1H), 6.32-6.22 (m, 1H), 5.36-5.30 (m, 2H), 4.00 (p, J=7.82 Hz, 1H), 3.84 (h, J=6.10 Hz, 1H), 3.17-3.08 (m, 1H), 2.25-1.92 (m, 4H), 1.44 (s, 9H); ¹³C-NMR (500 MHz, CDCl₃): δ

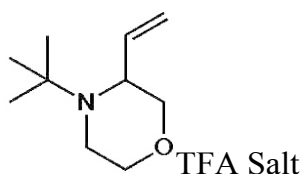
(ppm) = 23.3, 25.6, 32.9, 50.1, 63.0, 66.5, 119.9, 134.4. HRMS (ESI): C₁₀H₁₉N (M+H) calculated: 154.1596, found 154.1620.



1-(adamantan-2-yl)-2-vinylpyrrolidine (15b): General Procedure C: Into a 3 dram vial was placed 6-((adamantan-2-yl)amino)hex-2-en-1-ol (95 mg, 0.38 mmol) in 2 ml DCM. Thionyl chloride (0.03 ml, 0.38 mmol, 1 equiv) was slowly added at 0 °C. After stirring at room temperature for 1 hour, the solvent was removed and the resulting chloride was azeotroped with benzene by adding 2 ml benzene and then removing the solvent on the rotary evaporator. The vial containing the chloride was then taken into a glovebox. Next, 10 mg (0.01 mmol, 3 mol%) **1** was added and the reaction mixture dissolved in 1 ml DCM. Triethylamine (0.10 ml, 0.71 mmol, 2 equiv) was then added, the reaction was allowed to stir for 10 minutes, removed from the glove box, diluted with 1 ml DCM and loaded directly onto a column of silica gel and eluted with 5% MeOH in DCM saturated with NH₃. The product was isolated as an orange oil (79 mg, 96% yield). IR (film): ν = 2904, 2849, 1638, 1450, 1359, 1309, 994; ¹H-NMR (500 MHz, CDCl₃): δ (ppm) = 5.89 (p, J=8.55 Hz, 1H), 5.06 (d, J=17.03 Hz, 1H), 4.88 (d, J=10.09 Hz, 1H), 3.59 (s, 1H), 2.94 (s, 1H), 2.78 (q, J=8.75 Hz, 1H), 2.05 (s, 3H), 1.82-1.55 (m, 16H); ¹³C-NMR (500 MHz, CDCl₃): δ (ppm) = 23.9, 29.6, 33.3, 37.0, 40.0, 46.1, 58.2, 111.5, 146.1. HRMS (ESI): C₁₆H₂₅N (M+H) calculated: 232.2065, found 232.2080.



1-isopropyl-2-vinylpyrrolidine TFA Salt (15c): Synthesized according to general procedure B using 24.5 mg (0.155 mmol) 7-(*iso*-propylamino)hept-2-en-1-ol, 0.012 ml (0.155 mmol, 1 equiv) thionyl chloride, 4.4 mg (.0047 mmol, 3 mol%) of 1, and 0.043 ml (0.32 mmol, 2 equiv) triethylamine and purified on silica gel with 9:1 MeOH:H₂O in DCM. Due to the volatility of the products, the fractions containing the product were combined, treated with TFA (5 equiv) and the solvent removed *in vacuo*. The product TFA salt was isolated as a yellow oil as a hydrate/TFA adduct 45.9 mg. The yield was determined by addition of an internal standard (mesitylene) and then via analysis of the ¹H NMR spectrum. 98% yield (92% yield obtained using 0.06 g starting material alcohol). IR (film): ν = 2990, 2917, 1670, 1200, 1139; ¹H-NMR (500 MHz, CDCl₃): δ (ppm) = 10.06 (bs, 1H), 6.09-5.99 (m, 1H), 5.50-5.42 (m, 2H), 3.78-3.60 (m, 3H), 3.10-3.00 (m, 1H), 2.27-2.16 (m, 2H), 2.13-1.92 (m, 2H), 1.38 (d, J=6.64 Hz, 3H), 1.27 (d, J=6.62 Hz, 3H); ¹³C-NMR (500 MHz, CDCl₃): δ (ppm) = 14.9, 19.0, 21.5, 30.5, 46.8, 52.6, 67.8, 123.5, 131.3. HRMS (ESI): C₉H₁₇N (M+H) calculated: 140.1439, found 140.1457.

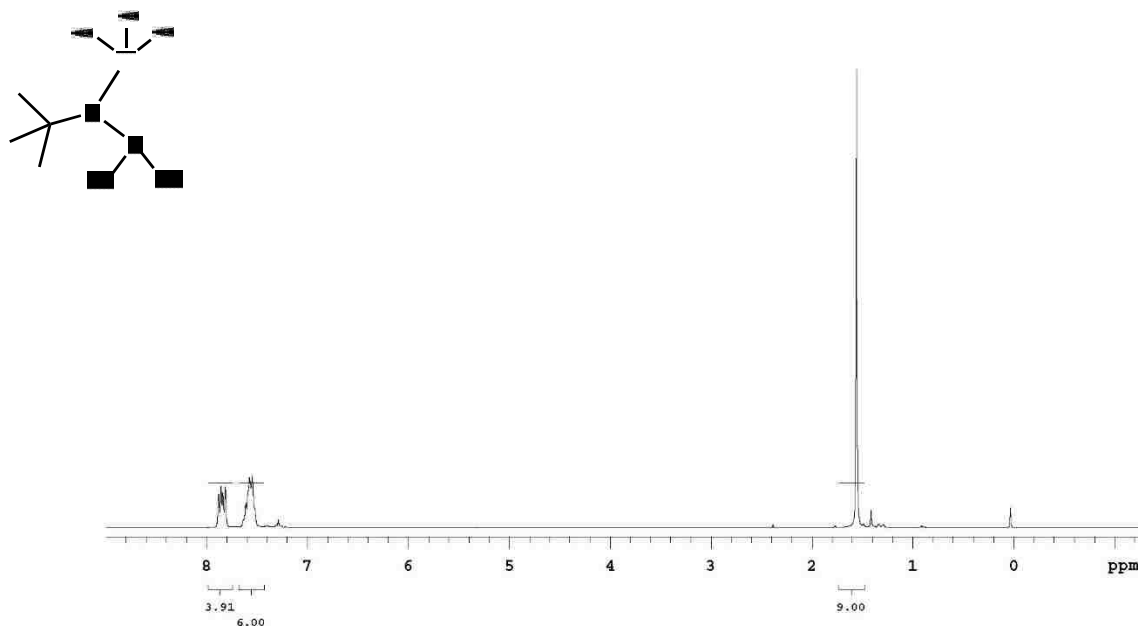


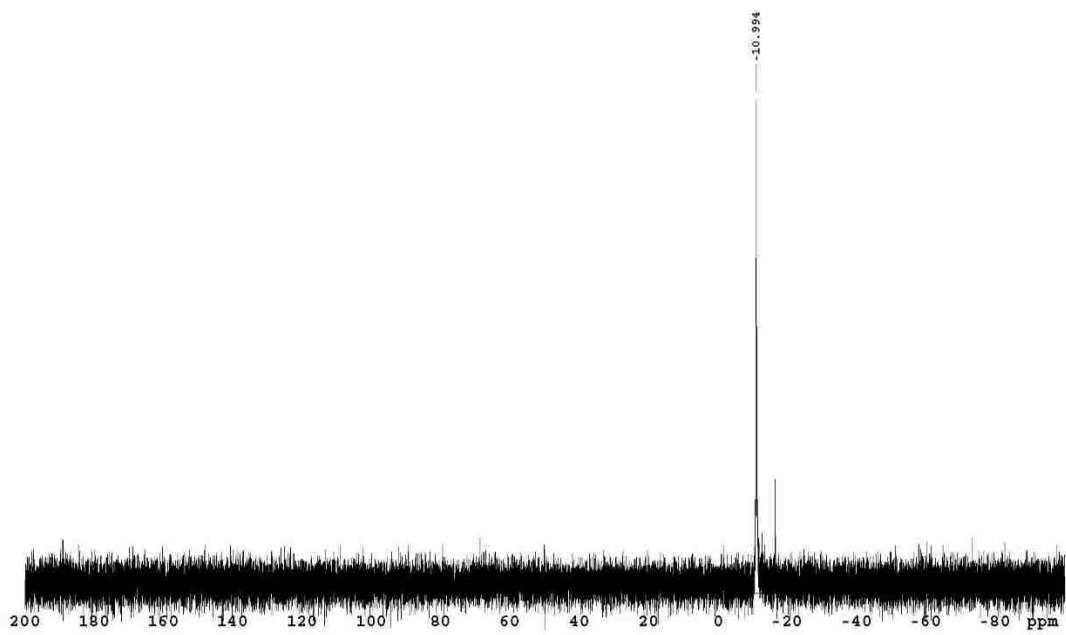
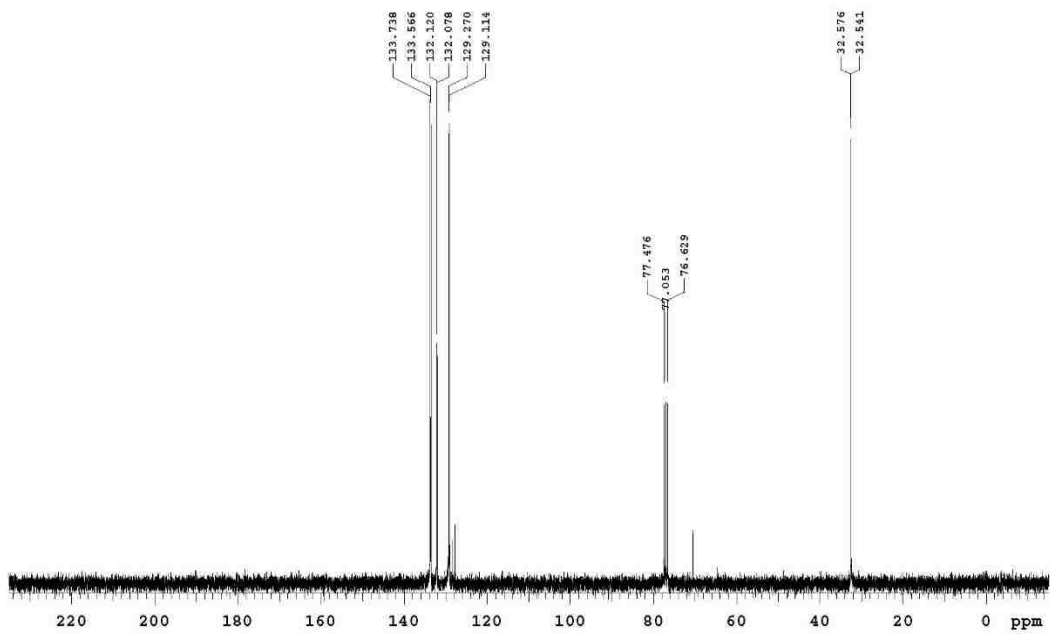
4-(*tert*-butyl)morpholine TFA Salt (16): Synthesized from the corresponding chloride as follows: In a glove box, into a 3 dram vial was placed 50 mg (0.24 mmol) N-(2-((4-chlorobut-2-en-1-yl)oxy)ethyl)-2-methylpropan-2-amine,⁴ 6.9 mg (.007 mmol, 3 mol%) of 1, 1 ml DCM, and finally 0.07 ml (0.48 mmol, 2 equiv) triethylamine. The reaction was stirred for 10 minutes, removed from the glove box, diluted with 1 ml DCM, and loaded directly onto a

⁴ Synthesized from *N-tert*-butylaminoethanol based on the following precedent: Arisawa, M.; Kato, C.; Kaneko, H.; Nishida, A.; Nakagawa, M. *J. Chem. Soc., Perkin Trans. 1*, **2000**, 12 1873.

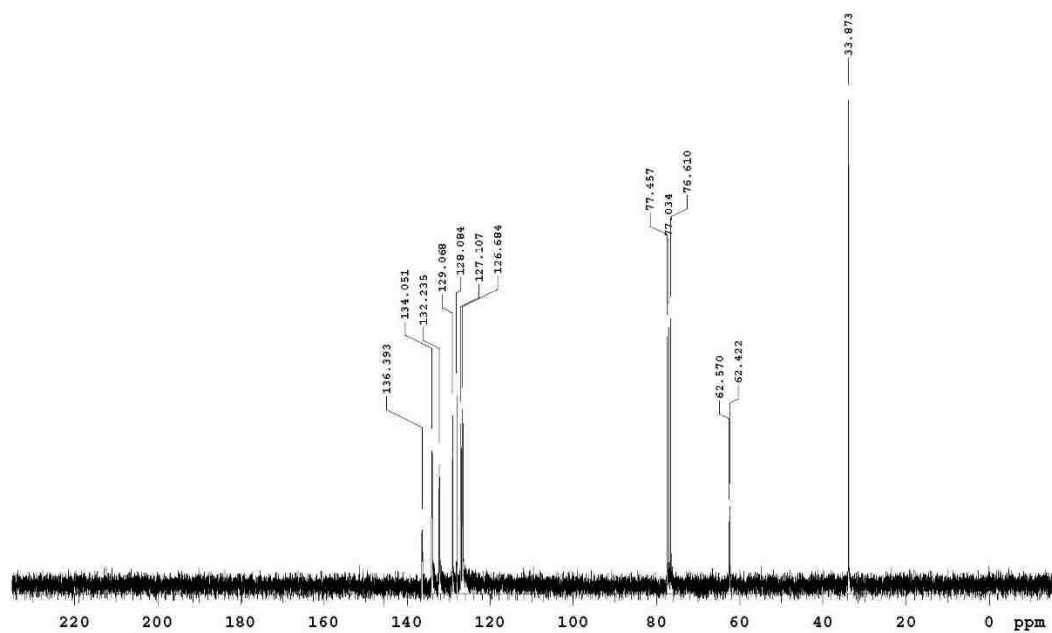
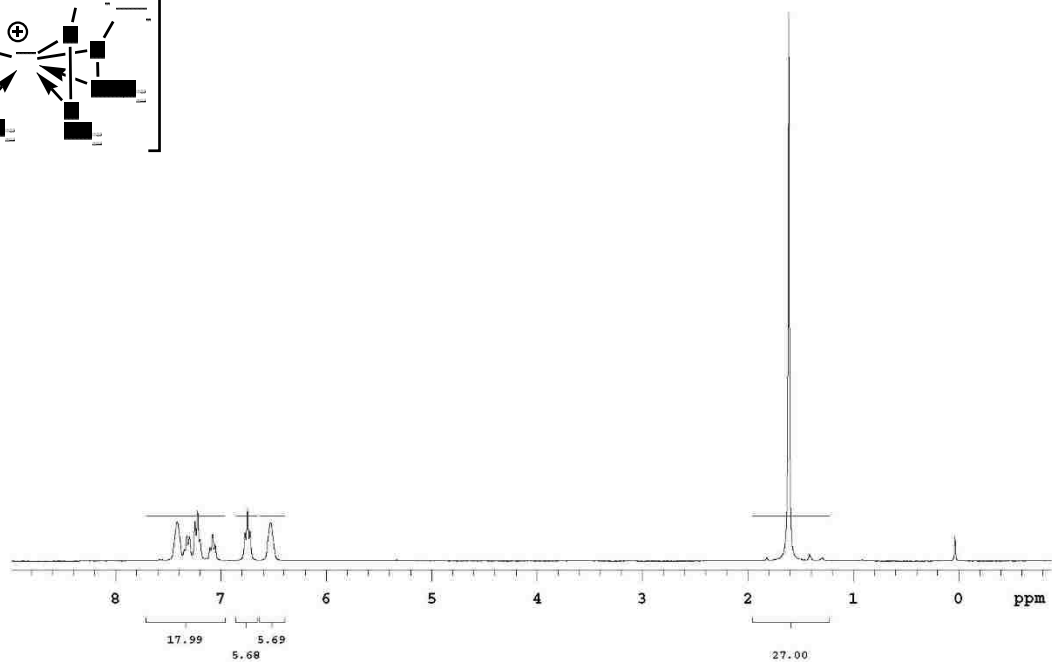
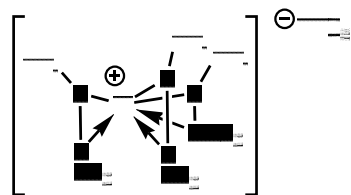
column of silica gel. The product was eluted with 9:1 MeOH:H₂O in DCM. Due to the volatility of the products, the fractions containing the product were combined, treated with TFA (5 equiv) and the solvent removed *in vacuo*. The product TFA salt was isolated as a yellow oil as a hydrate/TFA adduct 104 mg. The yield was determined by addition of an internal standard (mesitylene) and then via analysis of the ¹H NMR spectrum. 89% yield. IR (film): $\nu = 2988, 2918, 2877, 2768, 2636, 1671, 1383, 1202, 1136$; ¹H-NMR (500 MHz, CDCl₃): δ (ppm) = 10.65 (bs, 1H), 6.43-6.34 (m, 1H), 5.65-5.56 (m, 2H), 4.32 (d, J=10.10 Hz, 1H), 4.24 (d, J=13.07 Hz, 1H), 4.13-4.07 (m, 2H), 3.82 (d, J=13.00 Hz 1H), 3.41-3.28 (m, 2H), 1.46 (s, 9H); ¹³C-NMR (500 MHz, CDCl₃): δ (ppm) = 25.1, 26.3, 42.1, 60.1, 64.6, 71.6, 123.3, 129.9. HRMS (ESI): C₁₃H₂₃N (M+H) calculated: 170.1545, found 170.1565.

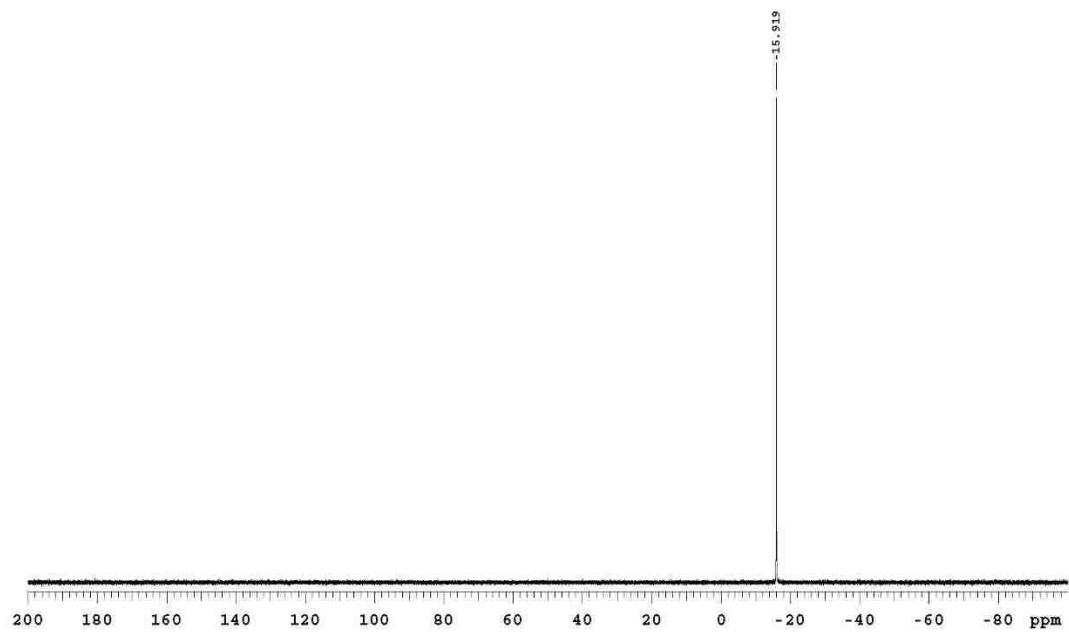
(*tert*-butyl(diphenylphosphanyl)amino)titanium(IV) trichloride (12):



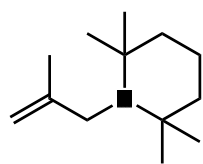


Titanium Tris(*N*-*tert*-butyl-diphenylphosphinoamide) pentachlorotitanate (13):

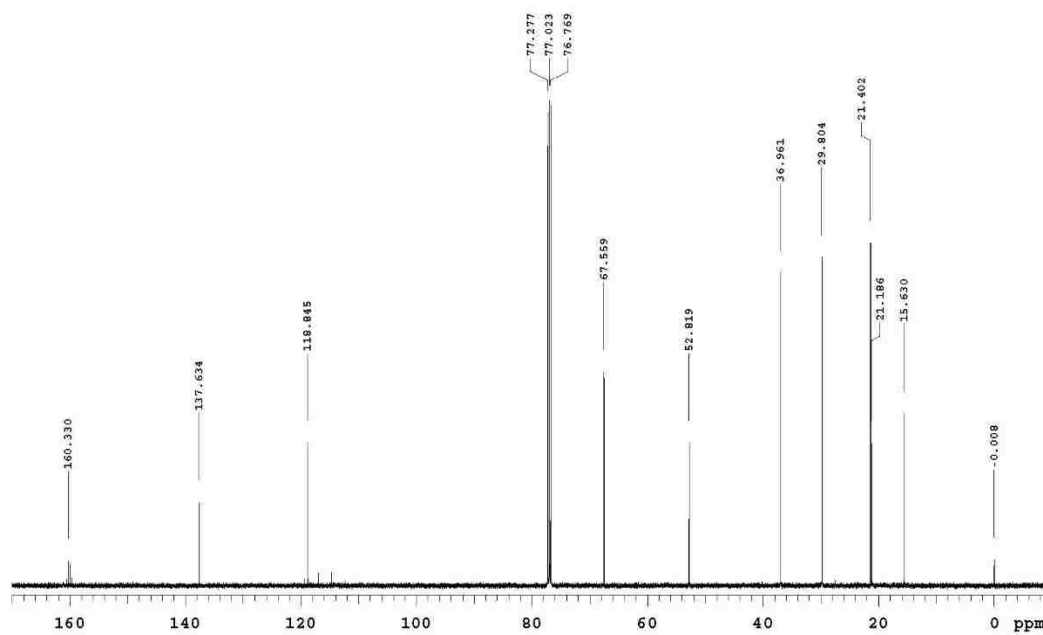
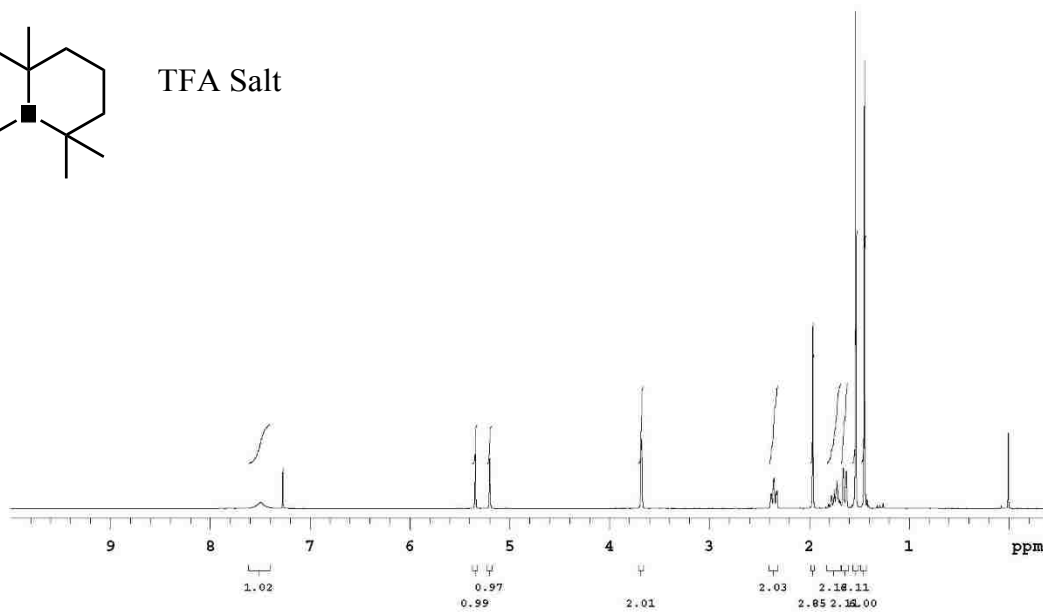




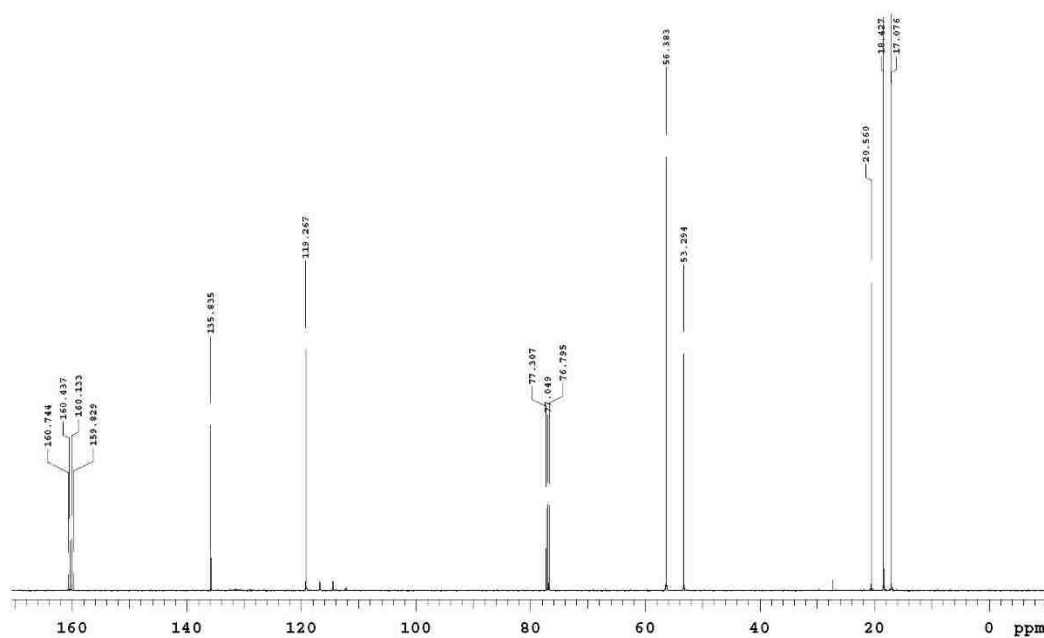
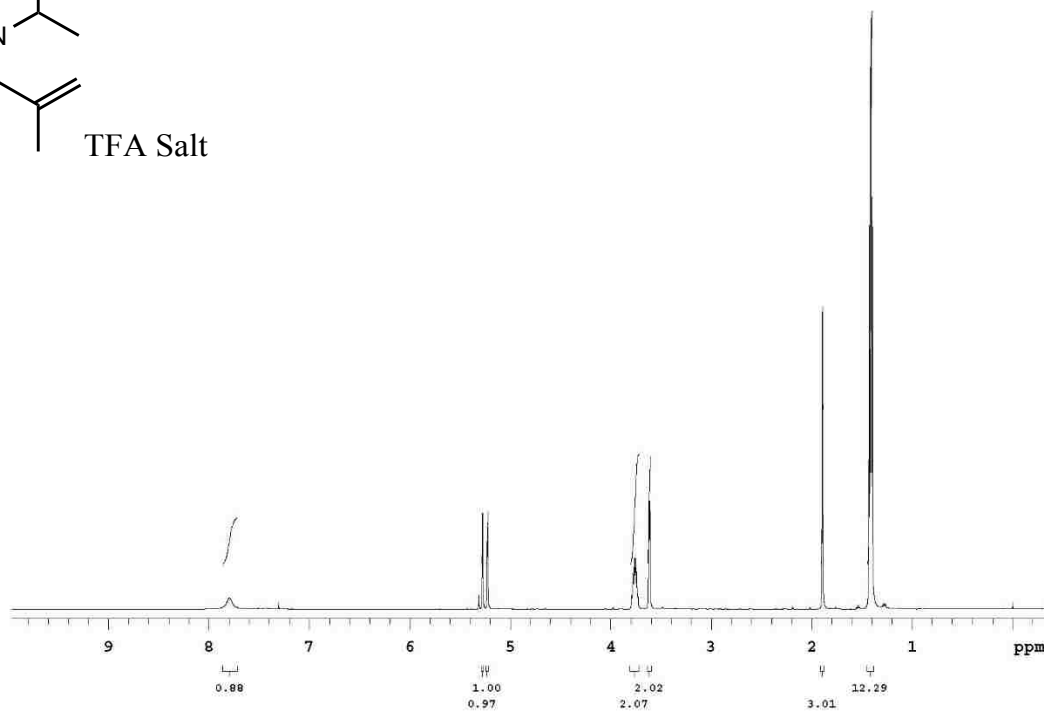
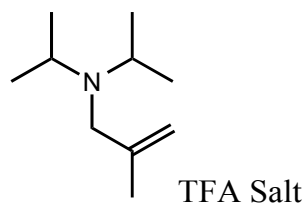
2,2,6,6-tetramethyl-1-(2-methylallyl)piperidine TFA Salt (4a):



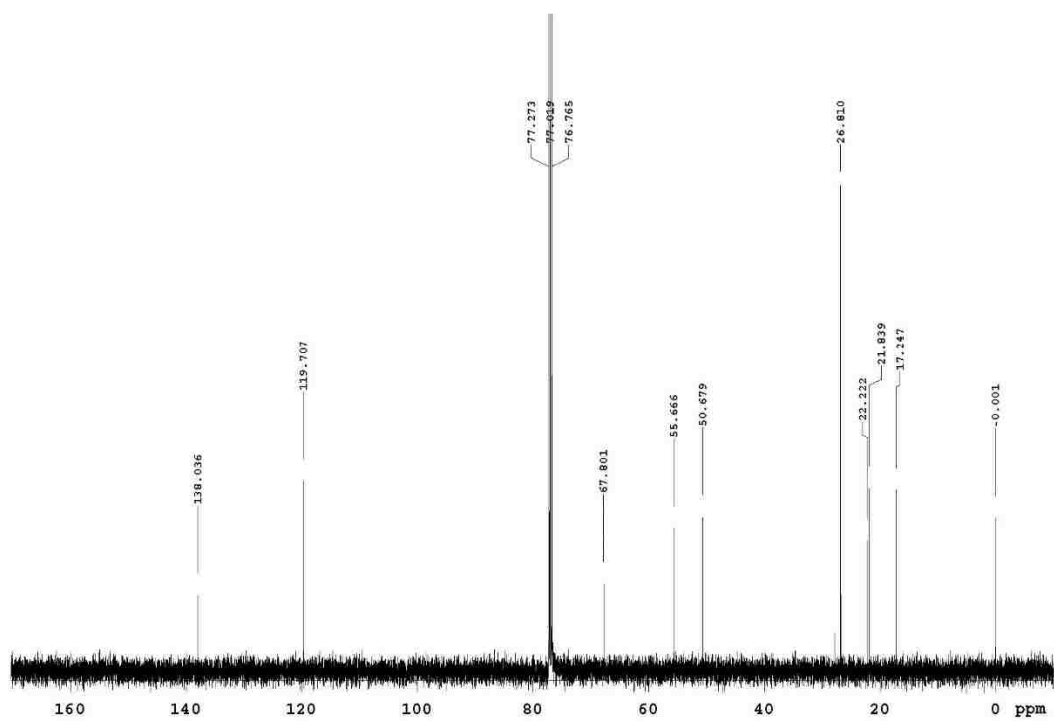
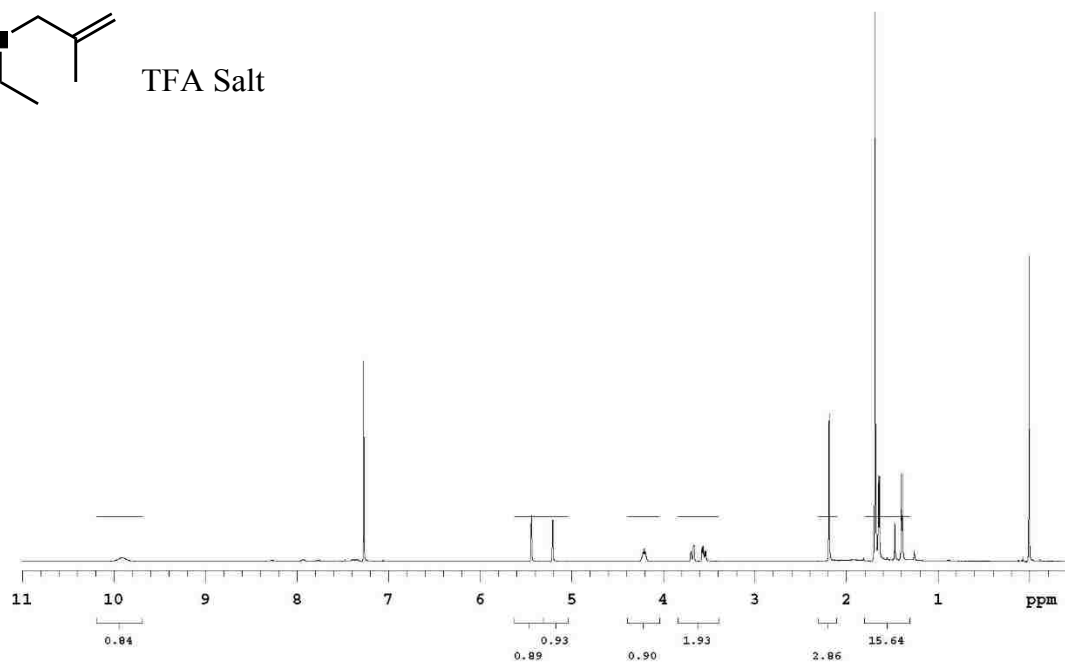
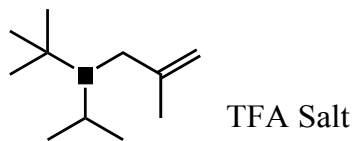
TFA Salt



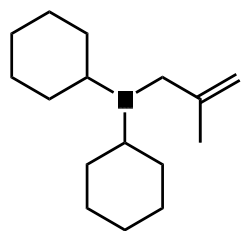
N,N-diisopropyl-2-methylprop-2-en-1-amine TFA Salt (4b):



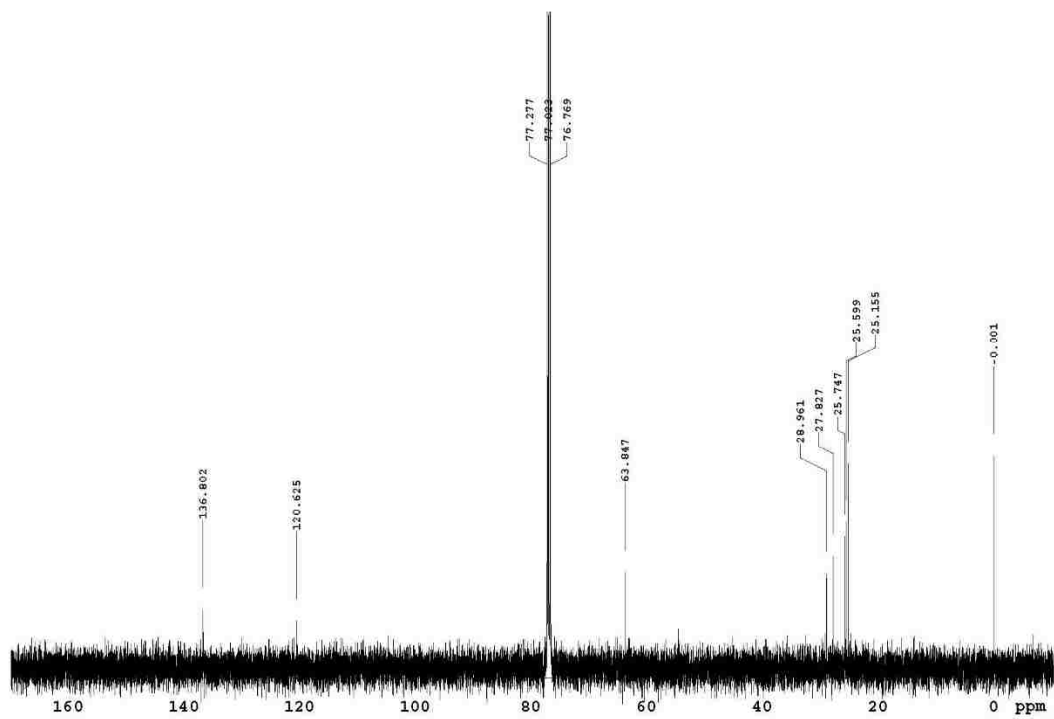
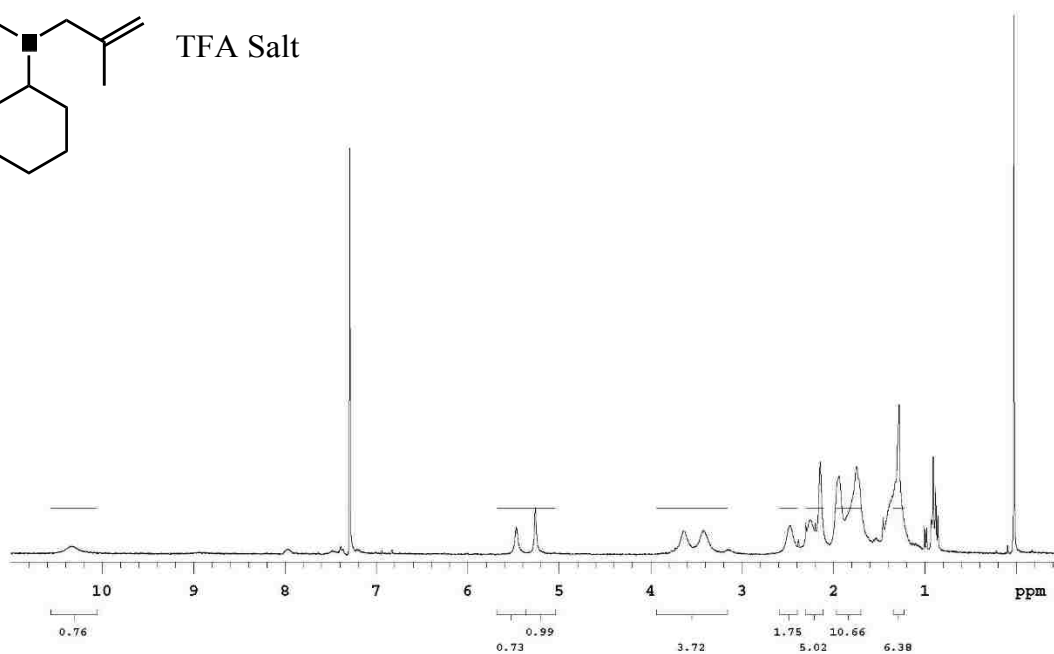
N-(*tert*-butyl)-N-isopropyl-2-methylprop-2-en-1-amine TFA Salt (4c):



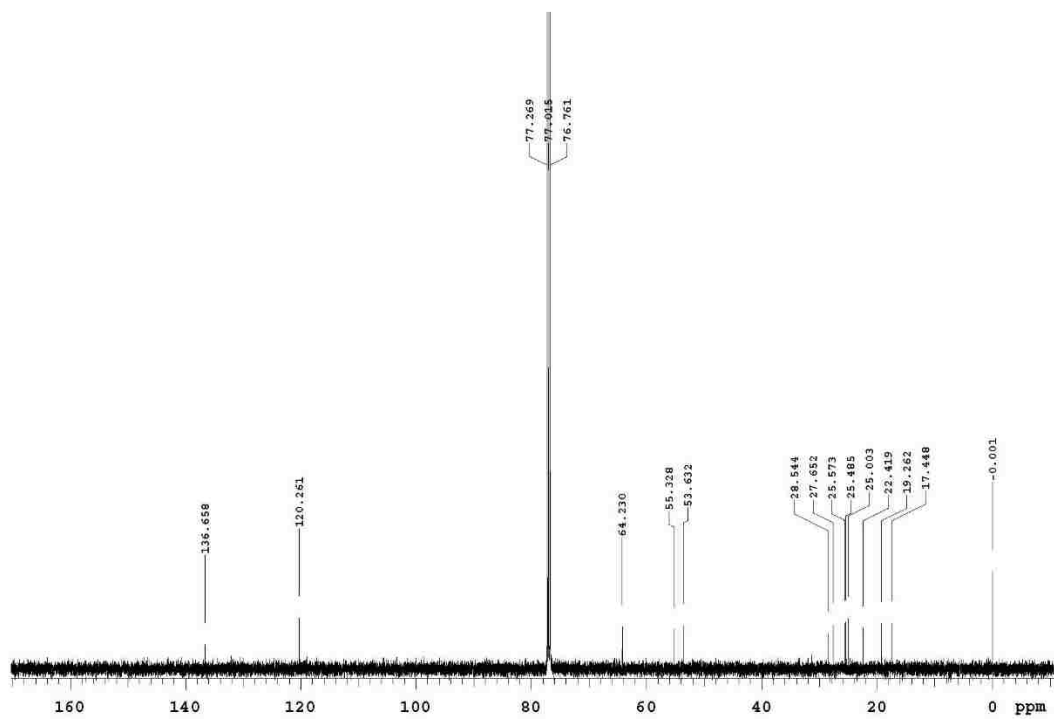
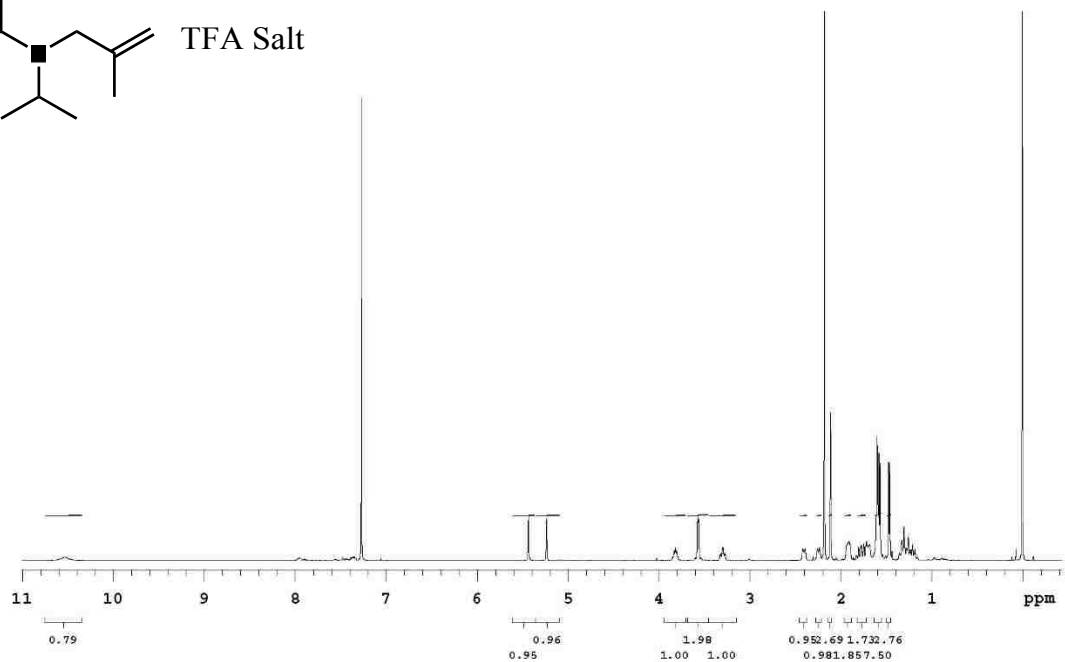
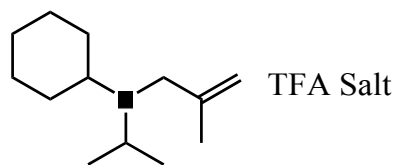
N-cyclohexyl-N-(2-methylallyl)cyclohexanamine TFA Salt (4d):



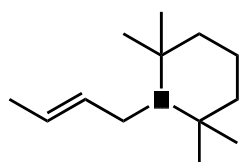
TFA Salt



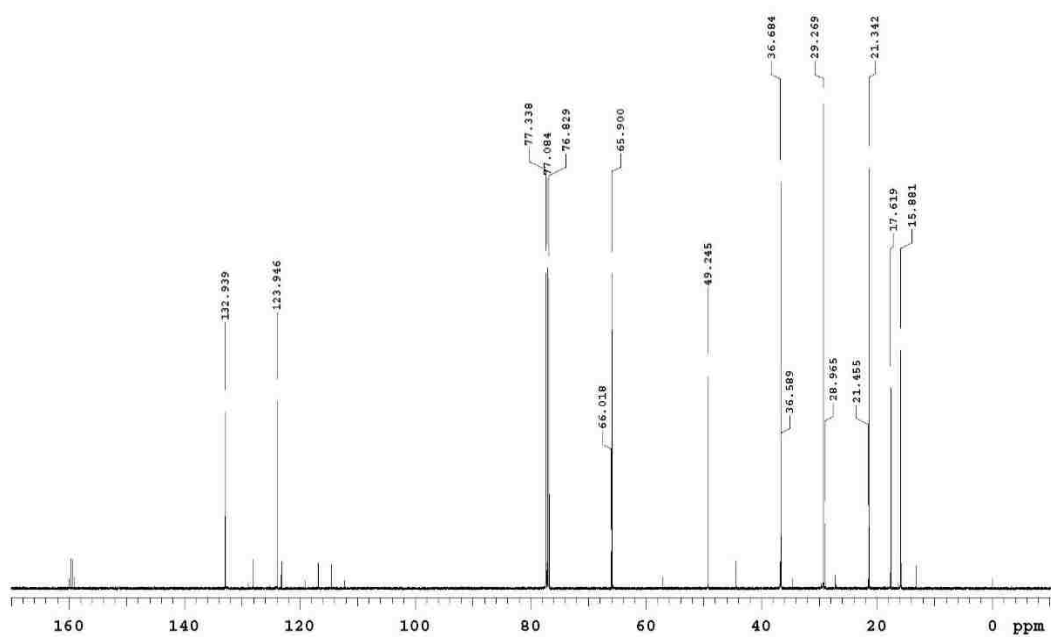
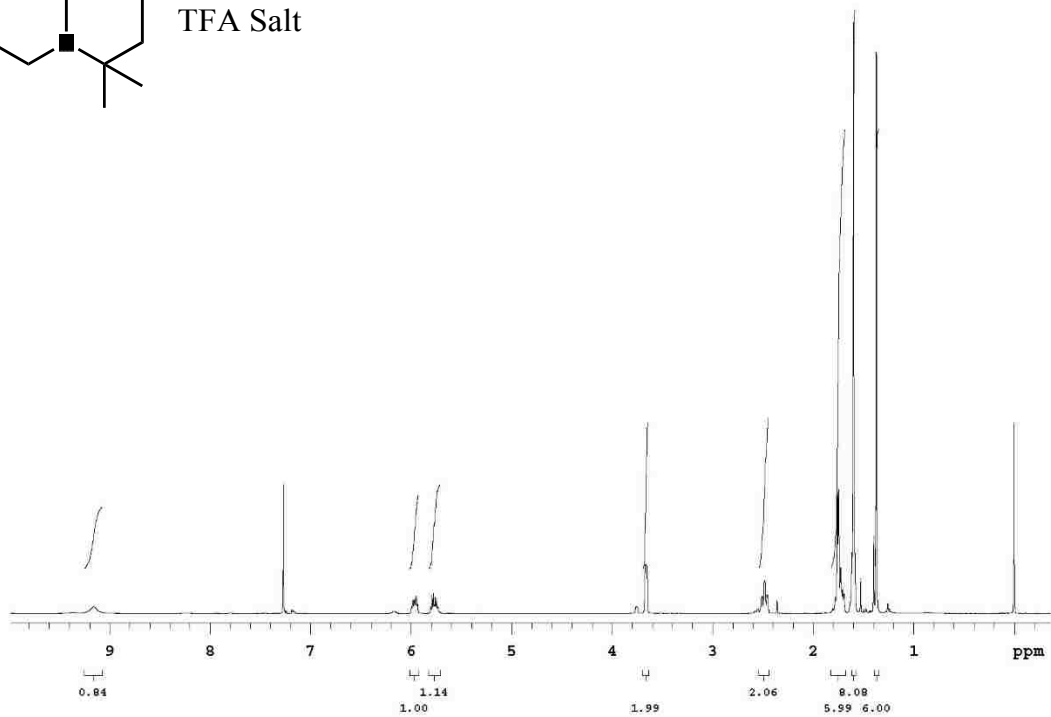
N-isopropyl-N-(2-methylallyl)cyclohexanamine TFA Salt (4e):



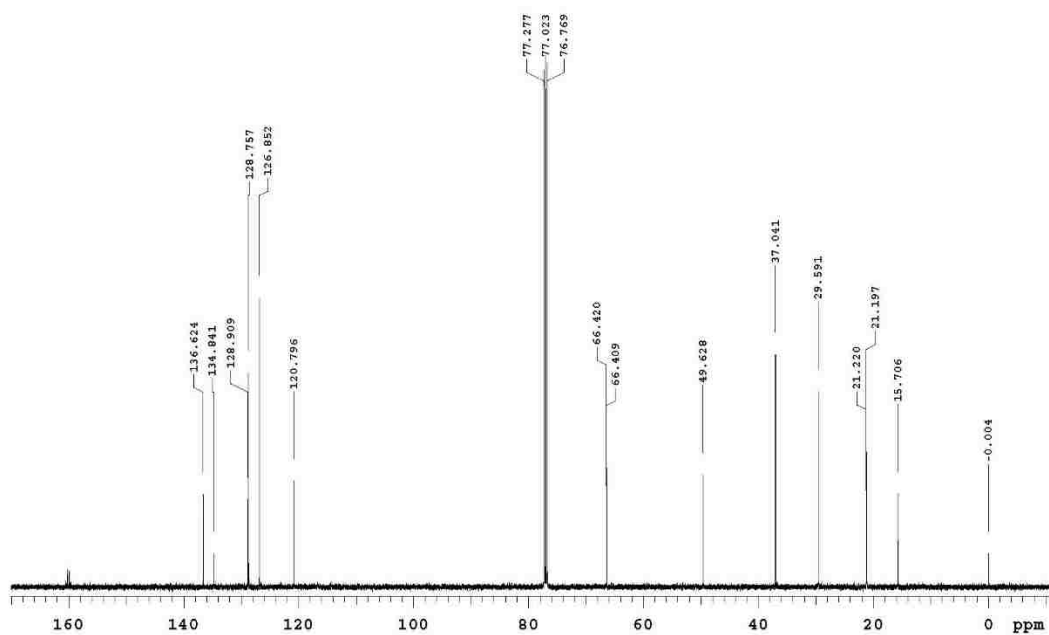
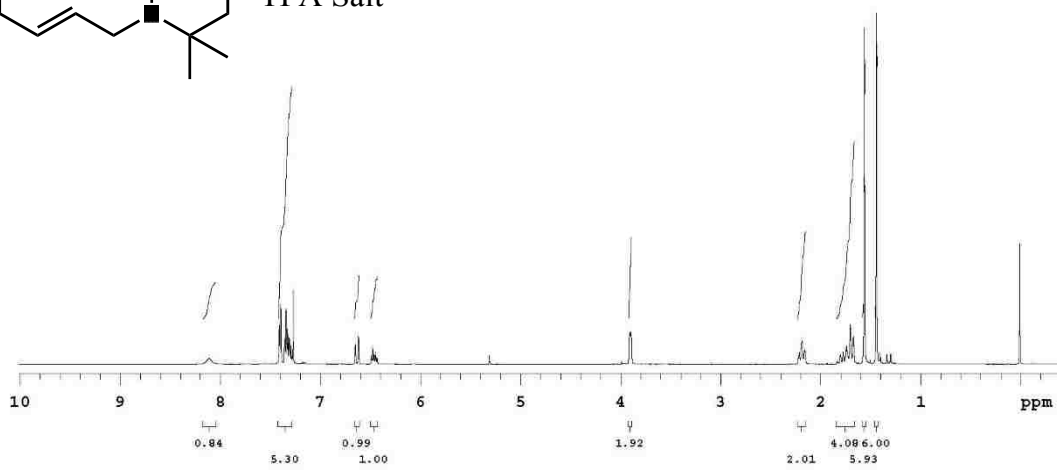
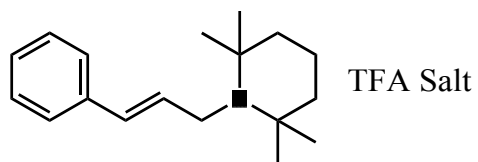
1-(but-2-en-1-yl)-2,2,6,6-tetramethylpiperidine TFA Salt (4h):



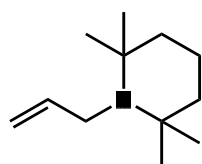
TFA Salt



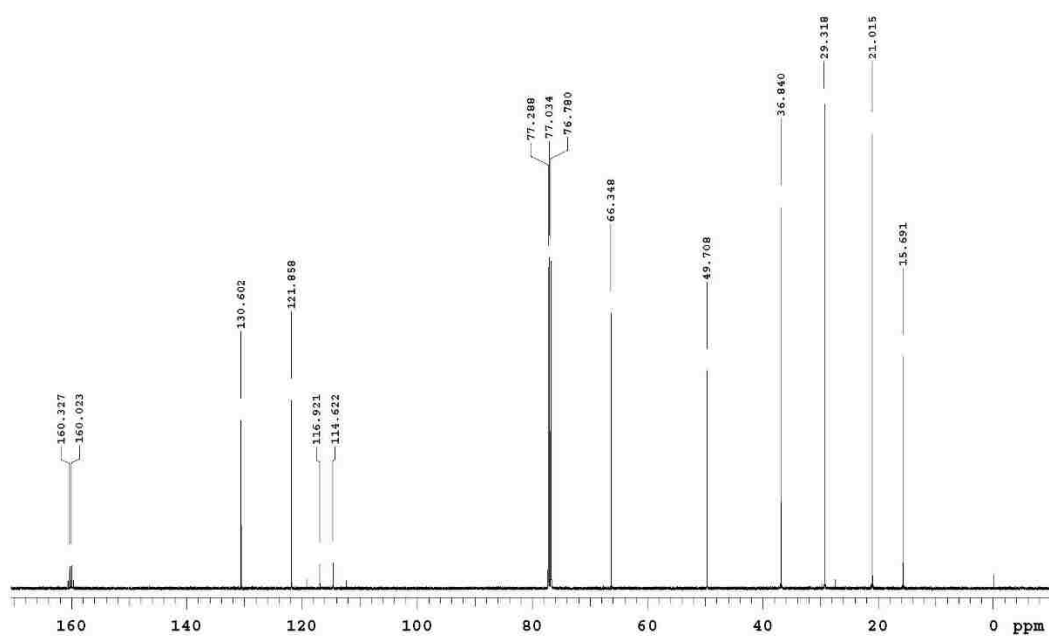
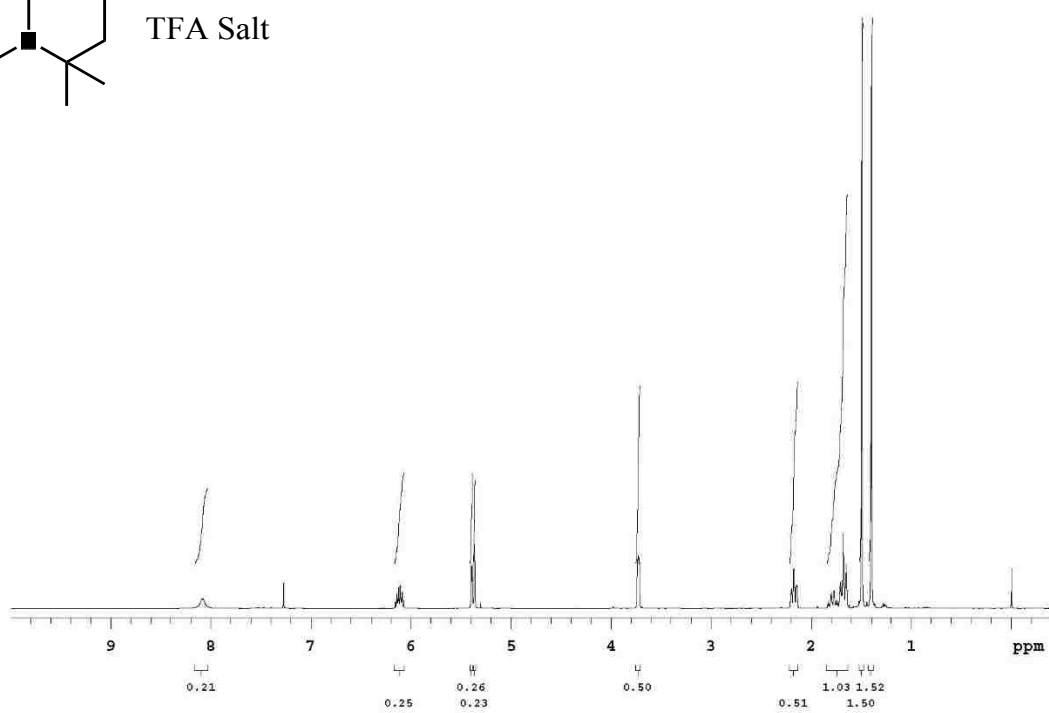
1-cinnamyl-2,2,6,6-tetramethylpiperidine TFA Salt (4i):



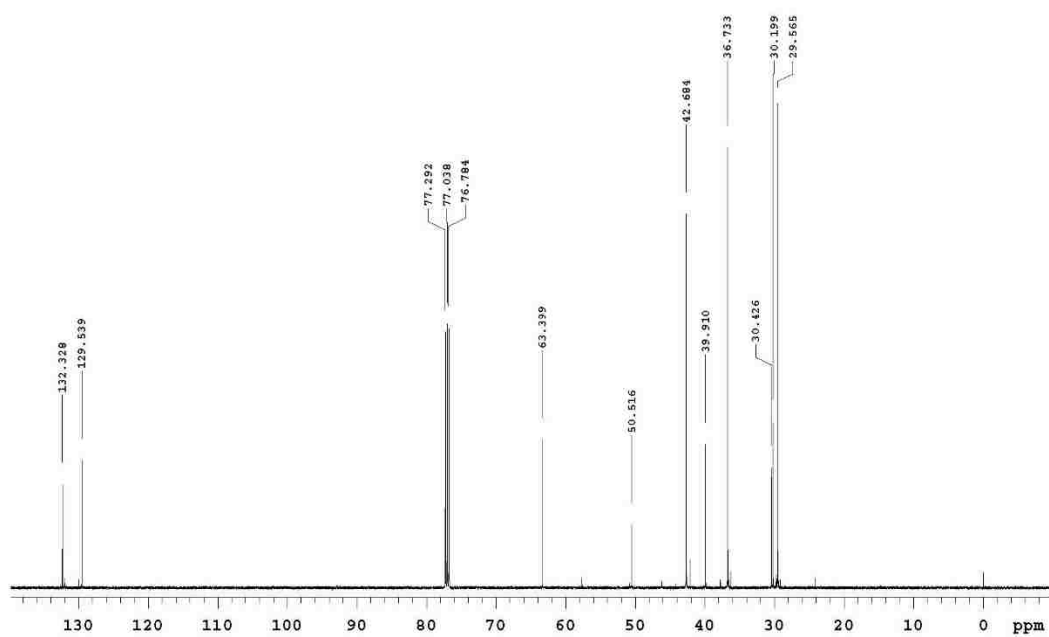
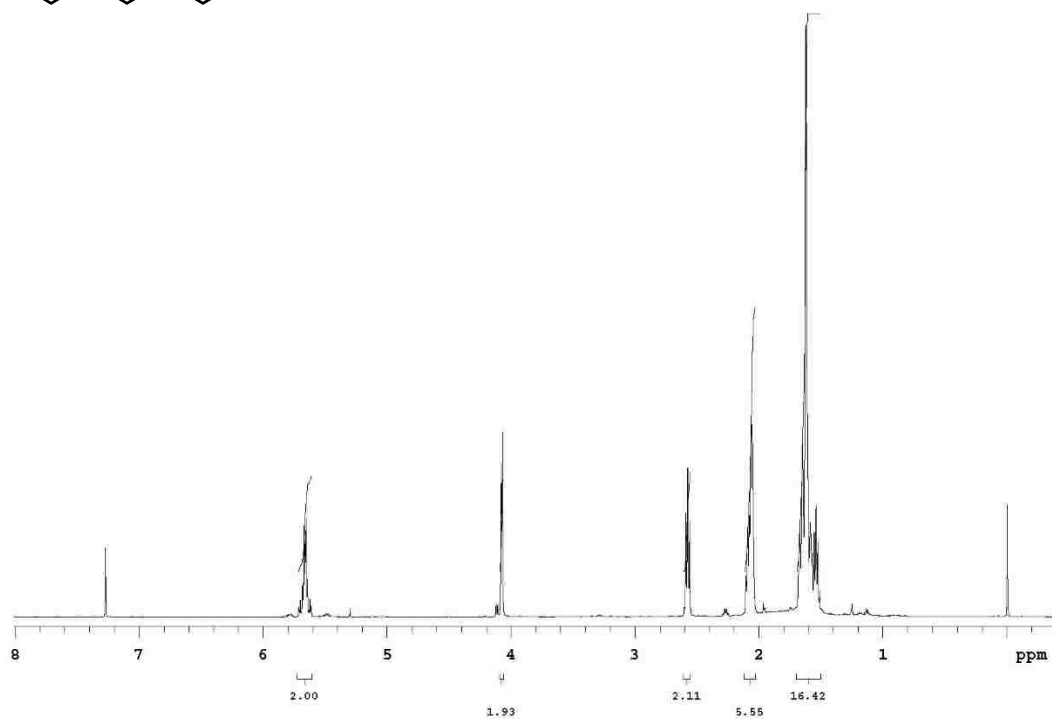
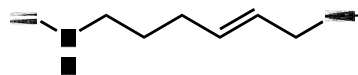
1-allyl-2,2,6,6-tetramethylpiperidine TFA Salt (4j):



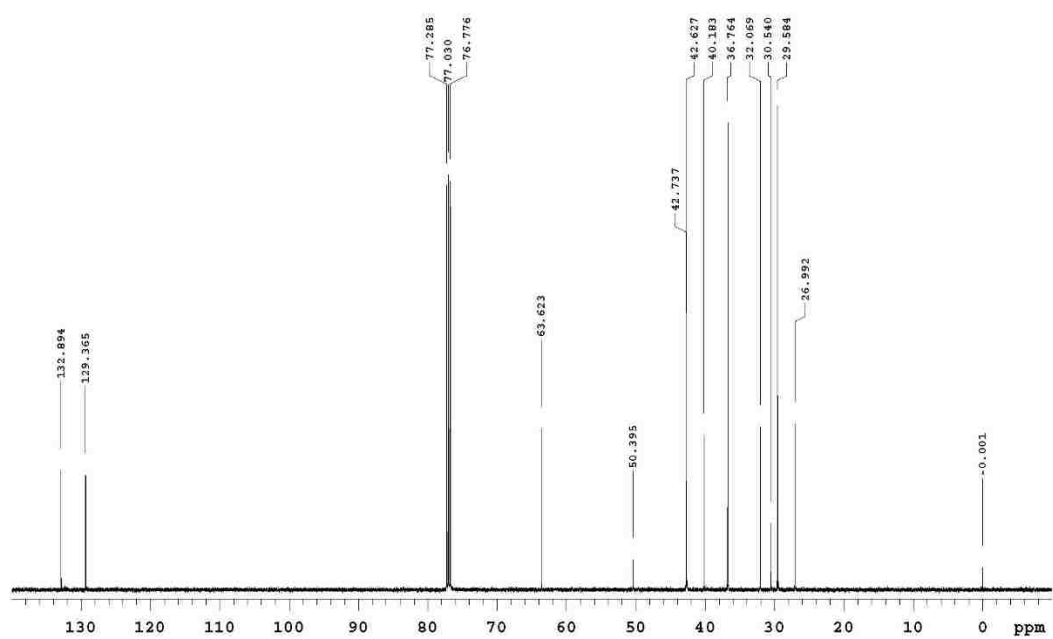
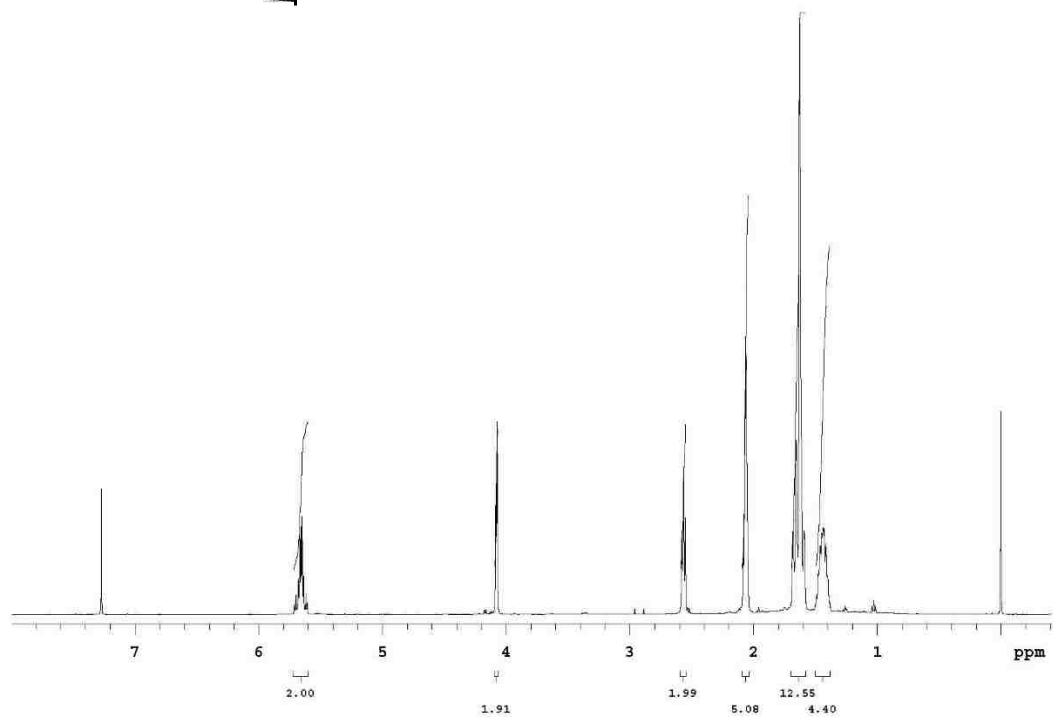
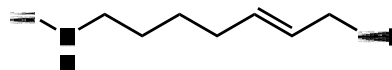
TFA Salt



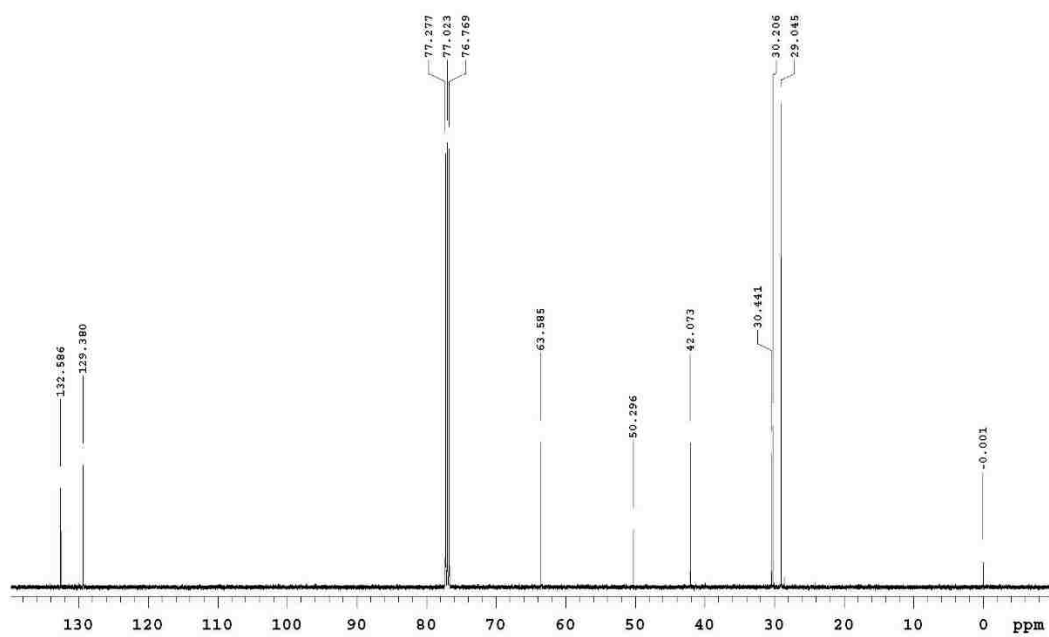
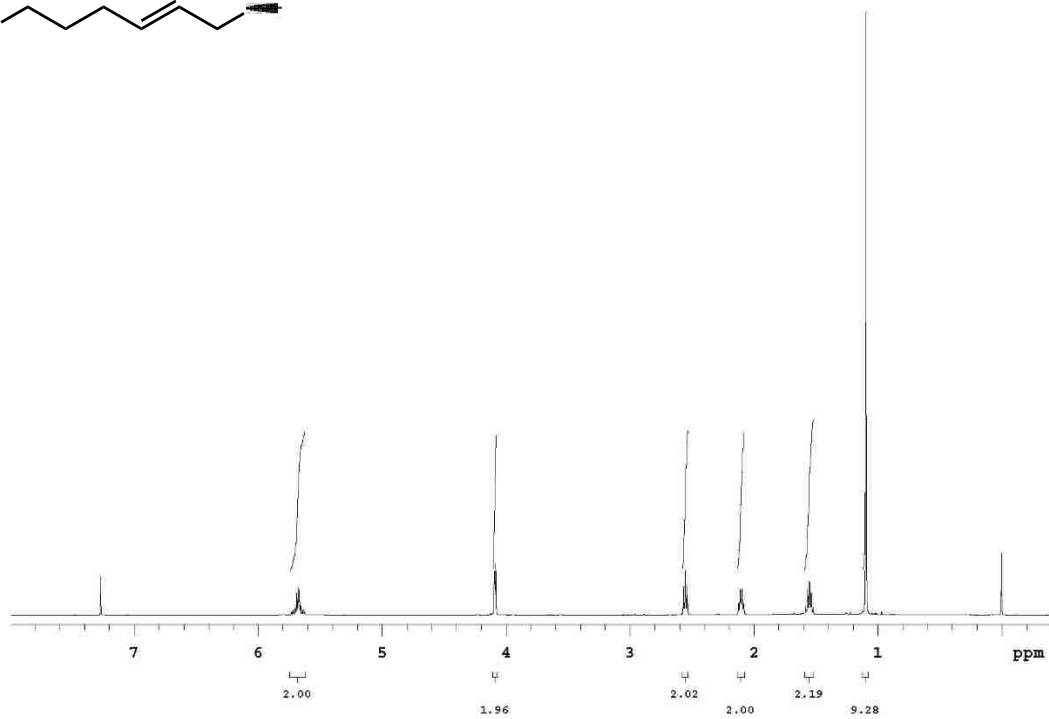
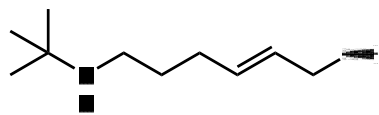
6-((adamantan-2-yl)amino)hex-2-en-1-ol (S1):



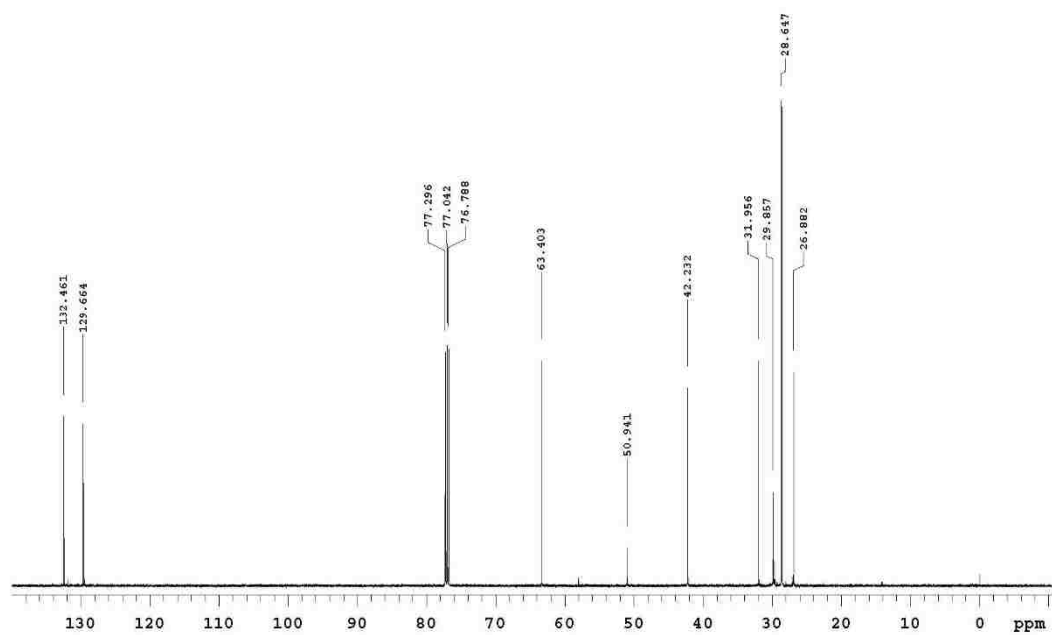
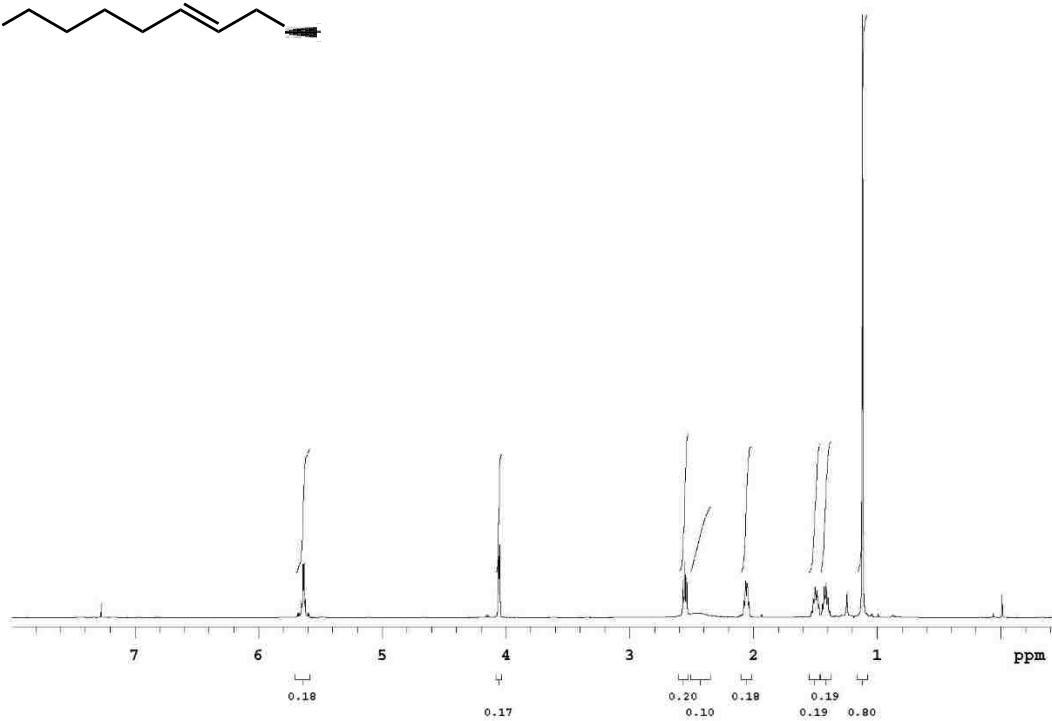
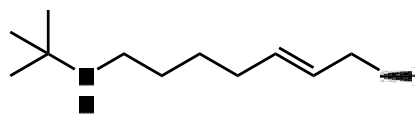
7-((adamantan-2-yl)amino)hex-2-en-1-ol (S2):



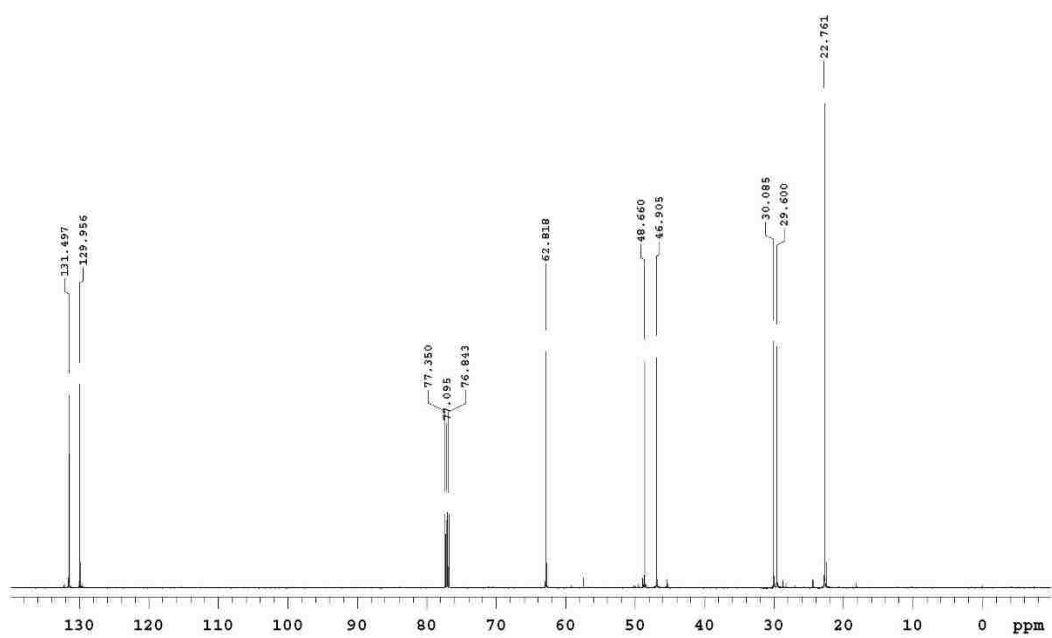
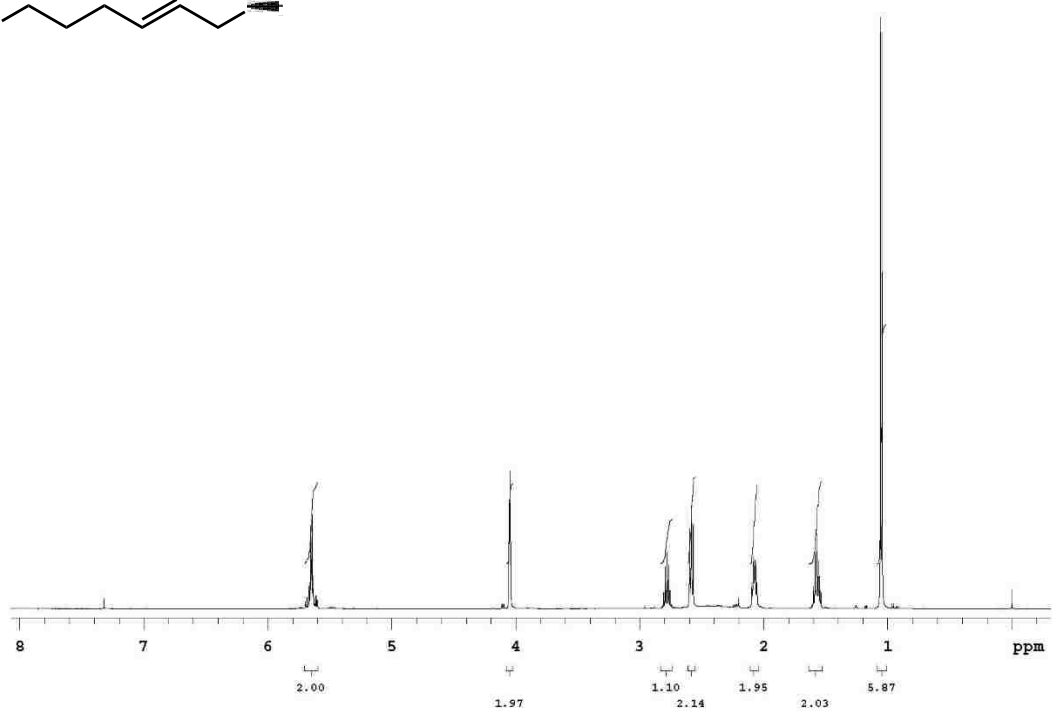
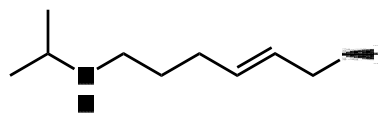
6-(*tert*-butylamino)hex-2-en-1-ol (S3):



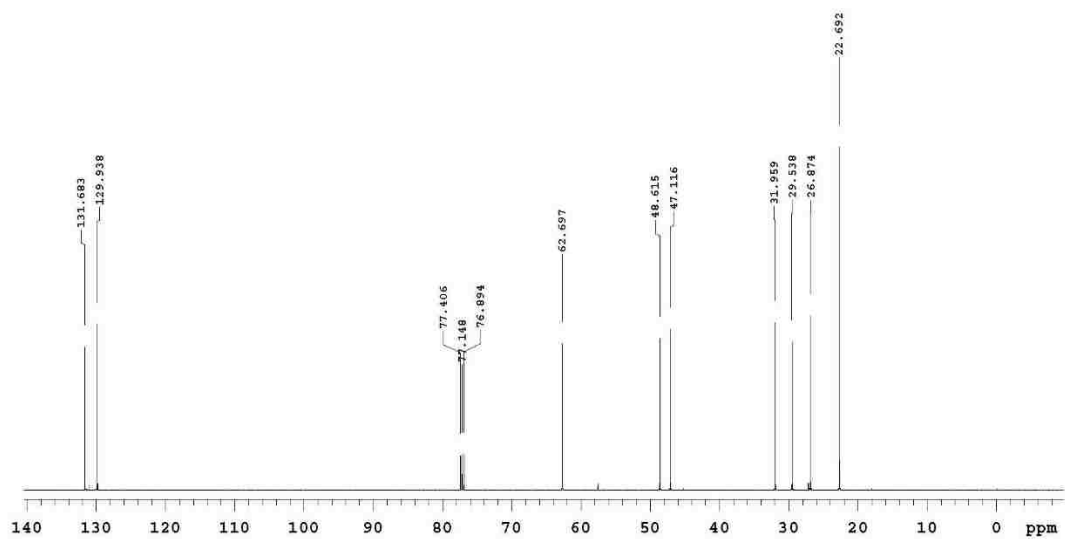
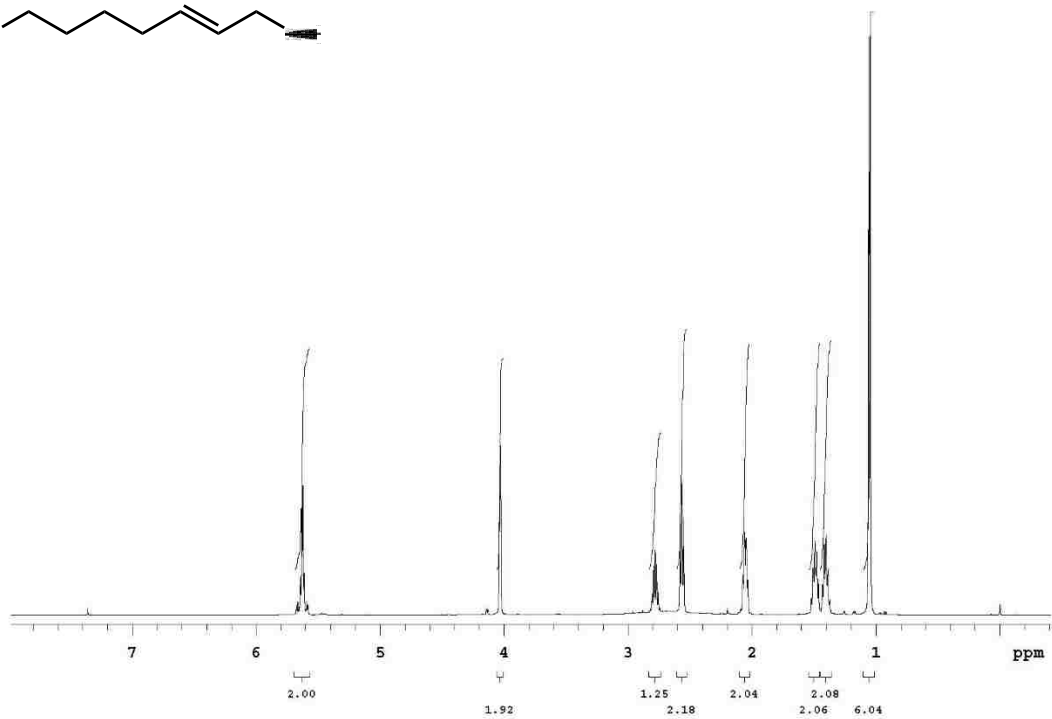
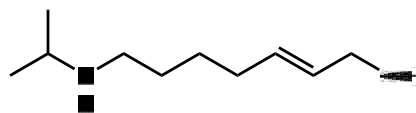
7-(*tert*-butylamino)hept-2-en-1-ol (S4):



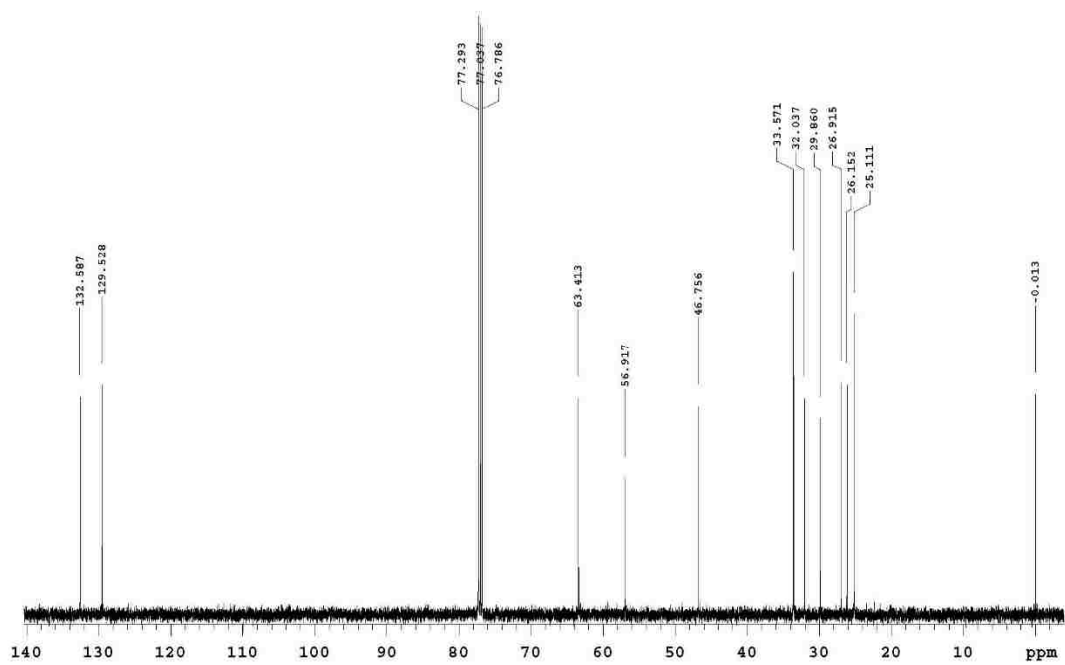
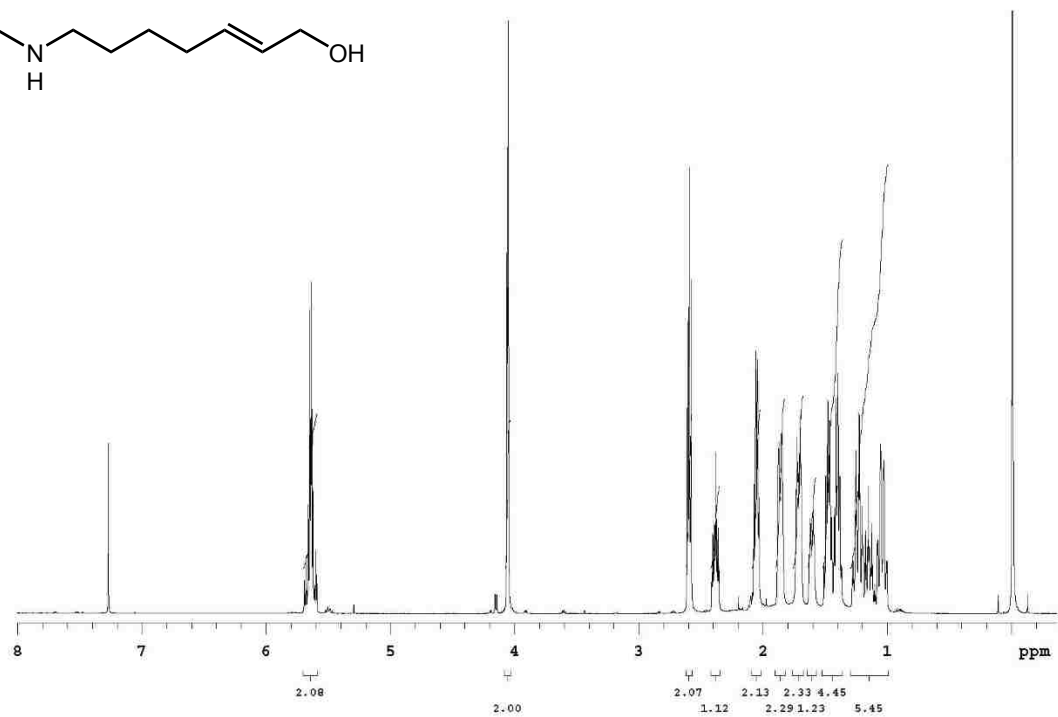
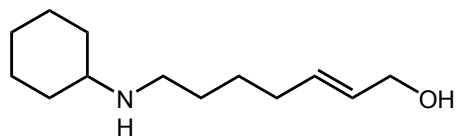
6-(isopropylamino)hex-2-en-1-ol (S5):



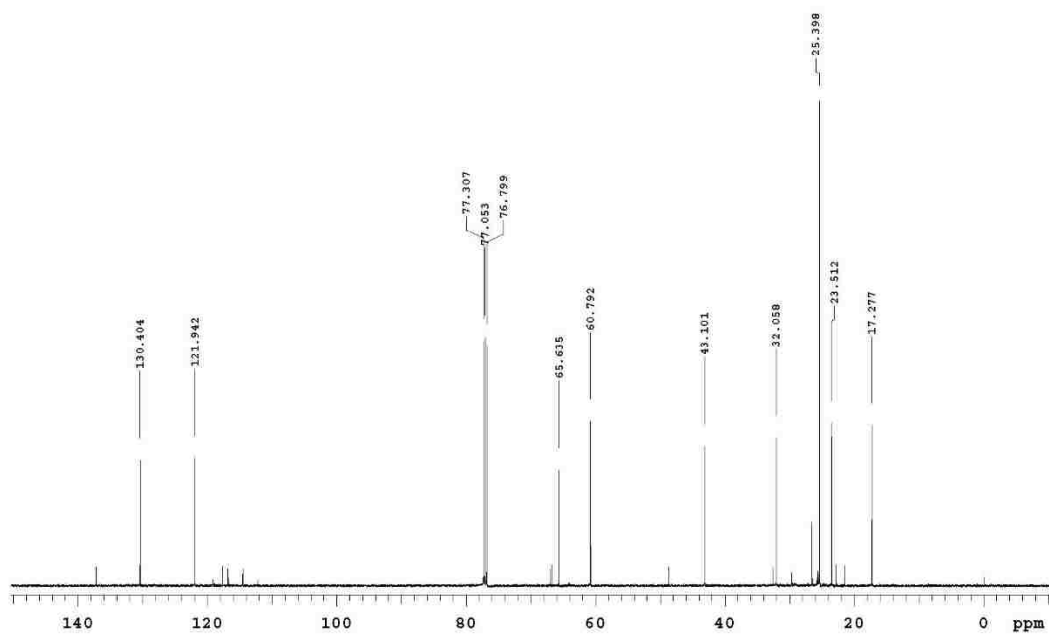
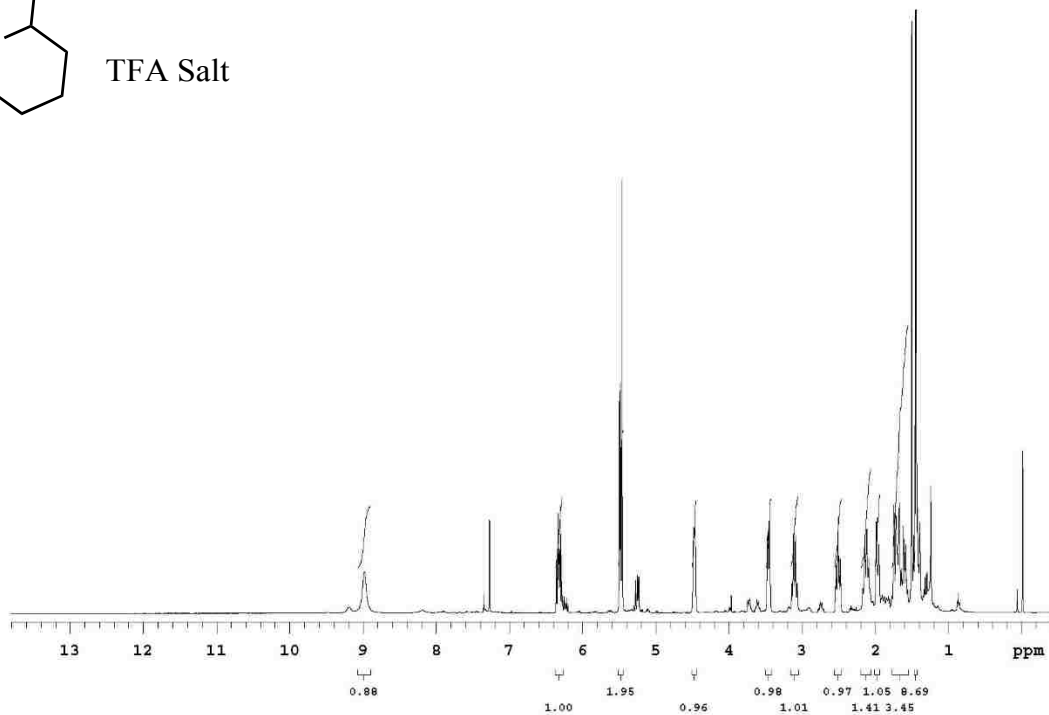
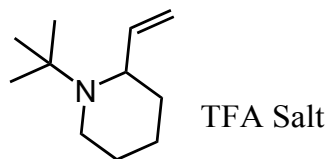
7-(isopropylamino)hept-2-en-1-ol (S6):



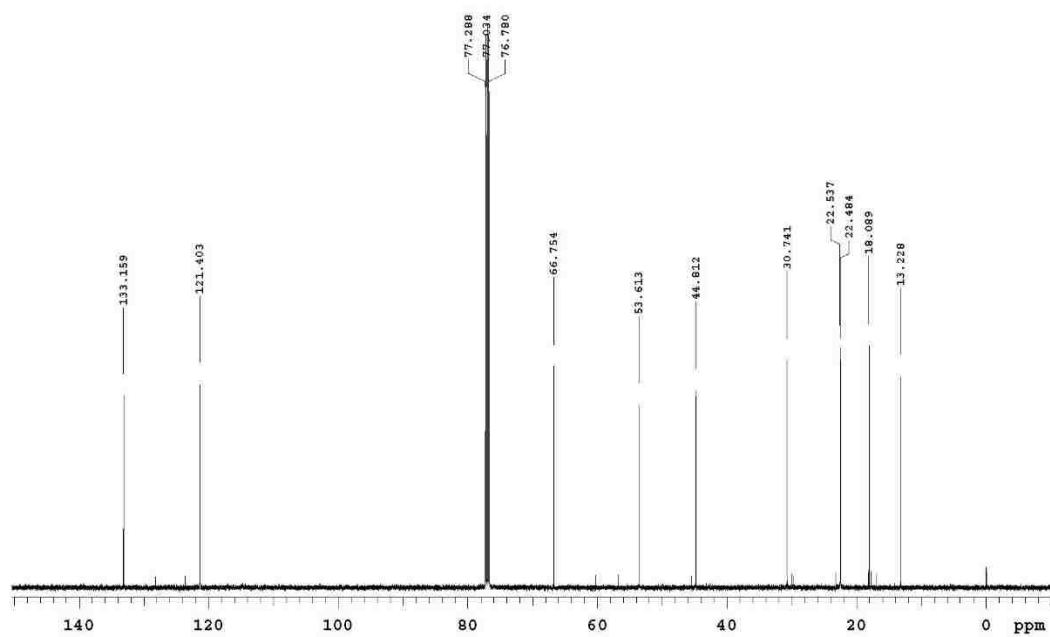
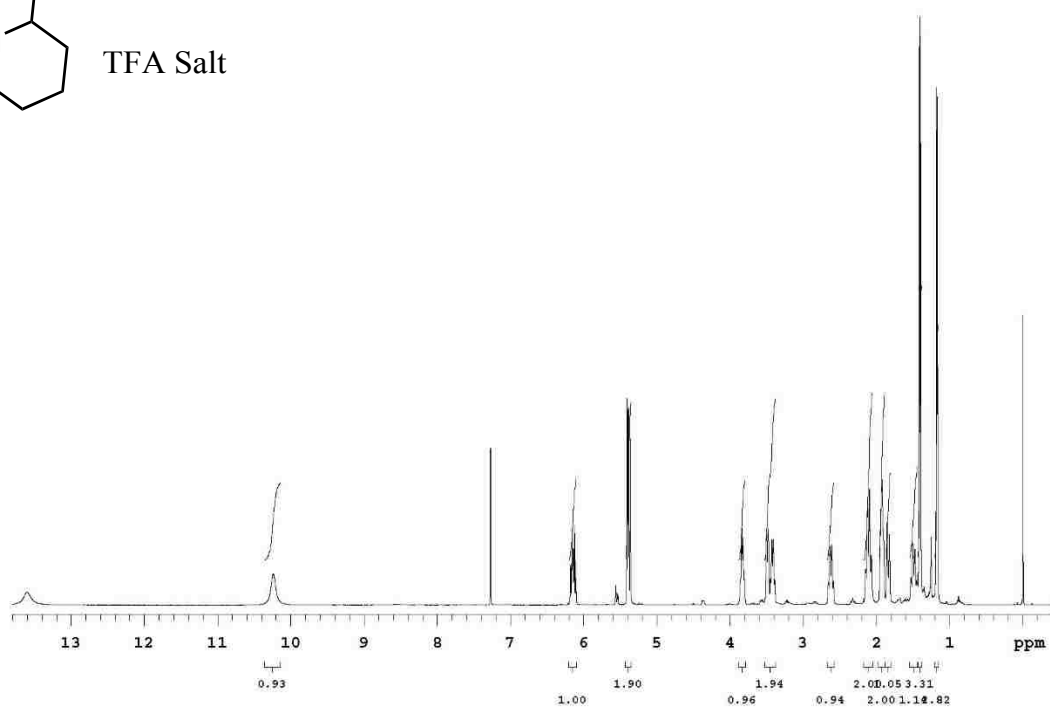
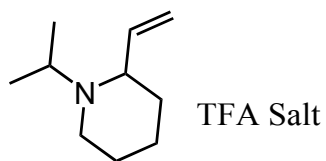
7-(cyclohexylamino)hept-2-en-1-ol (S7):



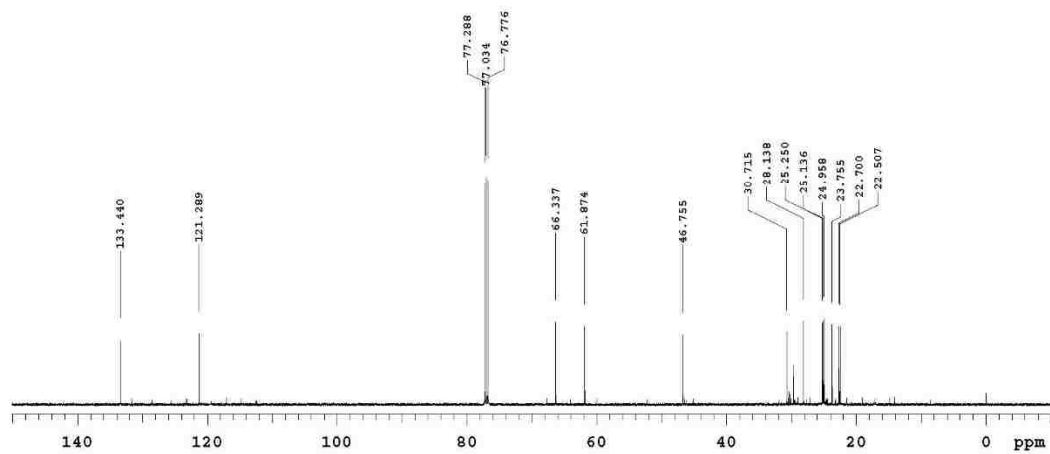
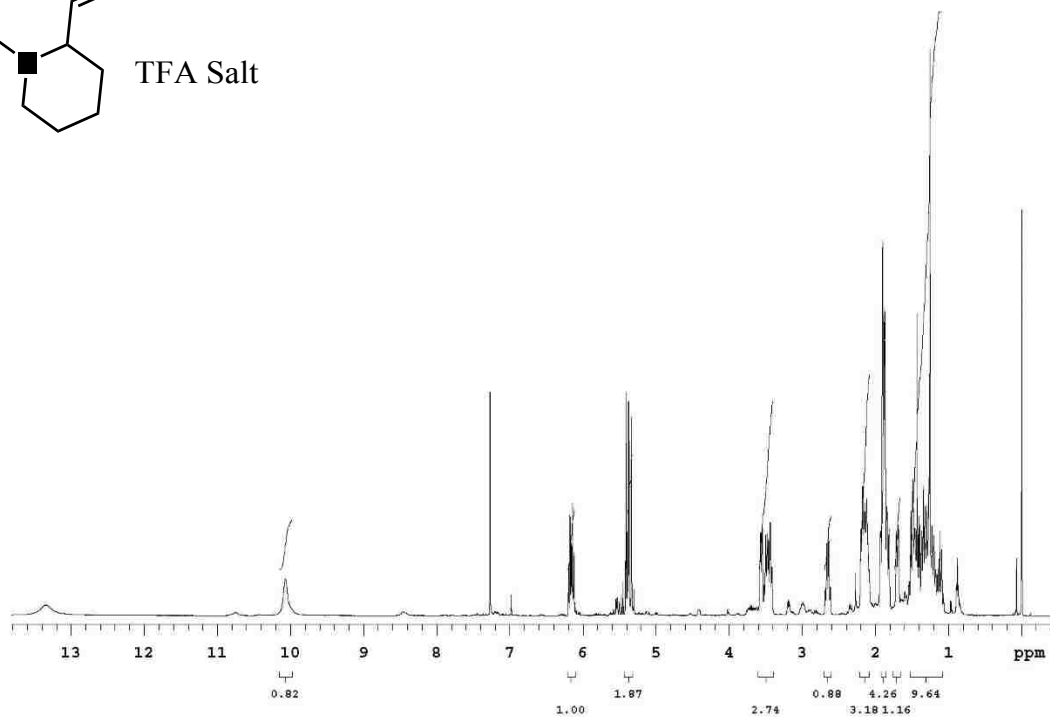
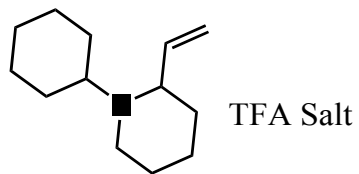
1-(*tert*-butyl)-2-vinylpiperidine TFA Salt (14a):



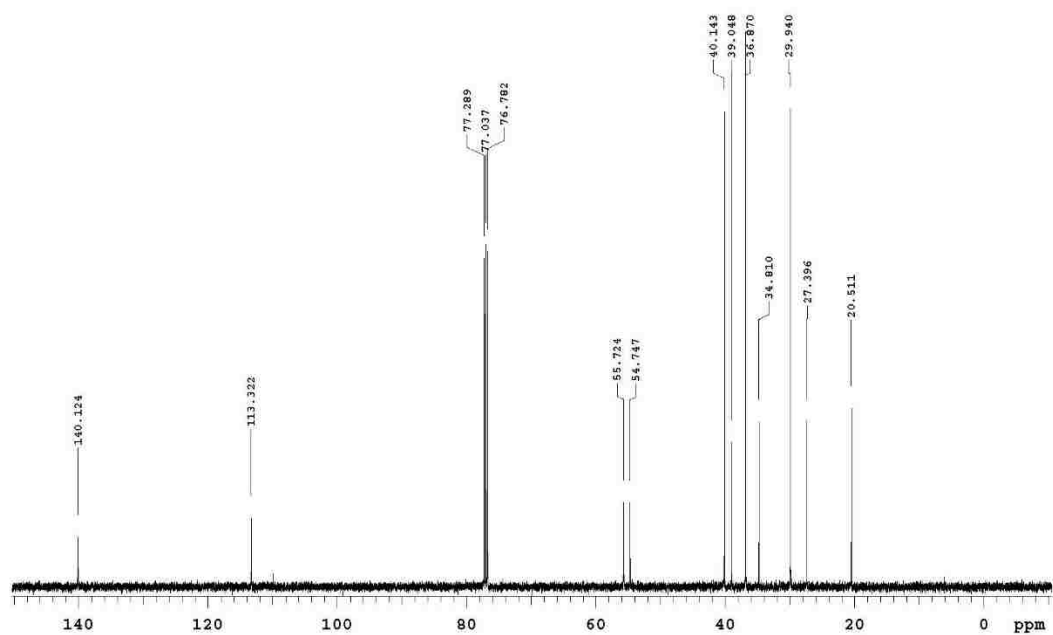
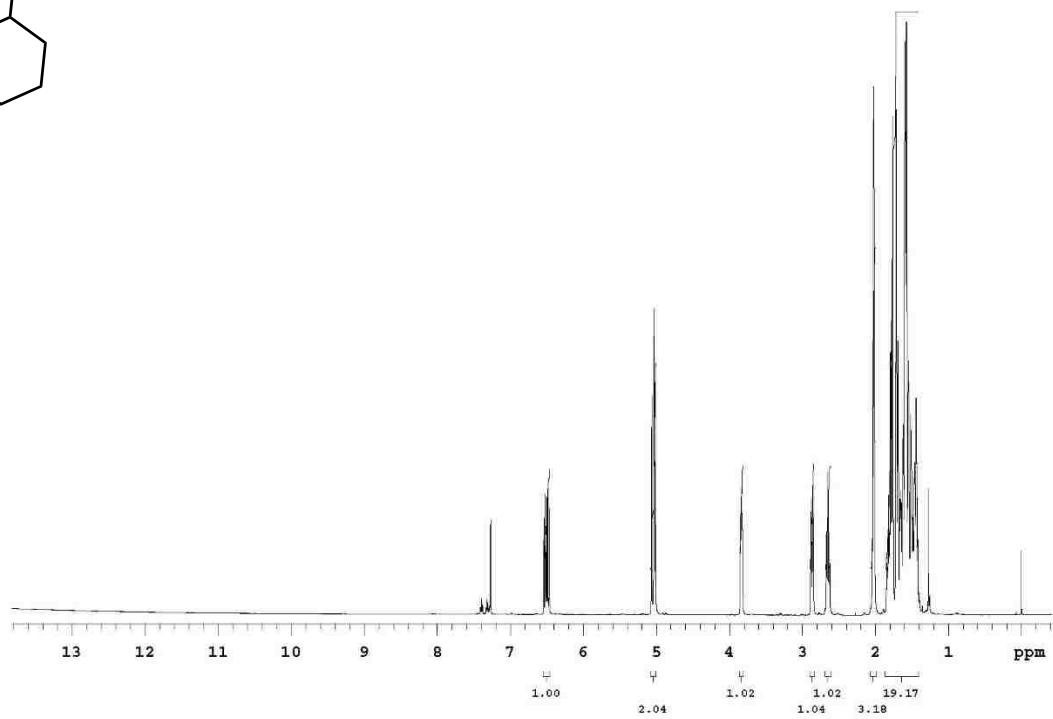
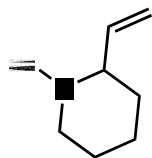
1-isopropyl-2-vinylpiperidine TFA Salt (14b):



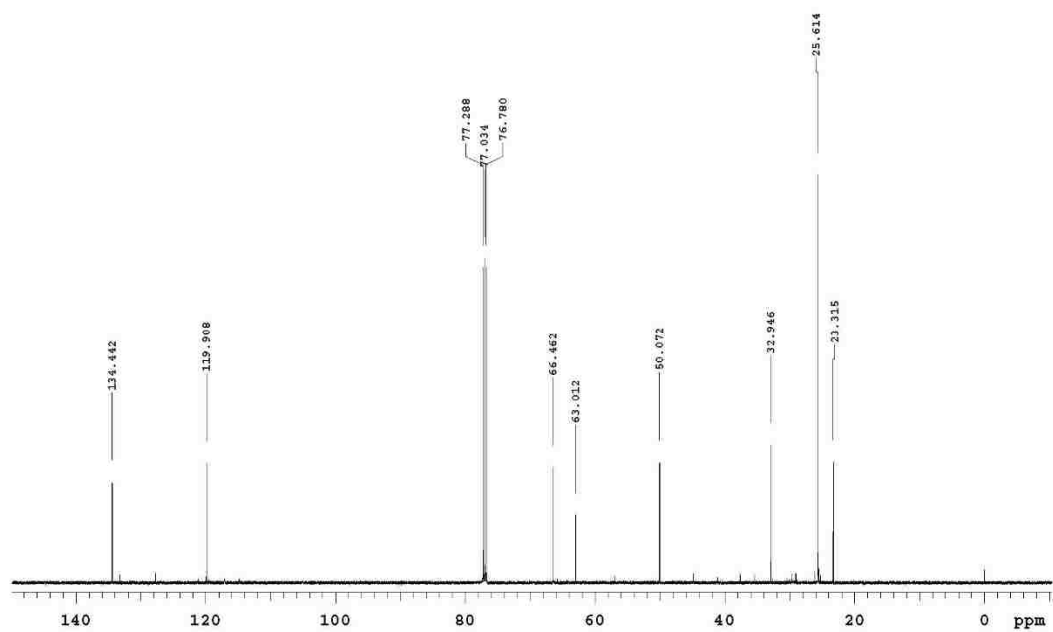
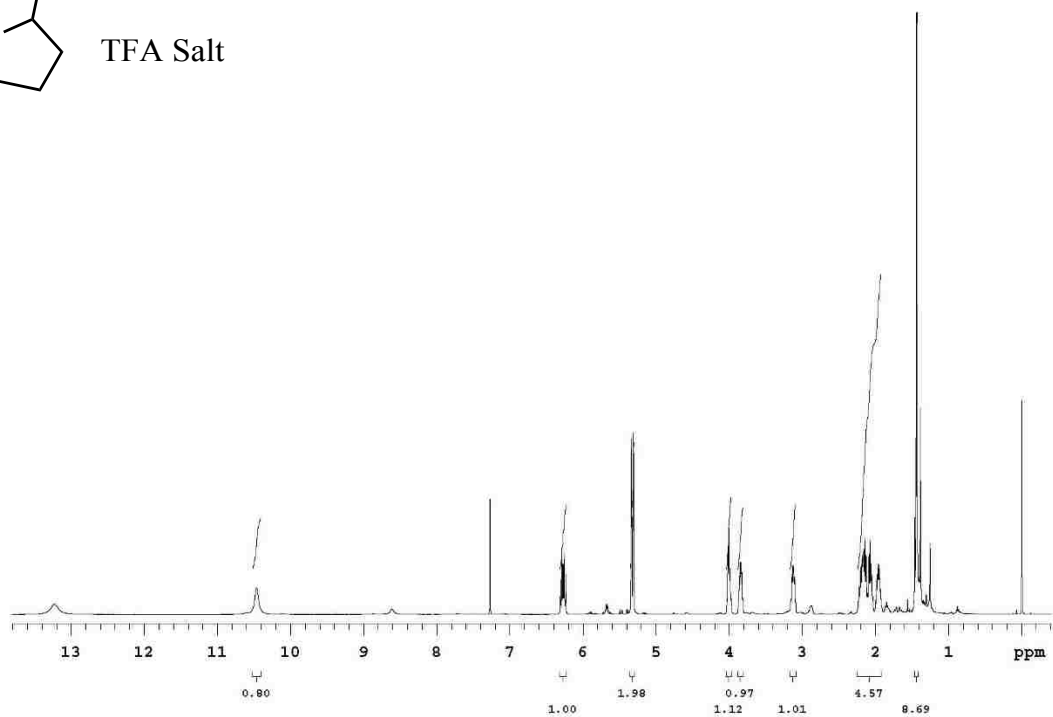
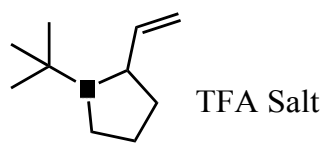
1-cyclohexyl-2-vinylpiperidine TFA Salt (14c):



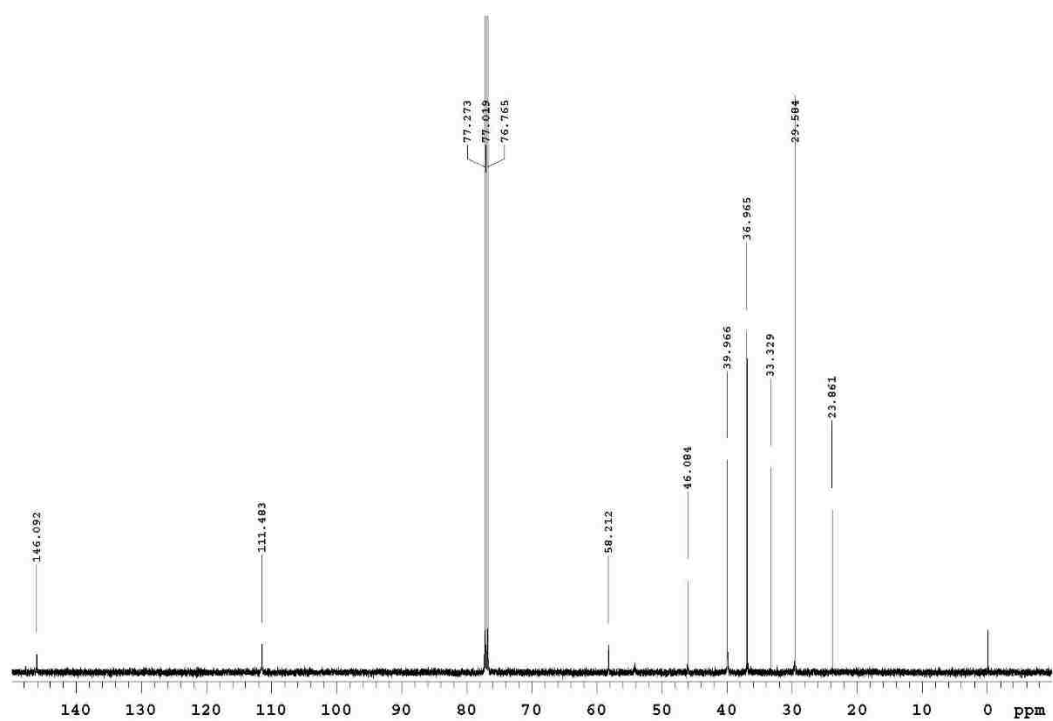
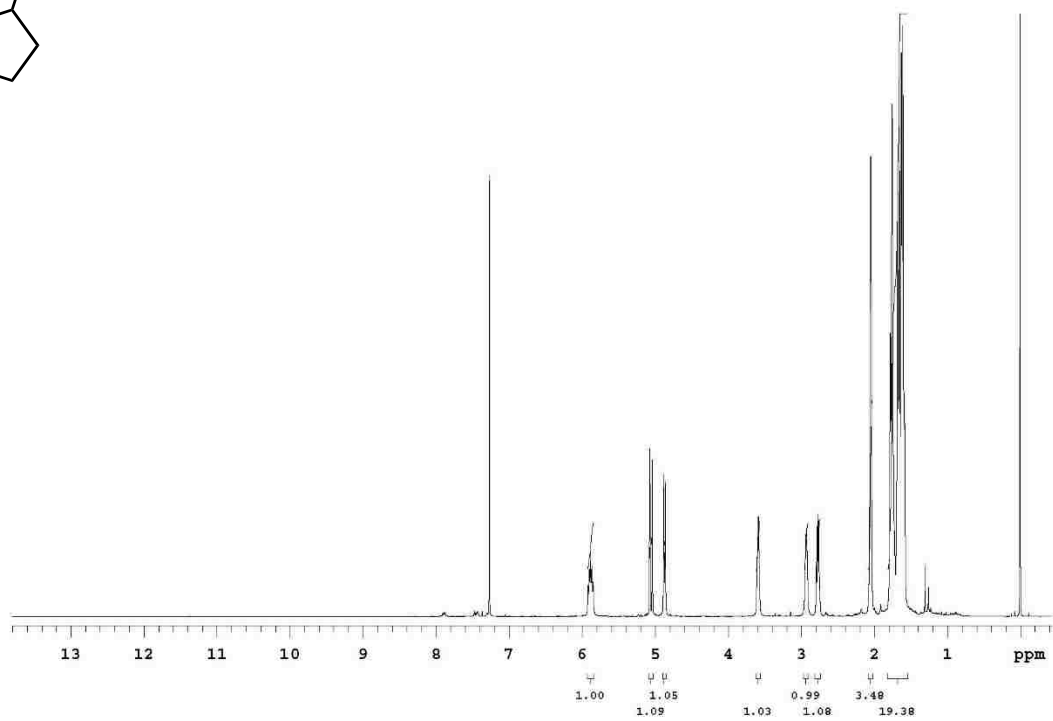
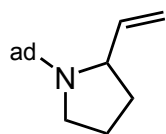
1-(adamantan-2-yl)-2-vinylpiperidine (14d):



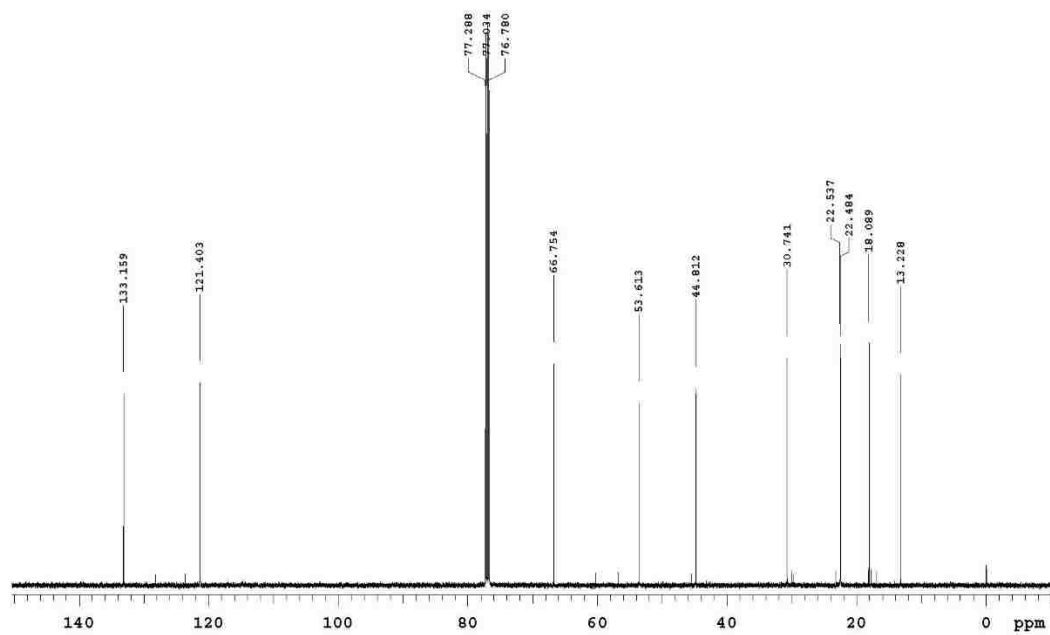
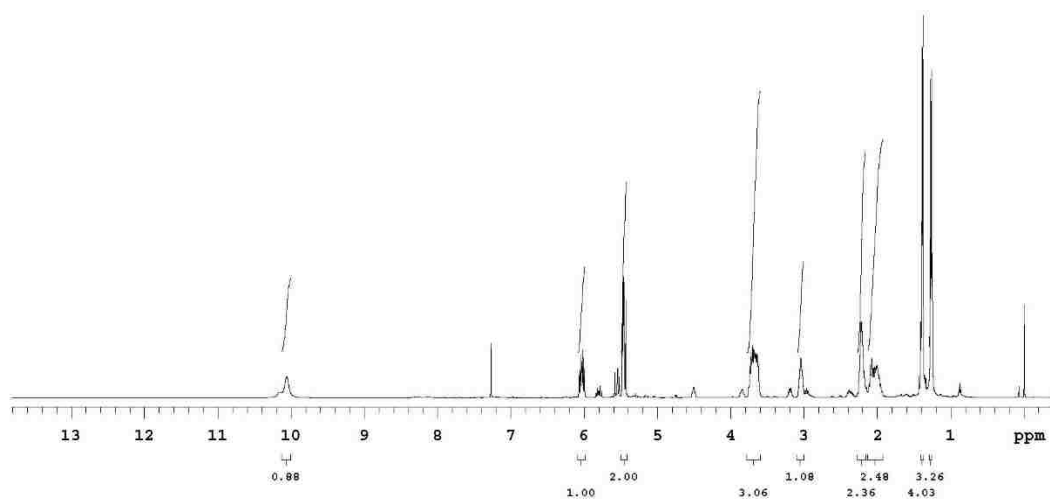
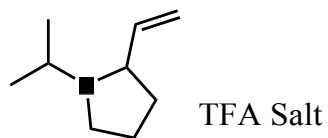
1-(*tert*-butyl)-2-vinylpyrrolidine TFA Salt (15a):



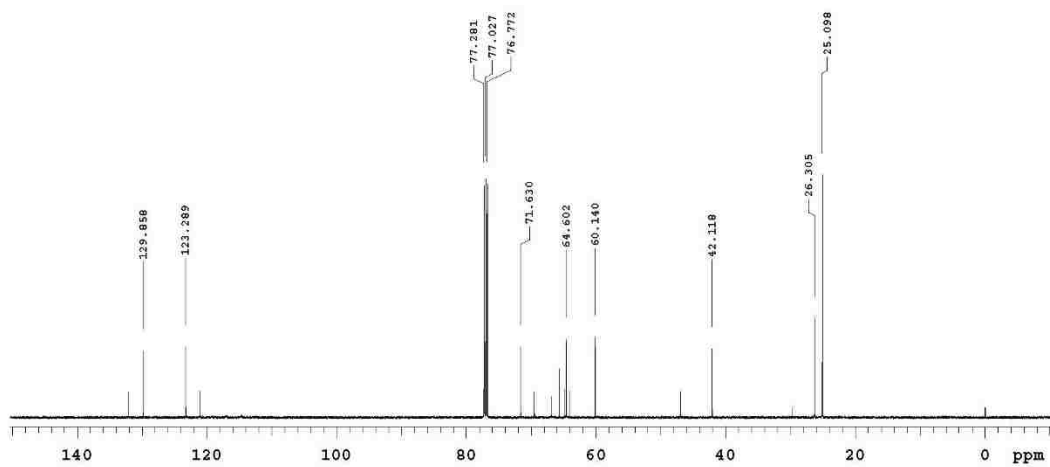
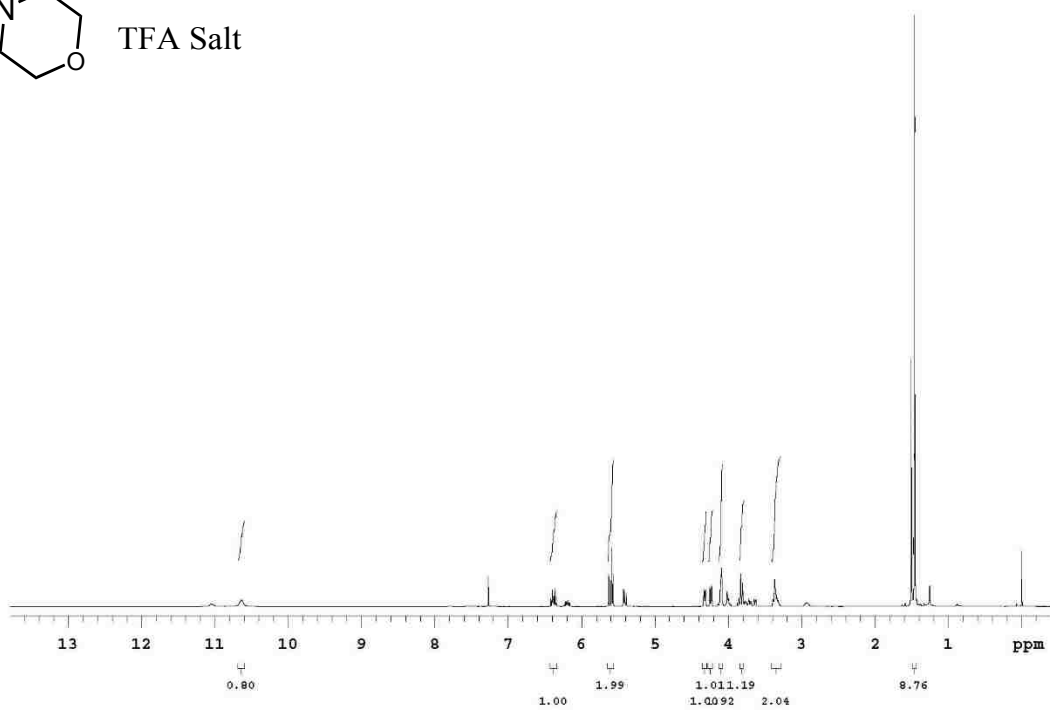
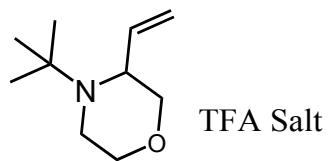
1-(adamantan-2-yl)-2-vinylpyrrolidine (15b):



1-isopropyl-2-vinylpyrrolidine TFA Salt (15c):



4-(*tert*-butyl)-3-vinylmorpholine TFA Salt (16):



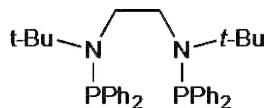
4.2 Supporting Information for Chapter 3

I. General Information

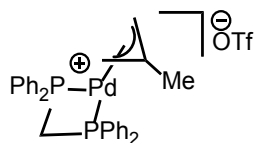
All reactions were carried out in oven-dried glassware with magnetic stirring, unless otherwise indicated. All the reagents were used as obtained unless otherwise noted. All commercially available amines were distilled from calcium hydride under nitrogen and stored over 4Å molecular sieves for at least 12 h before use. Reactions requiring a moisture-free environment were conducted in a nitrogen atmosphere glove box (Innovative Technology, PureLab HE system, double glove box). Analytical thin-layer chromatography was performed with 0.25 mm coated commercial silica gel plates (E. Merck, DC-Plastikfolien, kieselgel 60 F254). Flash Chromatography was performed with EM Science silica gel (0.040-0.063µm grade) Proton nuclear magnetic resonance (¹H-NMR) data were acquired on a Inova 300 (300 MHz) or on a Inova-500 (500 MHz) spectrometer. Chemical shifts are reported in delta (δ) units, in parts per million (ppm) downfield from tetramethylsilane. Carbon-13 nuclear magnetic resonance (¹³C-NMR) data were acquired on a Inova 500 at 125 MHz. Signals are reported as follows: s (singlet), d (doublet), t (triplet), q (quartet), dd (doublet of doublets), qd (quartet of doublets), brs (broad singlet), m (multiplet). Coupling constants are reported in hertz (Hz). Chemical shifts are reported in ppm relative to the center line of a triplet at 77.0 ppm for chloroform-d. Mass spectral data were obtained using ESI techniques (Agilent, 6210 TOF). Heterobimetallic complex 1⁵ was synthesized as previously described.

II. Synthesis of bisphosphinepalladium methallyl triflate complexes

⁵ Tsutsumi, H.; Sunada, Y.; Shiota, Y.; Yoshizawa, K.; Nagashima, H. *Organometallics* **2009**, 28, 1988–1991.



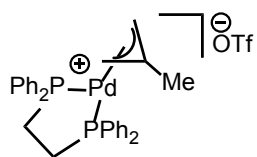
N,N'-di-tert-butyl-*N,N'*-bis(diphenylphosphino)ethane-1,2-diamine: Into a 5 dram vial containing a stir bar was placed *N,N'*-di-tert-butylethylenediamine (0.50 g, 2.9 mmol), dry toluene (5 ml), chlorodiphenylphosphine (1.04 ml, 5.8 mmol, 2 equiv), then triethylamine (0.89 ml, 6.38 mmol, 2.2 equiv). the reaction was heated to 75 °C overnight (14 hrs). The reaction was then diluted with 10 ml CH₂Cl₂ and loaded directly onto a short column of silica gel and eluted with 4:1 hexanes:EtOAc. The product was isolated as a white solid, 0.570 g, (36% yield) (M.P. = 148–150 °C). IR (film): ν = 3071, 3052, 2963, 2916, 2849, 1260, 1087, 1019, 798; ¹H NMR (CDCl₃, 500 MHz) δ (ppm): 7.27–7.43 (m, 20 H), 2.78 (apparent s, 4H), 0.94 (s, 18H); ¹³C NMR (CDCl₃, 125 MHz): 139.8 (doublet), 131.9 (doublet), 128.8 (doublet), 127.8, 56.0 (doublet), 50.0 (doublet), 31.1 (doublet); ³¹P NMR (CDCl₃, 202 MHz) δ (ppm): 49.6; HRMS (ESI): C₃₄H₄₃N₂P₂ (M+H) calculated: 541.2901, found 541.2884.



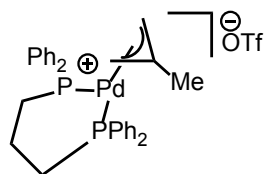
(bis(diphenylphosphino)methane)palladium(η^3 -methallyl) triflate (6a):

General Procedure: Into a flame dried vial containing a stir bar were placed [η^3 -methallylPdCl]₂ (43.7 mg, 0.111 mmol) and Ag(OTf) (57.0 mg, 0.222 mmol, 1 equiv), and the mixture was dissolved in dry dichloromethane (4 mL). Acetone (163 μ L, 2.22 mmol, 20 equiv) was added and the solution was allowed to stir 10 minutes. In a separate vial, 1,1-bis(diphenylphosphino)methane (85.3 mg, 0.222 mmol, 2 equiv) was dissolved in dichloromethane (1 mL) and then added to the reaction mixture. The resulting solution was allowed to stir for an addition 30 minutes, the solvent was removed, and the remaining

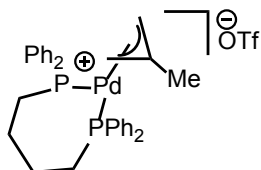
precipitate was dissolved in dichloromethane (2 ml). The solution was then filtered over celite into a 5 dram vial, layered with hexanes, and the product was allowed to drystalize overnight. The product was obtained as tan crystals (125 mg, 81% yield, Melting Point: 235 °C (decomp)). ¹H-NMR (500 MHz, CDCl₃): δ (ppm) = 7.47-7.43 (m, 2H), 7.41-7.33 (m, 6H), 7.23 (t, J=7.62 Hz, 4H), 7.07 (s, 4H), 6.95 (s, 4H), 4.30 (s, 2H), 4.24 (s, 2H), 3.80 -3.71 (m, 1H), 3.54- 3.44 (m, 1H) 1.54 (s, 3H); ¹³C-NMR (125 MHz, CDCl₃): δ (ppm) = 138.4 (t, J=2.48 Hz), 134.1 (t, J=3.53 Hz), 131.5 (d, J=69.74 Hz), 131.3 (t, J=3.03 Hz), 129.7 (dt, J=92.75, J=2.20 Hz), 78.4 (t, J=7.18 Hz), 28.5 (s), 22.5 (s); ³¹P-NMR (202 MHz, CDCl₃): δ (ppm) = 9.98 (s). HRMS (ESI): C₂₉H₂₉P₂Pd calculated: 545.0785, found 545.0703.



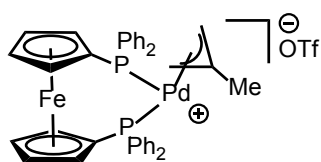
(bis(diphenylphosphino)ethane)palladium(η^3 -methallyl) triflate (6b): Synthesized according to the general procedure using 88.4 mg 1,2-bis(diphenylphosphino)ethane (0.222 mmol, 2 equiv). The product was obtained as white crystals (136 mg, 86% yield, Melting Point: 245 °C (decomp)). ¹H-NMR (500 MHz, CDCl₃): δ (ppm) = 7.65-7.58 (m, 4H), 7.55-7.46 (m, 16H), 4.62 (s, 2H), 3.31-3.26 (m, 2H), 2.89-2.62 (m, 4H), 1.95 (s, 3H); ¹³C-NMR (125 MHz, CDCl₃): δ (ppm) = 137.6 (t, J=5.91 Hz), 132.5 (q, J=5.99 Hz), 132.0 (s), 129.7 (ddt, J=88.85 Hz, J=44.29 Hz, J=18.08 Hz), 129.8 (dt, J=16.21 Hz, J=5.52 Hz), 70.3 (t, J= 16.86 Hz), 27.5 (d, J=22.06 Hz), 27.3 (d, J=22.06 Hz), 24.4 (s); ³¹P-NMR (202 MHz, CDCl₃): δ (ppm) = 52.13 (s). HRMS (ESI): C₃₀H₃₁P₂Pd calculated: 559.0941, found 559.0838.



(bis(diphenylphosphino)propane)palladium(η^3 -methallyl) triflate (6c): Synthesized as previously reported.¹

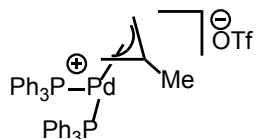


(bis(diphenylphosphino)butane)palladium(η^3 -methallyl) triflate (6d): Synthesized according to the general procedure using 94.7 mg 1,4-bis(diphenylphosphino)butane (0.222 mmol, 2 equiv). The product was obtained as grey crystals (129 mg, 79% yield, Melting Point: 250 °C (decomp)). ¹H-NMR (500 MHz, CDCl₃): δ (ppm) = 7.56-7.44 (m, 16H), 7.42-7.36 (m, 4H), 3.67 (s, 2H), 3.24-3.20 (m, 2H), 2.83-2.75 (m, 2H), 2.64-2.55 (m, 2H), 1.99-1.87 (m, 2H) 1.86-1.73 (m, 2H), 1.69 (s, 3H); ¹³C-NMR (125 MHz, CDCl₃): δ (ppm) = 137.4 (t, J=5.64 Hz), 133.1 (dt, J=24.87 Hz, J=19.96 Hz), 132.4 (dt, J=27.26 Hz, J=6.25 Hz), 131.2 (d, J=21.88 Hz), 129.3 (dt, J=7.15 Hz, J=5.26 Hz), 75.2 (t, J=16.07 Hz), 26.6 (d, J=12.04 Hz), 26.5 (d, J=12.04 Hz), 23.7, 23.3 (t, J=3.23 Hz); ³¹P-NMR (202 MHz, CDCl₃): δ (ppm) = 21.04 (s). HRMS (ESI) C₃₂H₃₅P₂Pd calculated: 587.1254, found 587.1139.

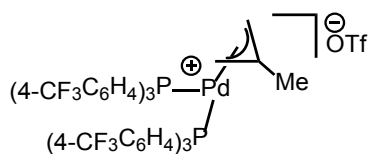


(bis(diphenylphosphino)ferrocene)palladium(η^3 -methallyl) triflate (7): Synthesized according to the general procedure using 123.1 mg 1,1-bis(diphenylphosphino)ferrocene (0.222 mmol, 2 equiv). The product was obtained as orange crystals (131 mg, 68% yield, Melting Point: 260 °C (decomp)). ¹H-NMR (500 MHz, CDCl₃): δ (ppm) = 7.65-7.58 (m, 4H), 7.58-7.46 (m, 16H), 4.49 (s, 2H), 4.45 (d, J=13.13 Hz, 4H), 4.18 (s, 2H), 3.70 (s, 2H), 3.46 (s, 2H), 1.87 (s, 3H); ¹³C-NMR (125 MHz, CDCl₃): δ (ppm) = 138.2 (t, J=5.54 Hz), 133.3 (q,

J=7.52 Hz), 133.0 (ddt, J=106.14 Hz, J=46.25 Hz, J=23.50 Hz), 131.6 (d, J=6.13 Hz), 129.3 (dt, J=15.50 Hz, J=5.38 Hz), 76.8 (t, buried in CDCl₃, retaken in CD₂Cl₂, δ =76.1 (t, J=15.74 Hz)), 75.7 (dt, J=59.34 Hz, J=5.91 Hz), 74.5 (dt, J=56.62 Hz, J=27.18 Hz), 73.5 (dt, J=33.40 Hz, J=3.58 Hz), 23.9 (s); ³¹P-NMR (202 MHz, CDCl₃): δ (ppm) =24.14 (s). HRMS (ESI) C₃₈H₃₅FeP₂Pd calculated: 715.0604, found 715.0482.

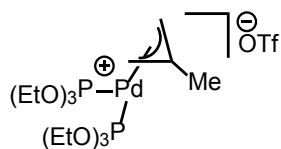


(bis(triphenylphosphino)palladium(η^3 -methallyl) triflate (8): Synthesized according to the general procedure using 116.5 mg triphenylphosphine (0.444 mmol, 4 equiv). The product was obtained as light orange crystals (176 mg, 95 % yield, Melting Point: 215 °C (decomp)). ¹H-NMR (500 MHz, CDCl₃): δ (ppm) =7.39 (t, J=7.21 Hz, 6H), 7.32-7.23 (m, 24H), 3.80-3.75 (m, 2H), 3.63 (s, 2H), 1.87 (s, 3H); ¹³C-NMR (125 MHz, CDCl₃): δ (ppm) =138.0 (t, J=5.03 Hz), 133.5 (t, J=6.59 Hz), 131.1 (dt, J=44.34 Hz, J=21.00 Hz), 131.0 (s), 129.0 (t, J=5.24 Hz), 78.7 (t, J=15.03 Hz), 23.6 (s); ³¹P-NMR (202 MHz, CDCl₃): δ (ppm) =24.00 (s). HRMS (ESI) C₄₀H₃₇P₂Pd calculated: 685.1411, found 685.1259.



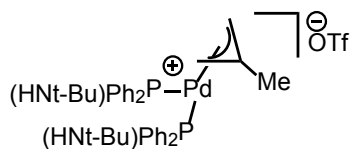
(bis(tris(4-trifluoromethylphenyl))phosphino)palladium(η^3 -methallyl) triflate (9): Synthesized according to the general procedure using 207.0 mg tris(4-trifluoromethylphenyl)phosphine (0.444 mmol, 4 equiv). The product was obtained as white crystals (183 mg, 69% yield, Melting Point: 265 °C (decomp)). ¹H-NMR (500 MHz, CDCl₃): δ (ppm) = 7.62 (d, J=7.96 Hz, 12H) 7.51-7.45 (m, 12H), 4.22-4.17 (m, 2H), 3.84 (s, 2H), 1.92

(s, 3H); ^{31}P -NMR (202 MHz, CDCl_3): δ (ppm) = 22.83 (s). HRMS (ESI) $\text{C}_{46}\text{H}_{31}\text{F}_{18}\text{P}_2\text{Pd}$ calculated: 1093.0654, found 1093.0424.



(bis(triethylphosphite)palladium(η^3 -methallyl) triflate (10):

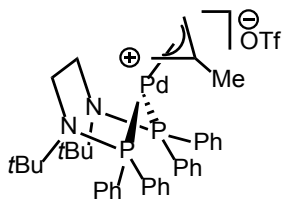
Synthesized according to the general procedure using 76.1 μL triethyl phosphite (0.444 mmol, 4 equiv). The product was obtained as a grey oil. IR (film): ν = 2984, 2937, 2906, 1390, 1272, 1223, 1151, 1098, 1009, 954, 788; ^1H -NMR (500 MHz, CDCl_3): δ (ppm) = 4.42 (s, 2H), 4.11-4.03 (m, 12H), 3.49 (s, 2H), 1.86 (s, 3H), 1.33 (t, $J=6.91$ Hz, 18H); ^{13}C -NMR (125 MHz, CDCl_3): δ (ppm) = 138.5 (s), 71.5 (s), 61.7 (s), 24.1 (s), 16.3 (s); ^{31}P -NMR (202 MHz, CDCl_3): δ (ppm) = 128.52 (s). HRMS (ESI) $\text{C}_{16}\text{H}_{37}\text{O}_6\text{P}_2\text{Pd}$ calculated: 493.1106, found 493.1075.



(bis(*N-tert*-butyldiphenylphosphoamido)palladium(η^3 -methallyl) triflate (11):

Synthesized according to the general procedure using 114.1 mg *N-tert*-butyl-1,1-diphenylphosphanamine (0.444 mmol, 4 equiv). The product was obtained as grey crystals (94 mg, 51% yield, Melting Point: 180 °C (decomp)). ^1H -NMR (500 MHz, CDCl_3): δ (ppm) = 7.64-7.58 (m, 4H), 7.48-7.39 (m, 12H), 7.33 (t, $J=7.36$ Hz, 4H), 3.97-3.91 (m, 2H), 3.44 (s, 2H), 3.36-3.31 (m, 2H), 1.23 (s, 3H), 1.05 (s, 18H); ^{13}C -NMR (125 MHz, CDCl_3): δ (ppm) = 136.8 (t, $J=5.38$ Hz), 135.7 (ddd, $J=159.98$ Hz, $J=24.96$ Hz, $J=21.87$ Hz), 131.9 (td, $J=6.79$ Hz, $J=2.53$ Hz), 130.1 (d, $J=27.01$), 128.3 (q, $J=5.08$ Hz), 75.7 (t, $J=16.78$ Hz), 56.0

(t, J=6.26 Hz), 31.9 (t, J=1.85 Hz), 22.6 (s); ^{31}P -NMR (202 MHz, CDCl_3): δ (ppm) = 47.94 (s). HRMS (ESI) $\text{C}_{36}\text{H}_{49}\text{N}_2\text{P}_2\text{Pd}$ calculated: 675.2255, found 675.2114.



(*N,N'*-di-*tert*-butyl-*N,N'*-bis(diphenylphosphino)ethane-1,2-diamine)palladium(η^3 -methallyl) triflate (12): Synthesized according to the general procedure using 84.5 mg *N,N*-di-*tert*-butyl-*N,N*-bis(diphenylphosphanyl)ethane-1,2-diamine (0.156 mmol, 2 equiv). The product was obtained as light yellow crystals (116 mg, 87% yield, Melting Point: 175 °C (decomp)). ^1H -NMR (500 MHz, CDCl_3): δ (ppm) = 7.82-7.76 (m, 4H), 7.57-7.46 (m, 12H), 7.45-7.40 (t, J=7.33 Hz, 4H), 3.98-3.87 (m, 2H), 3.81-3.69 (m, 2H), 3.11 (s, 2H), 2.76-2.71 (m, 2H), 1.29 (s, 3H), 1.10 (2, 18H); ^{13}C -NMR (125 MHz, CDCl_3): δ (ppm) = 137.7 (t, J=4.64 Hz), 135.4 (dd, J=41.51 Hz, J=28.00 Hz), 131.5 (q, J=7.45 Hz), 130.9 (d, J=28.73 Hz), 128.9 (dt, J=15.04 Hz, J=5.34 Hz), 77.5 (t, buried in CDCl_3 , retaken in CD_2Cl_2 , δ = 77.5 (t, J=16.82 Hz)), 60.7 (t, J=5.64 Hz), 54.3 (t, J=13.18 Hz), 30.6 (s), 22.2 (s); ^{31}P -NMR (202 MHz, CDCl_3): δ (ppm) = 73.15 (s). HRMS (ESI) $\text{C}_{38}\text{H}_{49}\text{N}_2\text{P}_2\text{Pd}$ calculated: 701.2411, found 701.2506.

III. Allylic Amination Rate Studies

General procedure for allylic aminations with diethylamine (Table 1): In a glove box: Into an NMR tube was weighed the bisphosphine palladium(η^3 -methallyl) triflate (0.005 mmol, .05 equiv) and 1 ml CDCl_3 was added. Diethylamine (103 μl , 1 mmol, 10 equiv) was then added, followed by methallyl chloride (9.8 μl , 0.1 mmol) and finally mesitylene (5 μl , internal

standard). The vial was capped, mixed vigorously and ^1H NMR was taken at several different time intervals. Conversion to product was determined by comparison to the internal standard. General Procedure for allylic aminations with 2,2,6,6-tetramethylpiperidine (Table 2, room temperature): In a glove box: Into an NMR tube was weighed the bisphosphine palladium(η^3 -methallyl) triflate (0.005 mmol, .05 equiv) and 1 ml CDCl_3 was added. 2,2,6,6-tetramethylpiperidine (169 μl , 1 mmol, 10 equiv) was then added, followed by methallyl chloride (9.8 μl , 0.1 mmol) and finally mesitylene (5 μl , internal standard). The vial was capped, mixed vigorously and ^1H NMR was taken at several different time intervals. Conversion to product was determined by comparison to the internal standard.

Procedure for amination at 90 $^\circ\text{C}$ with 8 (Table 2): In a glove box: Into a 2 dram vial was weighed the bis(triphenylphosphine)palladium(η^3 -methallyl) triflate (4.28 mg, 0.005 mmol, .05 equiv) and 1 ml CDCl_3 was added. 2,2,6,6-tetramethylpiperidine (169 μl , 1 mmol, 10 equiv) was then added, followed by methallyl chloride (9.8 μl , 0.1 mmol) and finally mesitylene (5 μl , internal standard). The vial was capped with a teflon cap, mixed vigorously and heated to 90 $^\circ\text{C}$ for 24 hrs. The contents of the vial were then transferred to an NMR tube and ^1H NMR was taken. Conversion to product was determined by comparison to the internal standard. Reaction was also run using bis((4- $\text{CF}_3\text{C}_6\text{H}_4$) $_3\text{P}$)Pd(methallyl)Triflate using (6.7 mg, 0.005 mmol, 0.05 equiv).

Allylic amination with complex 12: In a glove box: Into an NMR tube was weighed 12 (4.3 mg, 0.005 mmol, .05 equiv) and 1 ml CDCl_3 was added. Diethylamine (103 μl , 1 mmol, 10 equiv) was then added, followed by methallyl chloride (9.8 μl , 0.1 mmol) and finally mesitylene (5 μl , internal standard). The vial was capped, mixed vigorously and ^1H NMR was taken at several different time intervals. Conversion to product was determined by

comparison to the internal standard. The reaction was found to proceed to 51% conversion after 3 hr.

IV. Observation of catalytic intermediates.

Phosphorous NMR was used to track the formation of new intermediates during allylic amination catalysis as follows:

In the following example, 2 equivalents of methallyl chloride were used WRT amine base to ensure that the catalyst remained at the Pd(II) oxidation state at the end of the reaction. In a glove box, 9.4 mg (0.01 mmol, 1 mol%) **1** was added to an NMR tube and 1 ml of CDCl₃ added. 2,2,6,6-tetramethylpiperidine (141 mg, 1 mmol) was then added, followed by methallyl chloride (199 mg, 2.2 mmol, 2.2 equiv). The reaction was allowed to run to completion (20 minutes) and ³¹P NMR taken (³¹P NMR (300 MHz, CDCl₃): δ (ppm) major peaks at -16.75, 24.18 were observed.

Addition of tetrabutylammonium chloride to complex **1** was accomplished as follows: In a glove box, 9.4 mg (0.01 mmol) **1** was added to an NMR tube and 1 ml of CDCl₃ added. Tetrabutylammonium chloride (27.7 mg, 0.1 mmol, 10 equiv) was added. A ³¹P NMR was then taken. ³¹P NMR (300 MHz, CDCl₃): δ (ppm) major peaks at -16.72, 24.20 were observed, suggesting formation of the same intermediates as observed in the catalytic reaction. When attempts were made to isolate any complex formed by addition of exogenous chloride, only complex **1** was re-isolated (as confirmed via X-ray crystallography of the crystals obtained), suggesting the dynamic and reversible nature of formation of chloride adducts such as **1**-Cl.

V. Xyz coordinates and absolute energies

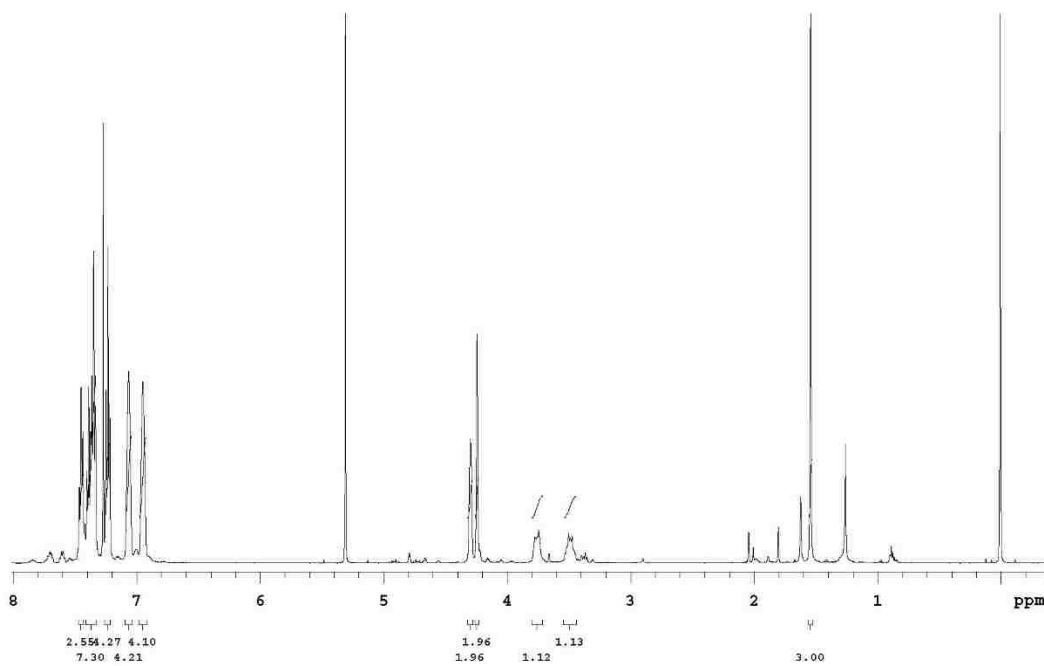
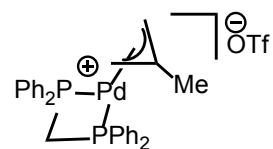
M06/6-31G(d,p)[LANL2DZ] optimized geometries in SMD dichloromethane solvent.

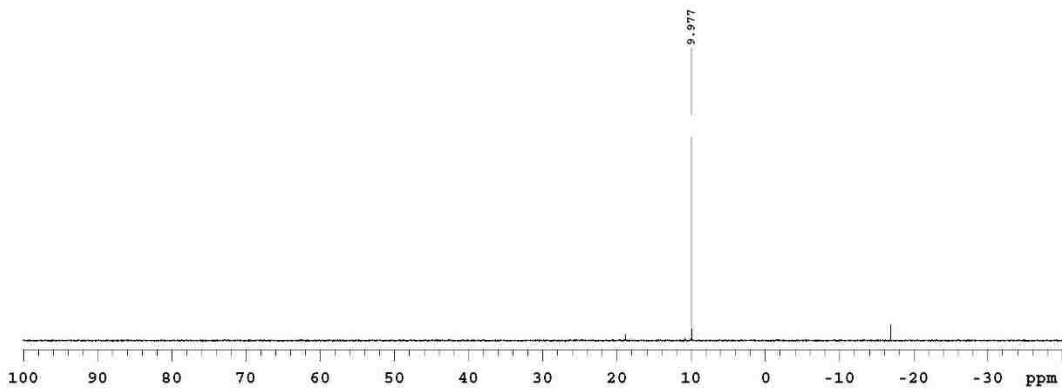
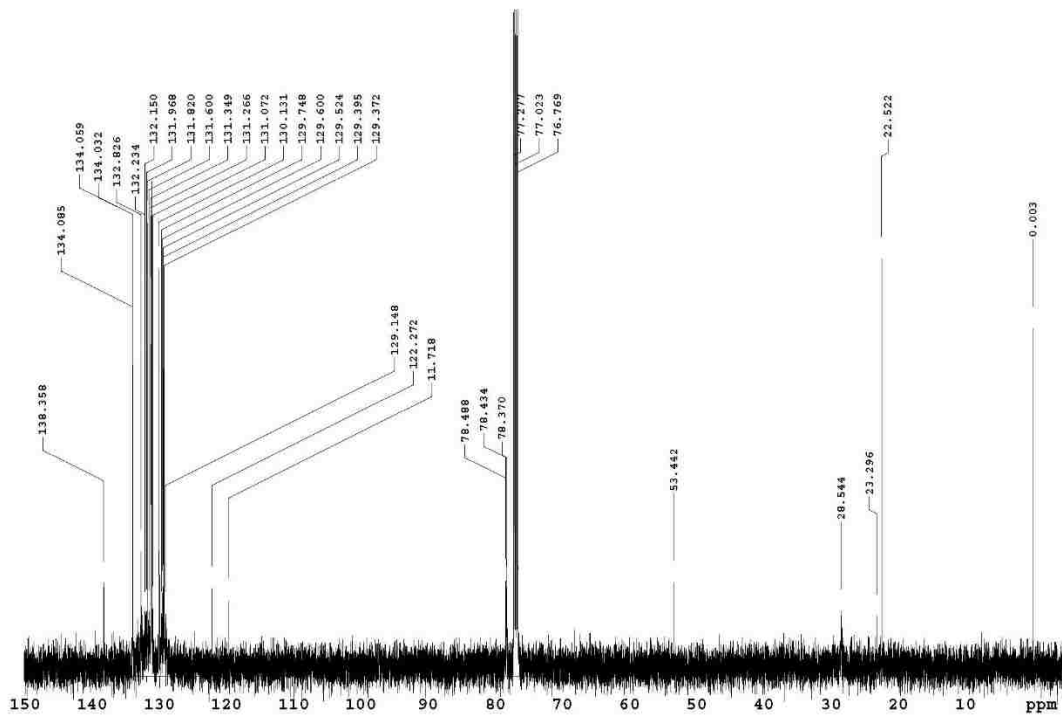
E large = M06/6-311+G(2d,2p)[LANL2TZ(f)

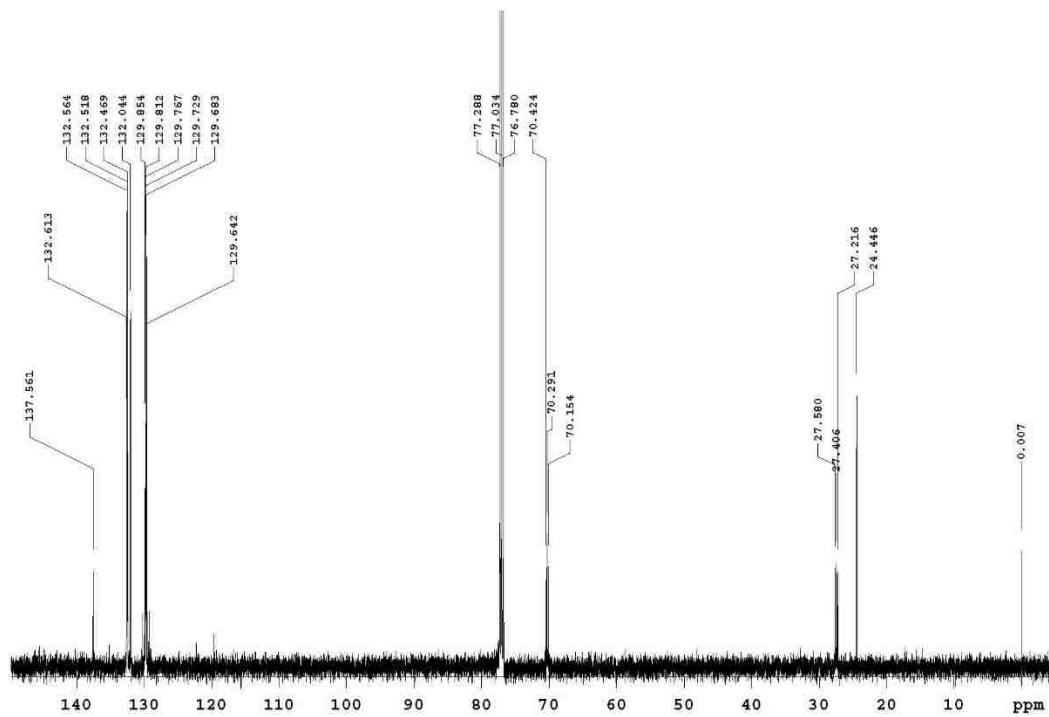
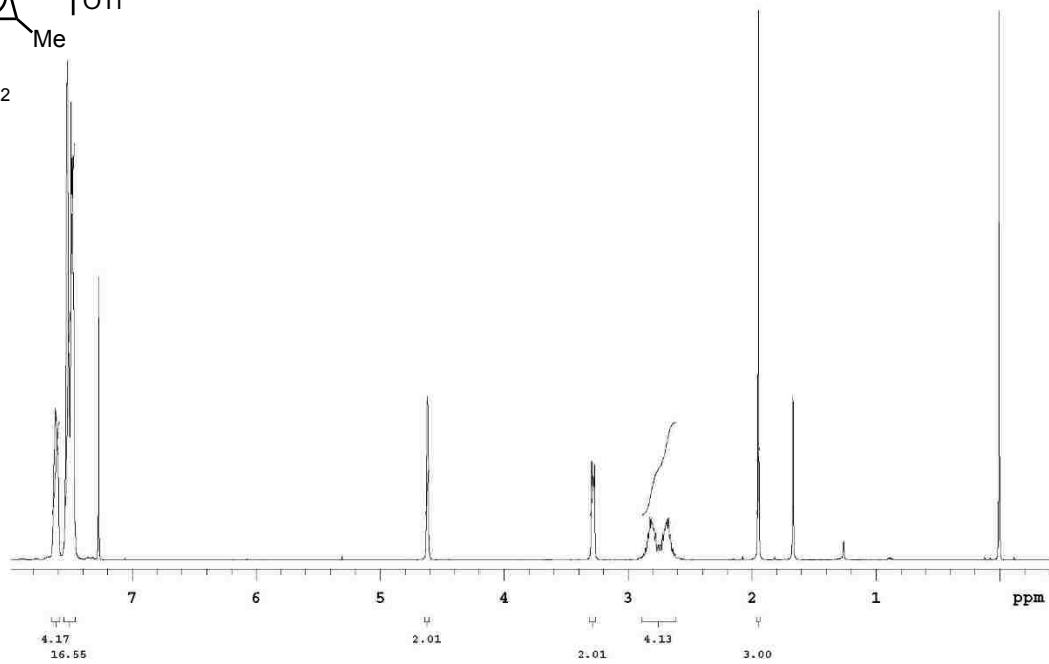
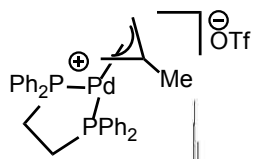
V. For XYZ coordinates of complexes, please see SI of work DOI: 10.1021/jacs. 5b02428

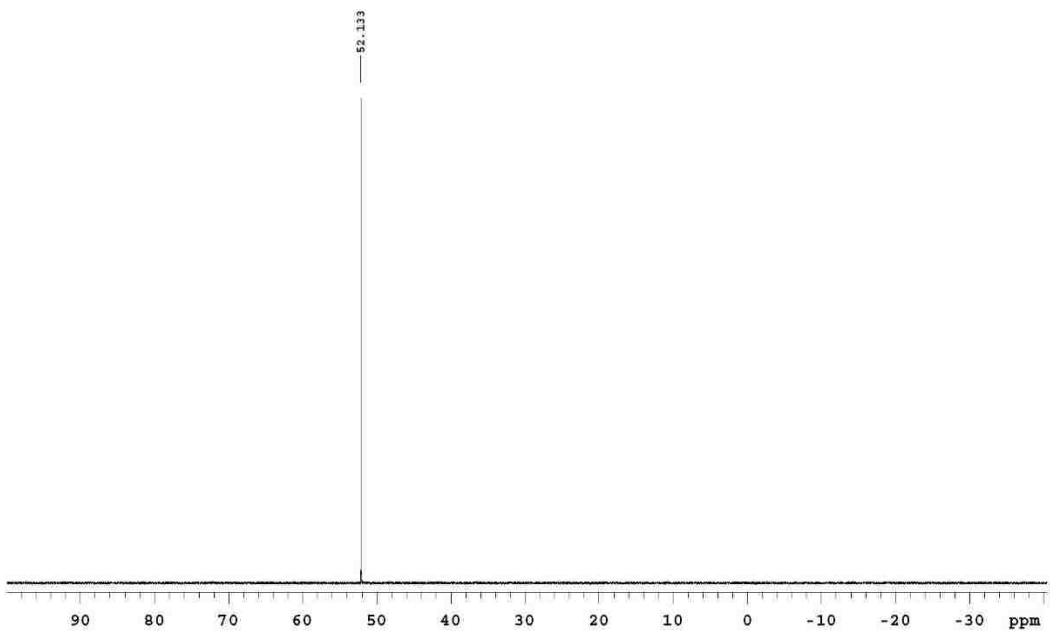
VI. Spectral Images

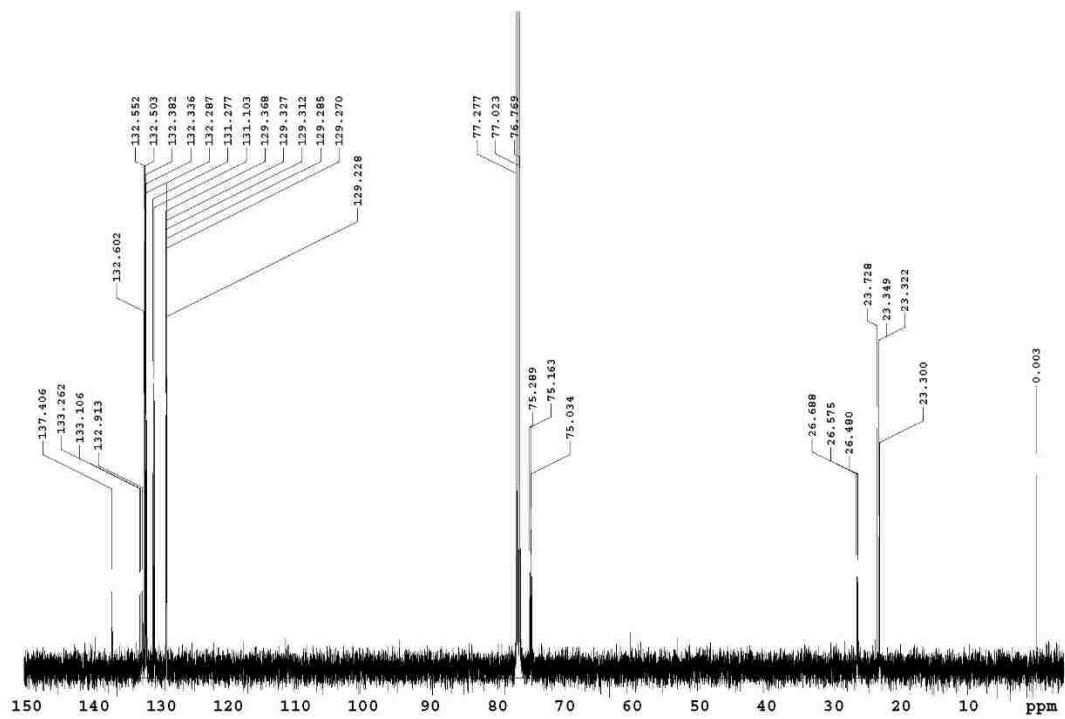
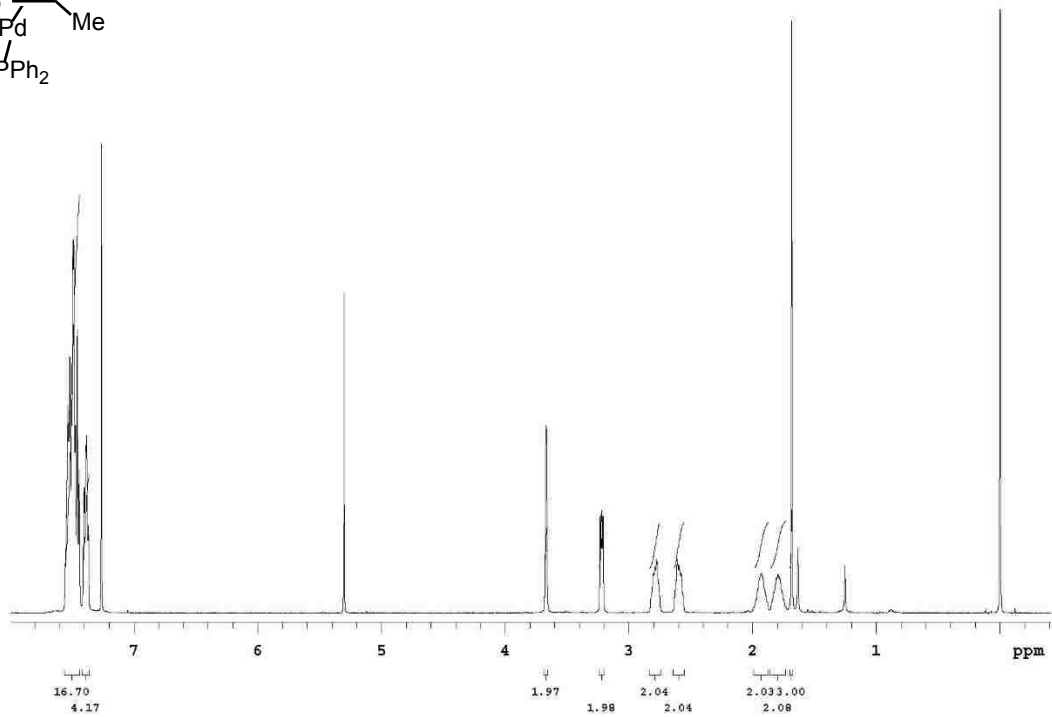
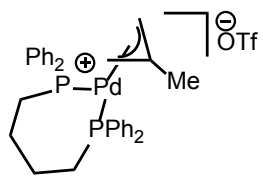
(bis(diphenylphosphino)methane)palladium(η^3 -methallyl) triflate (7a):

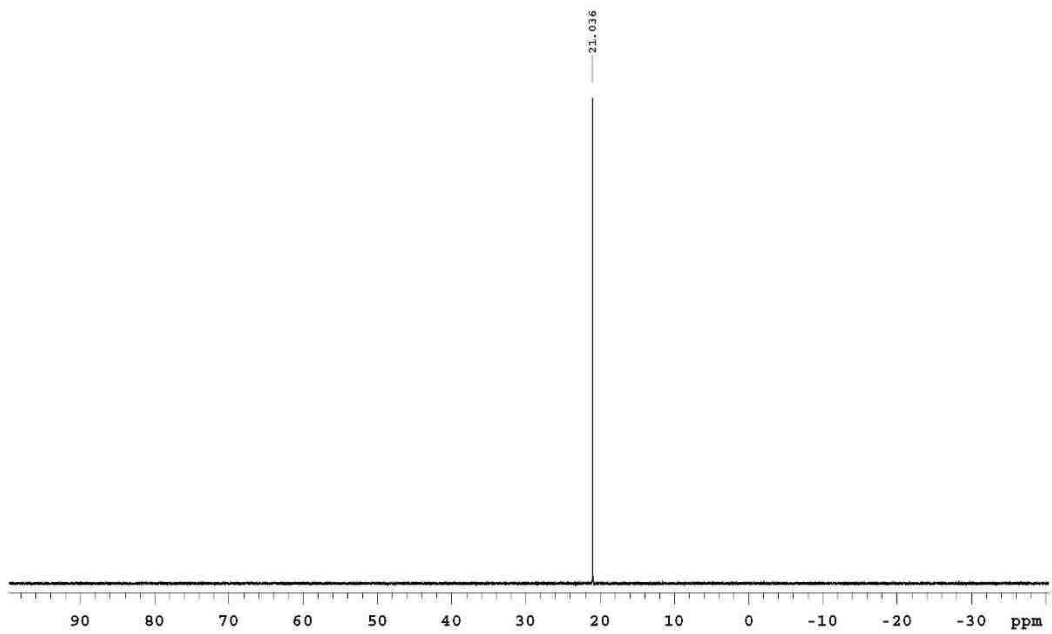


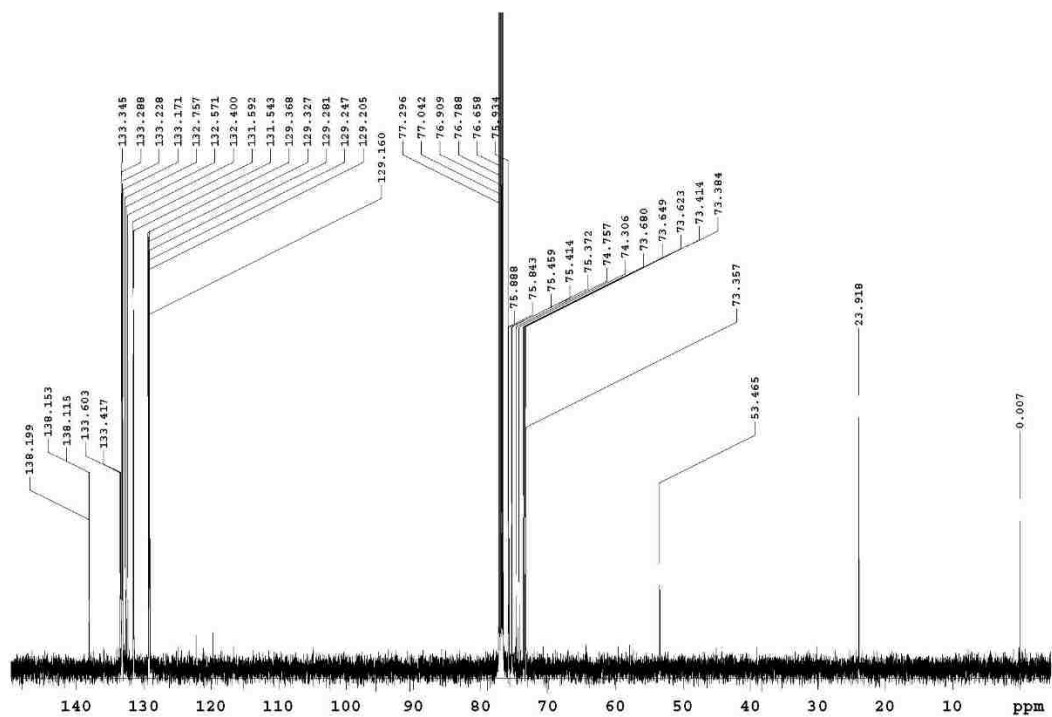
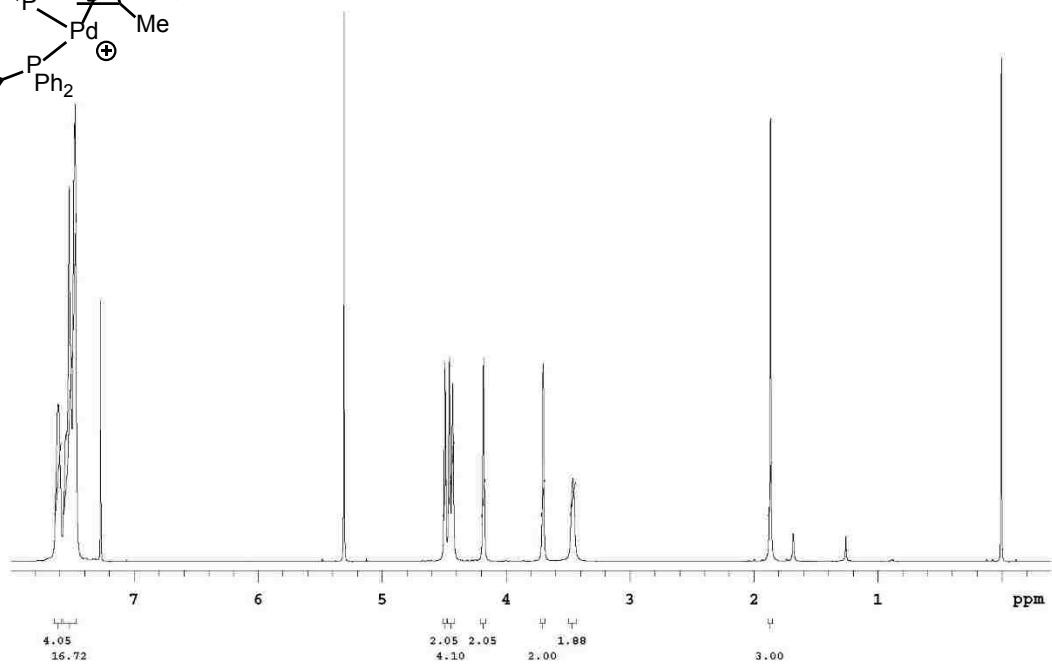
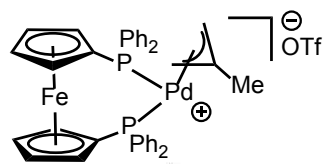


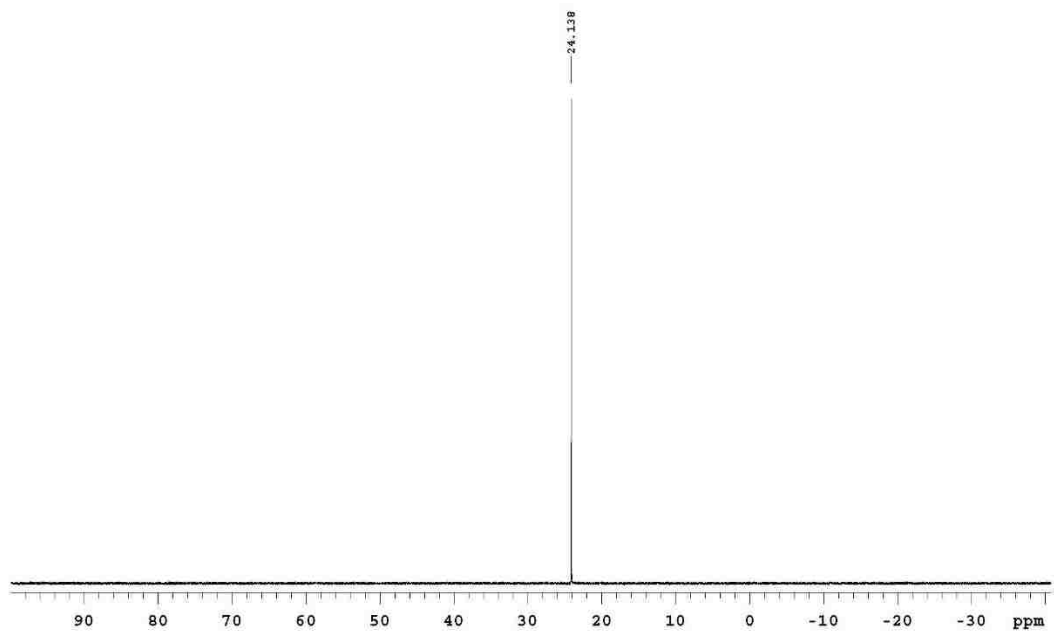


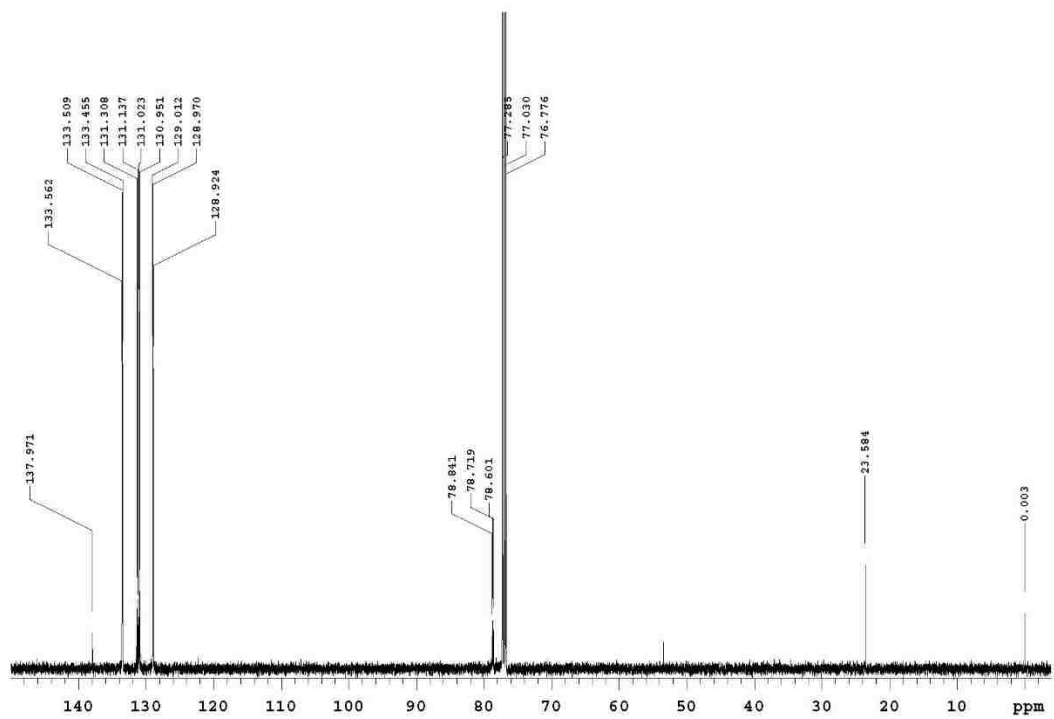
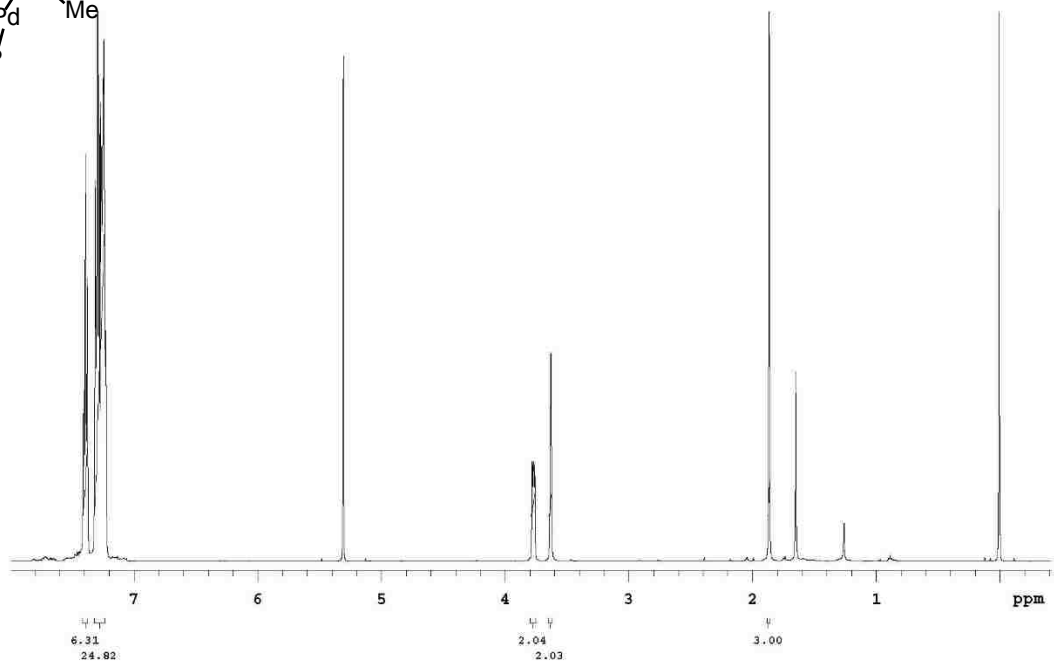
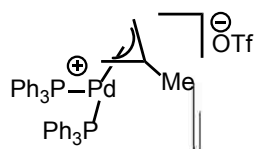


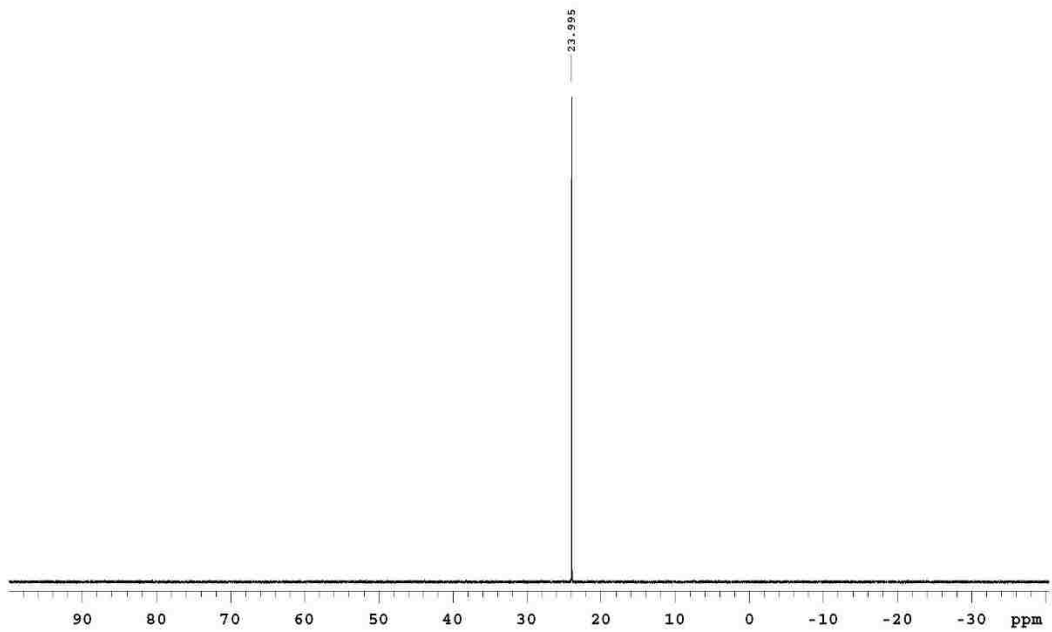




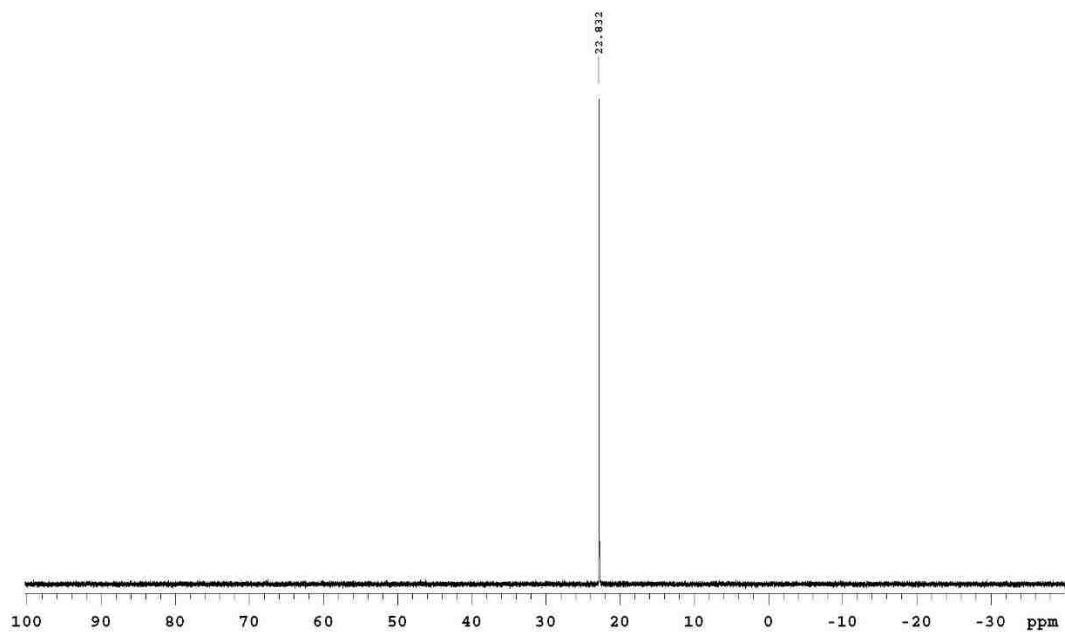
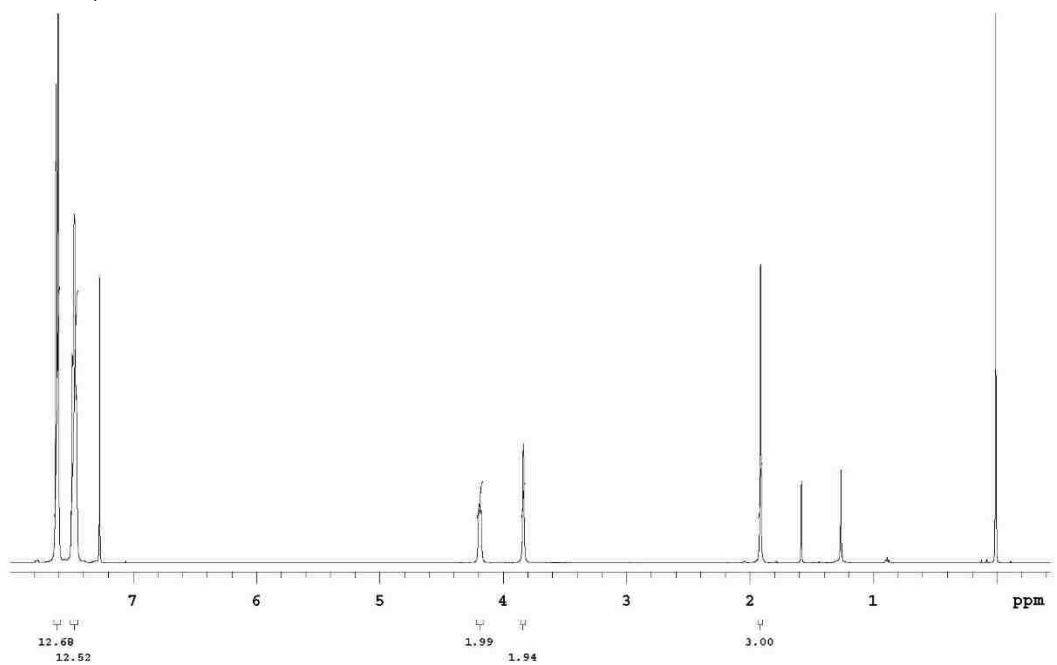
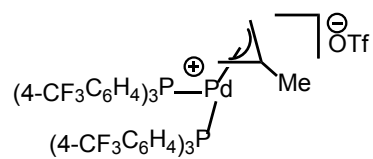


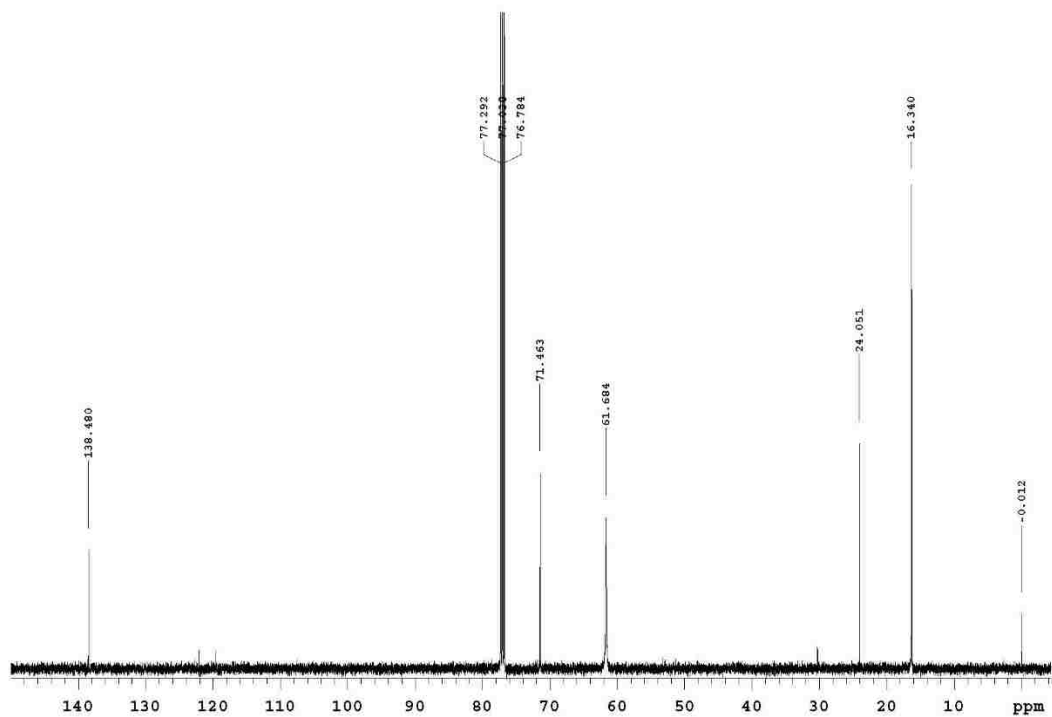
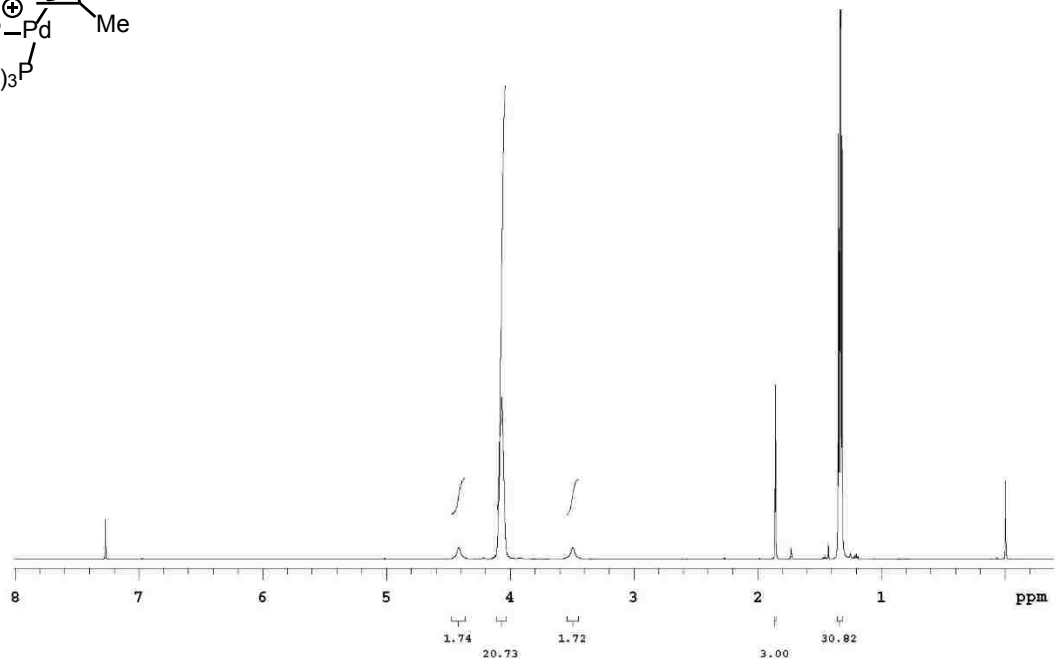
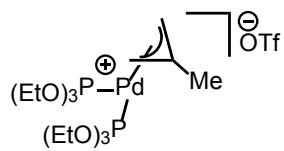


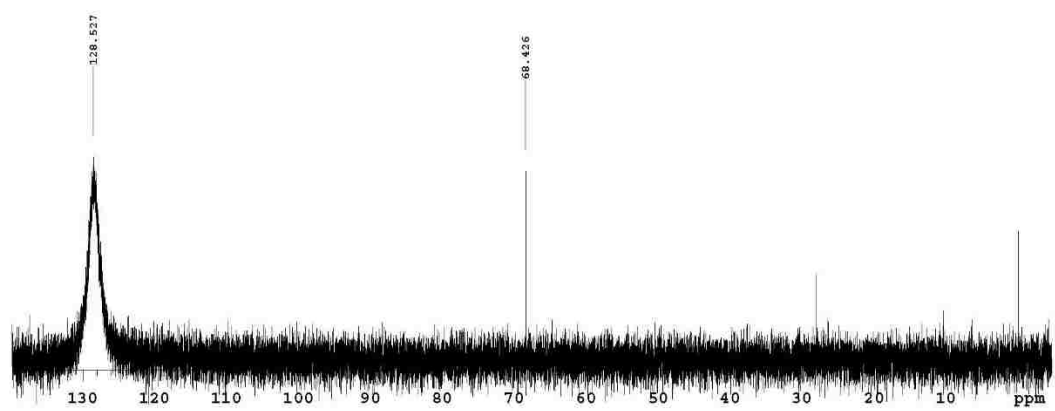


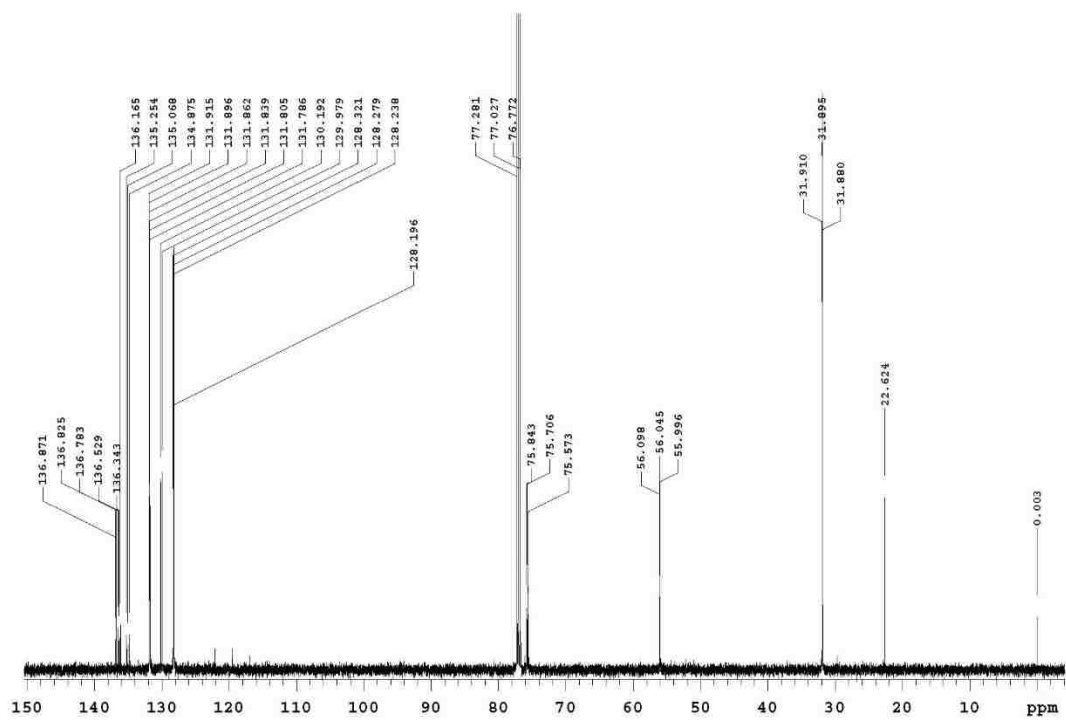
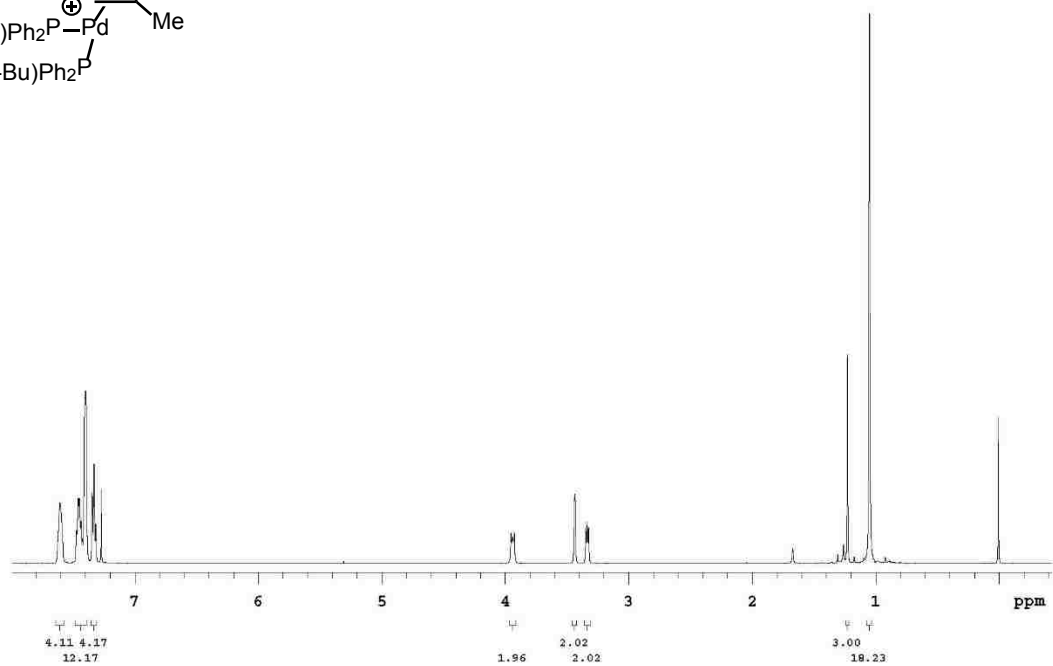
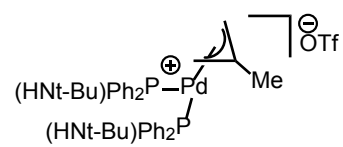


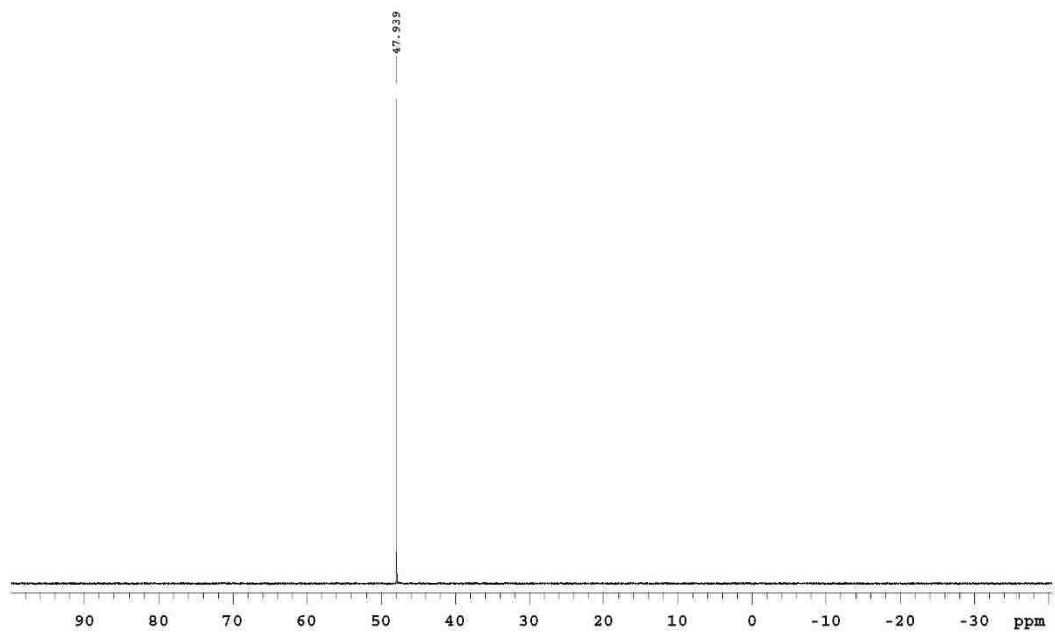
(bis(tris(4-trifluoromethylphenyl))phosphino)palladium(η^3 -methallyl) triflate (9):











Bridged Complex (6):

